UNIVERSITY OF OTTAWA

Department of Chemical and Biological Engineering

CONJUGATED LINOLEIC ACID/STYRENE/BUTYL ACRYLATE BULK AND EMULSION POLYMERIZATION

by

Stéphane Roberge

A thesis submitted to the Faculty of Graduate and Postdoctoral Studies in partial fulfillment of the requirements for the degree of

Doctor of Philosophy

in Chemical Engineering

Abstract

The potential for conjugated linoleic acid (CLA) incorporation into pressure-sensitive adhesive (PSA) formulations was evaluated. A series of free radical bulk copolymerizations of CLA/styrene (Sty) and CLA/butyl acrylate (BA) were designed to allow the estimation of reactivity ratios. Bulk terpolymerizations of CLA/Sty/BA were also evaluated before moving to emulsion terpolymerizations of CLA/Sty/BA. The polymers were characterized for composition, conversion, molecular weight and glass transition temperature while latexes were characterized for viscosity, particle size, tack, peel strength, and shear strength.

All experiments were performed at 80^{o}C and monitored with attenuated total reflectance Fourier transform infrared (ATR-FTIR) spectroscopy. While bulk experiments were monitored off-line, the emulsion experiments were monitored in-line. Absorbance peaks related to the monomers and polymer were tracked to provide conversion and polymer composition data using a multivariate calibration method. Off-line measurements using gravimetry and ^{1}H-NMR spectroscopy were compared to the ATR-FTIR data and no significant differences were detected between the measurement methods.

Pseudo-kinetic models, developed and validated with the copolymer experimental data, were used to estimate reactivity ratios. The copolymer pseudo-kinetic models were extended to a terpolymer pseudo-kinetic model and validated with experimental data. The pseudo-kinetic models incorporated the ability of oleic acid, a common impurity found in CLA, to trap electrons thus influencing the reaction kinetics significantly. The influence of terpolymer composition, chain transfer agent concentration, cross-linker concentration,

molecular weight, viscosity and particle size on tack, peel strength and shear strength was investigated by using a constrained mixture design. The final forms of the resulting empirical models allowed the creation of 3D response surfaces for PSA performance optimization. The incorporation of 30 wt.% CLA into a practical PSA application suitable for the removable adhesives category was achieved.

Résumé

Le potentiel d'incorporation de l'acide linoléique conjugué (ALC) dans des adhésifs sensible à la pression (ASP) a été évalué. Une série de copolymérisations en masse avec radicaux libres d'ALC/styrène (Sty) et d'ALC/acrylate de butyle (AB) ont été conçus pour estimer les rapports de réactivité des différents monomères. Des terpolymérisations en masse d'ALC/Sty/AB ont également été évalués avant de passer à des terpolymérisations en émulsion d'ALC/Sty/AB. Les polymères ont été caractérisés pour leurs composition, leur conversion, leur masse moléculaire et leur température de transition vitreuse tandis que les latex ont été caractérisés pour leur viscosité, leur taille de particule, leur adhérence, leur résistance à l'arrachement et leur résistance au cisaillement.

Toutes les expériences ont été effectuées à 80 °C et suivis à l'aide d'une méthode de surveillance d'atténuation du réfléchissement totale et transformation de Fourier d'une spectroscopie par infrarouge. Les polymérisations en masse ont été surveillées hors ligne, alors que les polymérisations en émulsion ont été surveillées en ligne. À l'aide d'un procédé d'étalonnage à variables multiples, les absorbances caractéristiques en relation avec les monomères et les polymères ont été suivies pour fournir la conversion et la composition des polymères. Cette méthode en ligne utilisant la spectroscopie par infrarouge fut comparé au méthode hors ligne tels que la gravimétrie et la résonnance magnétique nucléaire des protons et aucune différence significative n'a été décelée entre les méthodes.

Des modèles pseudo-cinétiques, développés et validés avec les données expérimentales de copolymère, ont été utilisés pour estimer les rapports de réactivité. Les

modèles pseudo-cinétique de copolymère ont été étendus à un modèle pseudo-cinétique de terpolymère et validés avec des données expérimentales. Les modèles pseudo-cinétique ont intégrés la capacité de l'acide oléique, une impureté commune dans ALC, à piéger des électrons influençant ainsi la cinétique de réaction de manière significative. L'influence de la composition des terpolymères, de la concentration des agents de transfert de chaine, de la concentration des agents de réticulation, de la masse moléculaire des terpolymères, de la viscosité et de la taille de particule sur l'adhérence, la résistance à l'arrachement et la résistance au cisaillement a été étudiée en utilisant une conception de mélange contraint. Les formes finales des modèles empiriques résultant permis la création de surfaces de réponse 3D pour l'optimisation de la performance des ASP. L'incorporation de 30% par poids d'ALC dans une application pratique d'ASP approprié pour la catégorie des adhésifs amovibles a été atteinte.

Statement of Contributions

I hereby declare that I am the sole author of this thesis. I performed the polymerization experiments, polymer characterizations, pressure-sensitive adhesive testing, and data analysis except for the acquisition of ^{1}H-NMR data, which were contracted out to the Department of Chemistry at the University of Ottawa. Ms. Liana Martel is also acknowledged for her assistance with some of the polymer experiments and characterizations.

My thesis supervisor Dr. Marc A. Dubé provided the scientific guidance throughout the project and editorial comments for the written work.

Stéphane Roberge Date: January 15, 2016

_____

Acknowledgements

I would like to express my gratitude to my supervisor Dr. Marc A. Dubé for all the support and guidance he provided to me throughout this thesis. I am grateful to all the members of the Polymer Reaction Engineering group and the technicians of the Department of Chemical and Biological Engineering at the University of Ottawa.

For the financial support during this project, I am grateful to the Natural Sciences and Engineering Research Council of Canada and to the University of Ottawa. Interest from Omnova Solutions (USA) in this work is also acknowledged.

Table of Contents

List of Tables

List of Figures

Nomenclature

Symbols

f_i	Instantaneous fraction of monomer i (dimensionless)
F_i	Instantaneous mole fraction of monomer i (dimensionless)
k_d	Decomposition of initiator rate constant (L/mol min)
$k_{i,j}$	Initiation of monomer j rate constant (L/mol min)
k_p	Polymerization rate constant (L/mol min)
$k_{p,ij}$	Propagation rate constant of monomer j to terminal monomer i, (L/mol min)
$k_{tc,ij}$	Termination by combination rate constant, terminal monomers for the radical chains are i and j, respectively (L/mol min)
$k_{td,ij}$	Termination by disproportionation rate constant, terminal monomers for the radical chains are i and j, respectively (L/mol min)
P_{n+m}	Dead polymer of length n+m (dimensionless)
r_i	Reactivity ratio of monomer i (dimensionless)
R_d	Rate of decomposition of initiator (mol/L min)
R_i	Rate of initiation (mol/L min)
R_p	Rate of polymerization (mol/L min)
$R_{r+1,i}$	Radical chain of length r+1, ending in monomer i and j, respectively (dimensionless)
R_t	Rate of termination (mol/L min)

$R\cdot$	Free radical (dimensionless)
$R\cdot_{1,i}$	Radical chain with 1 monomer, ending in monomer i (dimensionless)
$R\cdot_{m,i}$	Radical chain of length m, ending in monomer i (dimensionless)
$R\cdot_{n,i}$	Radical chain of length n, ending in monomer i (dimensionless)
$R\cdot_{r,i}$	Radical chain of length r, ending in monomer i (dimensionless)
X	Overall conversion (wt. % or mol fraction)
x_i	Conversion of monomer I (wt. % or mol fraction)

Abbreviations

AA	Acrylic Acid
ASTM	American Society for Testing and Materials
ATR-FTIR	Attenuated Total Reflectance Fourier Transform Infrared
BA	Butyl Acrylate
CMC	Critical Micelle Concentration
CLA	Conjugated Linoleic Acid
CTA	Chain Transfer Agent
DMA	Dynamic Mechanical Analysis
DSC	Dynamic Scanning Calorimetry
DVB	Divinylbenzene
GPC	Gel Permeation Chromatography
^{1}H-NMR	Proton Nuclear Magnetic Resonance Spectroscopy
KPS	Potassium Persulfate

NaOH	Sodium Hydroxide
NIR	Near Infrared
ODA	Octadecyl Acrylate
PET	Polyethylene Terephtalate
PLS	Partial Least Square
PRESS	Predicted Residual Error Sum of Square
PSA	Pressure Sensitive Adhesive
PSD	Particle size distribution
PSTC	Pressure Sensitive Tape Council
SDS	Sodium Dodecyl Sulfate
Sty	Styrene
T_g	Glass Transition Temperature
THF	Tetrahydrofuran

Chapter 1 – Introduction

Petroleum-based polymers are not sustainable and researchers worldwide are working on a variety of solutions to reduce our dependence on fossil fuels for polymer production. One such solution involves the incorporation of conjugated linoleic acid (CLA), a renewable monomer derived from plant oils, into polymer formulations and increasing our understanding of the different reaction mechanisms involved. This project followed many principles of green chemistry[1] by utilizing CLA as a safer, renewable, degradable and non-functionalized monomer, using a water-based (emulsion) polymerization technique, and employing real-time process monitoring. The replacement of a monomer will inevitably alter the polymer product properties and our goal was to balance product performance while increasing sustainability.

Caution must be applied when incorporating plant-based materials into commercial, non-comestible products. We must apply a smart agricultural philosophy to avoid competition between the polymer industry and the food industry for plant-based materials by considering land allocation, crop rotation, fertilizer, water usage and ultimately crop platforms dedicated to industrial usage[2]. Plant oils can be less energy intensive to produce than alcohols or sugars because they do not require solvent extraction or intensive heat input. Even if pressing can produce lower yields, the biomass residue called seedcake, comprised mainly of proteins, can be used elsewhere such as in animal feed[3].

Worldwide, the production of bioplastics, or polymers derived from renewable materials such as plant oils, was 0.3 million tons in 2010[4] and was projected to exceed 1 million tons by the end of 2015[4]. In comparison, regular plastic production was 160

million tons in 2000[5] and increased to 299 million tons in 2013[6]. In financial terms, the bioplastics market offers a substantial source of revenue with sales of 2.9 billion dollars projected for 2015[7]. Considering that, the present fossil fuel-based plastic market, not yet converted to bioplastics, achieved revenues of 743 billion dollars in 2010[4], the bioplastics market has a lot of potential for growth. Emerging economies from China and India are also expected to play a large role in the projected growth of the plastic market to 530 million tons by 2020[5]. This can be explained in part because, in 2010, the average per capita consumption of plastics was 109 kg for North America, 29 kg for China and 5.8 kg for India[8].

Plant oils derived from soybeans are easily available in Ontario (e.g., farm cash receipts exceeded 1 billion dollars in 2009)[9]. While Canadian soybean production has been concentrated in Ontario, new varieties, developed by Canadian researchers, are making it possible to grow them in other parts of the country. Canada exports well over 1 billion dollars' worth of soybeans annually[9]. Since 1999, the Government of Canada has put together many initiatives to increase the availability of soybean feedstock such as the Genomics Research and Development Initiative (GRDI), the Seed Program Modernization Initiative (SPMI) or the Co-operative Development Initiative (CDI). Since 2008, the Ontario SMART initiative (Strategic Management Adding Revenue Today) is helping farmers increase the yield and productivity of soybean and wheat.

Plant oils, or triglycerides, are made of three fatty acid chains bonded to a glycerol backbone (see Figure 1.1.a). Mostly low molecular weight polymers are obtained during the polymerization of plant oils [11, 12]. The polymer molecular weight can be increased by copolymerization[13, 14], pre-oxidation[15], polymerization in supercritical

carbon dioxide[16], functionalization[17-27] and with bacterial methods[28]. For this research project, and in the interest of green chemistry principles, we sought to evaluate the potential of plant oils to be polymerized without additional functionalization.

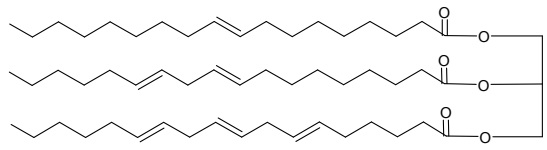

a) Triglyceride

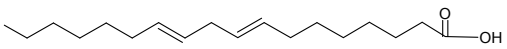

b) Linoleic acid

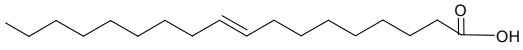

d) Oleic acid

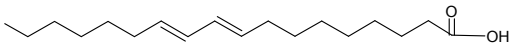

c) Conjugated linoleic acid

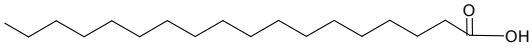

e) Saturated fatty acid
(Stearic acid)

Figure 1.1: a) Triglyceride, b) Linoleic acid, c) Conjugated linoleic acid, d) Oleic acid, and e) Saturated fatty acid

The polymerization of plant oils is made difficult due to steric hindrance which can be overcome by the use of its component fatty acid chains such as linoleic acid (see Figure 1.1.b)[29, 30]. Soybean oil can be easily and inexpensively photo-isomerized to produce fatty acids[31]. Because of the ability of conjugated oils to copolymerize[32], CLA was chosen for free radical polymerization (see Figure 1.1.c). With the prohibitive cost of high purity CLA[33, 34], an affordable CLA containing impurities such as oleic acid (see

Figure 1.1.d) and saturated fatty acids (see Figure 1.1.e) presents an interesting option for polymerization. Oleic acid has been used as a surfactant replacement in the emulsion homopolymerization of styrene without any signs of copolymerization[35] and is also known for its electron trapping ability[36] where the oleic acid radicals are resonance stabilized[37]. Saturated fatty acids are not expected to participate in free radical reactions, other than to impart some viscosity to the reaction medium, because they do not contain the proper reactive sites (i.e., the double bonds) for free radical polymerization.

Free-radical polymerization can be carried out in different media such as bulk or emulsion. While the main components of a bulk polymerization are monomer and initiator, the main components for an emulsion polymerization are generally, water, surfactant, monomer and a water-soluble initiator. From a greatly simplified perspective, an emulsion is formed by agitating and heating the water, surfactant and monomer. The emulsion therefore consists of a continuous water phase with suspended monomer droplets ranging in diameter from 1 to 10 μm[38], as well as monomer-swollen micelles generated when the surfactant concentration exceeds that of the critical micelle concentration. The initiator is subsequently added, and free radicals are produced by thermal decomposition of the initiator. The free radicals then preferentially enter the monomer-swollen micelles and polymerization begins wherein the micelles then become polymer particles; this process is known as particle nucleation. The preferential radical entry into the micelles as opposed to the monomer droplets is due to the significant surface area possessed by the micelles. The monomer droplets stabilized by surfactant at their surface act instead as monomer reservoirs. Thus, during the polymerization, monomers exit the droplets and diffuse through the aqueous phase to reach the polymer

particles, considered the main locus of polymerization. As noted above, polymer particles are generally formed by the entry of radicals into the micelle (heterogeneous nucleation) if micelles are present. However, an additional particle nucleation mechanism involving the precipitation of growing oligomers in the aqueous phase (homogeneous nucleation) can also occur. In conventional emulsion polymerization, the final product is a stable colloidal suspension of polymer particles having diameters from 0.1 to 1 μm [39].

Whether in emulsion or bulk, free radical chain growth polymerization is a chain reaction consisting of a sequence of three steps: initiation, propagation and termination. Initiation involves the decomposition of the initiator to free radicals by thermal, photochemical or redox methods. For this research project, we focused on the thermal homolytic dissociation of our initiator. Propagation involves the rapid addition of monomers to the growing radical chains while termination involves the mutual annihilation of two radical chains. Reactivity ratios[40] are important parameters used to predict copolymer composition via the Mayo-Lewis equation:

$$\frac{d[M_1]}{d[M_2]} = \frac{[M_1](r_1[M_1]+[M_2])}{[M_2](r_2[M_2]+[M_1])} \tag{1.1}$$

where r_1 and r_2 are the reactivity ratios associated with the concentrations of monomers 1 ($[M_1]$) and 2 ($[M_2]$), respectively. The reactivity ratios for the copolymerization propagation step are related to the propagation rate constant as:

$$r_1 = \frac{k_{p,11}}{k_{p,12}} \tag{1.2}$$

$$r_2 = \frac{k_{p,22}}{k_{p,21}} \tag{1.3}$$

where $k_{p,ij}$ is the propagation rate constant of a growing radical chain ending in monomer i adding a monomer j unit. Equation 1.1 can also be expressed in terms of mole fractions instead of concentrations:

$$F_1 = 1 - F_2 = \frac{r_1 f_1^2 + f_1 f_2}{r_1 f_1^2 + 2 f_1 f_2 + r_2 f_2^2} \tag{1.4}$$

where F_i is the instantaneous mole fraction of monomer *i* in the copolymer and f_i is the mole fraction of monomer *i* in the reaction mixture. The copolymer composition will drift during the reaction if one reactivity ratio is significantly different than the other. Thus, knowledge of the reactivity ratios is important if one wishes to control copolymer composition using, for example, semi-batch feed policies[42].

One form of adhesives called pressure-sensitive adhesives (PSAs) are characterized by instantaneous adhesion upon application of light pressure[43]. They are soft and tacky with a low glass transition temperature (T_g) within the -60 to 20 ^oC range. While an acrylic polymer such as poly(BA) can be soft and tacky, thus providing good tack and peel strength, it often lacks in shear strength. The addition of a "hard" monomer such as Sty is useful to regulate tack, peel strength and shear strength[44, 45]. Monomers

with functional groups such as acrylic acid (AA) can be added to improve peel strength, shear strength and film formation, but at the expense of reducing tack[46]. Tack is defined as the property that enables an adhesive to form a bond of measurable strength with a surface of another material upon brief contact under light pressure or no pressure. Peel strength represents the force required to remove a standard PSA strip from a specified test surface under a standard test angle (90^o or 180^o) and conditions. Shear strength is the internal or cohesive strength of the adhesive mass. Usually, it represents the length of time it takes for a standard PSA strip to fall from a test panel after application of a load.

In order to develop new application-specific products and improve existing processes, there is a need to identify the factors that influence the performance of PSAs. Reaction components and process conditions will affect latex properties and those latex properties can affect rheological properties and film formation processes. Furthermore, latex rheology and the film formation process can affect the performance of the adhesive. The relationship between the operating conditions and the latex properties can be obtained by mathematical modeling of the polymerization reactor and extensive experimentation. Considerable efforts have already been devoted to the modeling and control of latex properties[47, 48] and this research project will focus on discovering the impact of latex properties on adhesive performance. A seeded semibatch emulsion polymerization of n-BA, with varying amounts of styrene as comonomer using potassium persulfate as the initiator at 75^oC was investigated for its impact on adhesive performance[49, 50]. They increased the amount of styrene from 0 to 10% and found that they could control the amount of gel and the level of branching by using the styrene as a control variable. They also found that the adhesive properties could be modified by

adding small amounts of styrene. Furthermore, they investigated the effect of dodecane-1-thiol, a chain transfer agent (CTA), on the kinetics, gel fraction, level of branching, and MWD of the sol. By increasing the CTA concentration, they noticed that the gel fraction and the sol weight-average molecular weight showed a strong dependence. On the other hand, no effects were observed on the kinetics or the level of branching. The performance of PSAs made from a semi-continuous emulsion and a solution polymerization was compared[51]. The PSAs were made from two different polymers: poly(2-ethyl-hexyl acrylate-stat-acrylic acid) and poly(n-butyl acrylate-stat-acrylic acid) at 97.5/2.5 wt%. They found that the difference in film network morphology caused significantly lower shear holding power for the emulsion-based PSA compared with that of the solvent-borne film. Unlike shear holding power, the loop tack and peel of the acrylic PSAs were mainly controlled by the same sol/gel molecular parameters, regardless of originating from an emulsion or solution polymerization. The important molecular parameters were sol-to-gel ratio, entanglement molecular weight, weight average molecular weight, and to a lesser extent, glass transition temperature. Polymer molecular weight has a great influence on adhesive properties, especially in the low molecular weight range[32]. As the molecular weight increases, its effect starts to level off. Low molecular weight polymers exhibit good tack but their ability to peel is generally unacceptable for normal PSAs unless they can be cross-linked. Both tack and peel strength increase with molecular weight until a maximum is reached[52]. Shear strength increases with molecular weight but decreases strongly at fairly high molecular weights[52].

An important principle of green chemistry involves the real-time monitoring of processes[53]. The inline monitoring of polymerizations using an attenuated total

reflectance Fourier transform infrared (ATR-FTIR) spectroscopy has previously been applied to monitoring conversion and polymer composition in our laboratory[54-56]. In this technique, a sample is placed in contact with an internal reflection element (IRE) with a high refractive index and low infrared absorption in the region of interest. When the infrared beam enters the IRE at an angle just below the critical angle for total internal reflection, an evanescent wave is set up and is designed to penetrate 1-10 μm into the sample[57]. Since the infrared frequencies are similar to the vibrational movements of chemical bonds, the sample will only absorb infrared frequencies matching its own vibrational movements. The remaining infrared beam (or reflection spectra) can be detected to analyze which frequencies were absorbed. This remaining infrared beam intensity will not decrease significantly because the intensity of the evanescent wave decays exponentially with the distance from the IRE, thus allowing thick or strongly absorbing samples (e.g., water) to be analyzed[57]. The frequencies absorbed in the reflection spectra can be associated with functional groups in polymer chains[58]. A quantitative analysis is made possible by applying Beer's law, which stipulates that the absorbance intensity at a certain frequency is proportional to the concentration of the associated component[58]. For the measurement of the reflection spectra, an interferometer is used and a Fourier transform is applied to enhance the spectral resolution. Infrared spectroscopy includes three distinct spectral regions; namely near-infrared (NIR), mid-infrared (MIR) and far-infrared (FIR). The MIR spectral region encompasses the frequencies corresponding to the fundamental vibrations of virtually all functional groups of organic molecules[58].

1.1 Thesis Objectives

Our hypothesis is that CLA can be incorporated into a practical polymer application in commercially important quantities. Thus, the objective for this thesis was to incorporate 15-25 wt.% CLA into adhesive formulations to allow industry the opportunity of labeling their product as "green". We aspire to provide a transitional solution towards eventually incorporating 100% CLA into an adhesive formulation. To achieve this objective, an increased understanding of the polymerization kinetics when CLA is incorporated in the polymer formulation is required. Thus, a first step was to estimate the reactivity ratios of CLA when copolymerized in bulk with Sty or BA. This was to be followed by the bulk terpolymerization of CLA/Sty/BA. In parallel, the development of a pseudo kinetic model was deemed necessary to confirm our understanding. The next step was to bring us closer to our product formulation by focusing on the emulsion terpolymerization of CLA/Sty/BA. Using our improved understanding of the relationships between the CLA-containing polymer's properties and PSA performance, an optimized product formulation could then be achieved. The successful implementation of an ATR-FTIR monitoring tool for bulk and emulsion polymerization involving CLA, Sty and BA was also undertaken in this project. A schematic diagram of the research methodology is shown in Figure 1.2.

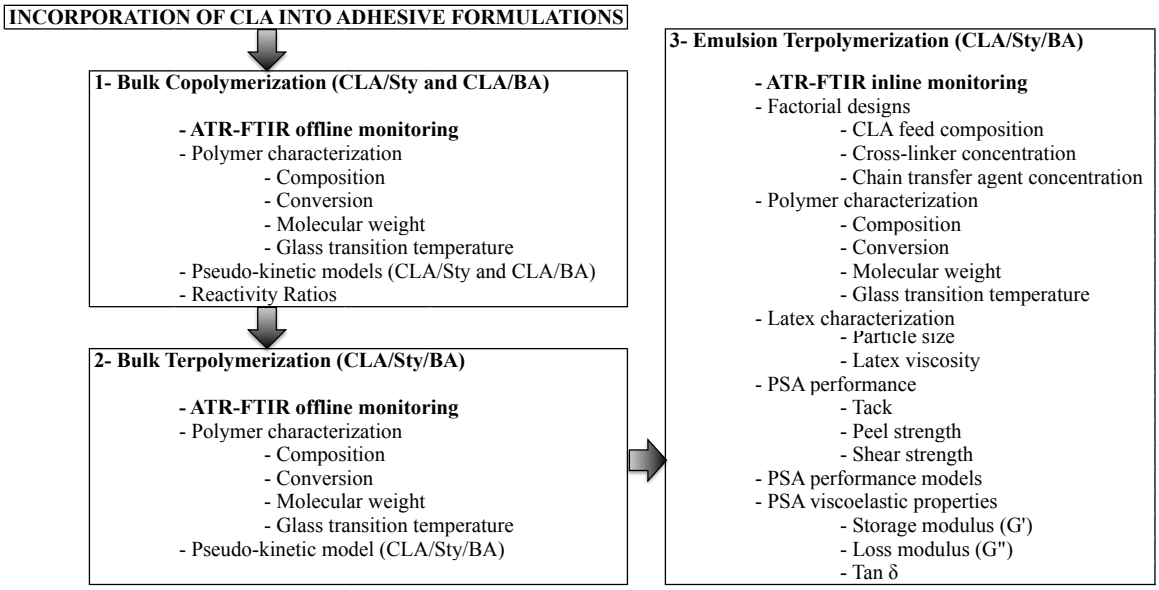

Figure 1.2: Schematic overview of research methodology.

1.2 Thesis Outline

This thesis consist of six chapters. Chapter 2 contains a published manuscript on bulk copolymerizations of CLA with Sty or BA. Chapter 3 contains a published manuscript on bulk terpolymerizations of CLA/Sty/BA. Chapter 4 contains a submitted manuscript on emulsion polymerizations of CLA/Sty/BA. Chapter 5 contains a submitted manuscript on ATR-FTIR monitoring of bulk and emulsion co- and terpolymerizations. The final chapter provides a general discussion of the thesis as well as conclusions based on the results obtained. Sample calculations are found in Appendix A, extra figures are shown in Appendix B, and the Matlab codes for copolymerization and terpolymerization are found in Appendix C and D, respectively. Because of the intention that some chapters could be read separately, the repetition of some common ideas and elements was inevitable.

1.3 References

1. M. A. Dubé, S. Salehpour, Applying the Principles of Green Chemistry to Polymer Production Industries. Macromol. React. Eng., 8, 7-28.
2. A. S. Carlsson, Plant oils as feedstock alternatives to petroleum – A short survey of potential crop platforms. Biochimie, 2009, 91, 665-670.
3. J. W. Lee, Advanced Biofuels and Bioproducts, Volume 1, Springer, New York, 2013, p. 1-1099.
4. Greener Package, December 2011, http://www.greenerpackage.com/bioplastics/world_demand_bioplastics_exceed_1_million_tons_2015, (last checked December, 2015).
5. Pardos Marketing, February 2006, http://www.pardos-marketing.com/paper_g04.htm (last checked December, 2015).
6. PlasticsEurope Association of Plastics Manufacturers, http://www.plasticseurope.org/documents/document/20150227150049-final_plastics_the_facts_2014_2015_260215.pdf (last checked December, 2015).
7. ICIS, December 2011, http://www.icis.com/Articles/2011/12/02/9513755/world-bio-plastics-demand-to-reach-2.9b-by-2015-us-firm.html (last checked December, 2015).
8. Central Institute of Plastics Engineering and Technology, Government of India, http://cipet.gov.in/plastics_statics.html (last checked December, 2015).
9. Department of Foreign Affairs and International Trade, Government of Canada, http://www.canadiansoybeans.com/UserFiles/File/exportsbycountry_12.pdf (last checked December, 2015).

10. S. Salehpour, M. A. Dubé, Biodiesel: a green polymerization solvent. Green Chem., 2008, 10, 329-334.

11. R. Jovanovic, M. A. Dubé, Solvent effects in butyl acrylate and vinyl acetate homopolymerizations in tolutene. J. Appl. Polym. Sci., 2004, 94, 871-876.

12. C. Li, H. Li, P. Liu, Free radical copolymerization of N-(4-carboxyphenyl)maleimide with hydropropyl methacrylate. J. Macromol. Sci., Pure Appl. Chem., 2004, 41, 1161- 1172.

13. F. S. Guner, Y. Yagci, A. T. Erciyes, Polymers from triglyceride oils. Prog. Polym. Sci., 2006, 31, 633-670.

14. F. Li, R. C. Larock, New Soybean oil – styrene – divinylbenzene thermosetting copolymers I. Synthesis and characterization. J. Appl. Polym. Sci., 2001, 80, 658-670.

15. B. Cakmakli, B. Hazer, I. O. Tekin, F. B. Comert, Synthesis and characterization of polymeric soybean oil-g-methyl methacrylate (and n-butyl methacrylate) graft copolymers: biocompatibility and bacterial adhesion. Biomacromolecules, 2005, 6, 1750-1758.

16. Z. Liu, B. K. Sharma, S. Z. Erhan, From oligomers to molecular giants of soybean oil in supercritical carbon medium: 1. Preparation of polymers with lower molecular weight from soybean oil. Biomacromolecules, 2007, 8, 233-239.

17. S. N. Khot, J. J. Lascala, E. Can, S. S. Morye, G. I. Williams, G. R. Palmese, S. H. Kusefoglu, R. P. Wool, Development and application of triglyceride-based polymers and composites. J. Appl. Polym. Sci., 2001, 82, 703-723.

18. T. Eren, S. H. Kusefoblu, Synthesis and characterization of copolymers of bromoacrylated methyl oleate. J. Appl. Polym. Sci., 2004, 91, 2700-2710.

19. Y. Deng, X. D. Fan, J. Waterhouse, Synthesis and characterization of soy-based copolyamides with different α-amino acids. J. Appl. Polym. Sci., 1999, 73, 1081-1088.

20. Z. S. Petrovic, A. Zlatanic, C. C. Lava, S. Sinadinovic-Fiser, Epoxidation of soybean oil in toluene with peroxoacetic and peroxoformic acids – kinetics and side reactions. Eur. J. Lipid Sci. Technol., 2002, 104, 293-299.

21. S. Park, F. Jin, J. Lee, Synthesis and thermal properties of epoxidized vegetable oil. Macromol. Rapid Commun., 2004, 25, 724-727.

22. C. Ozturk, H. Mutlu, M. A. R. Meier, S. H. Kusefoglu, 4-Vinylbenzenesulfonic acid adduct of epoxidized soybean oil: Synthesis, free radical ADMET polymerizations. Eur. Polym. J., 2011, 47, 1467-1476.

23. R. Hoogenboom, U. S. Schubert, Microwave-assisted cationic ring-opening polymerization of soy-based 2-oxazoline monomer. Green Chem., 2006, 8, 895-899.

24. F. Li, R. C. Larock, New Soybean oil – styrene – divinylbenzene thermosetting copolymers I. Synthesis and characterization. J. Appl. Polym. Sci., 2001, 80, 658-670.

25. Z. S. Petrovic, Polyurethanes from vegetable oils. Polym. Rev., 2008, 48, 109-155.

26. S. S. Narine, X. Kong, Bailey's Industrial Oil and Fat Products, 6th Edition, 6th Volume Set, Chapter 8: Vegetable Oils in the Production of Polymers and Plastics, John Wiley and Sons Inc., Edmonton 2005, p. 279-306.

27. J. John, M Bhattacharya, R. B. Turner, Characterization of polyurethane foams from soybean oil. J. Appl. Polym. Sci., 2002, 86, 3097-3107.

28. B. Hazer, S. I. Demirel, M. Borcakli, M. S. Eroglu, M. Cakmak, B. Erman, Free radical crosslinking of unsaturated bacterial polyesters obtained from soybean oily acids. Polym. Bull., 2001, 46, 389-394.

29. F. Li, M. V. Hanson, R. C. Larock, Soybean oil – divinylbenzene thermosetting polymers: synthesis, structure, properties and their relationships. Polymer, 2001, 42, 1567-1579.

30. Z. S. Petrovic, Polyurethanes from vegetable oils. Polym. Rev., 2008, 48, 109-155.

31. R. Gangidi, A. Proctor, Photochemical production of conjugated linoleic acid from soybean oil. Lipids, 2004, 39, 577-582.

32. D. H. Hewitt, F. Armitage, Styrene copolymers in surface coatings. J. Oil Colour Chem. Assoc., 1946, 29, 109-128.

33. S. Roberge, M. A. Dubé, Bulk Copolymerization of Conjugated Linoleic Acid with Styrene and Butyl Acrylate: Reactivity Ratio Estimation. J. Macromol. Sci., Pure Appl. Chem., 2015, 52, 961-970.

34. S. Roberge, M. A. Dubé, Bulk Terpolymerization of Conjugated Linoleic Acid with Styrene and Butyl Acrylate. Sust. Chem. Eng., 2015, DOI: 10.102/acssuschemeng.5b01106.

35. A. Eshuis, H. J. Leendertse, D. Thoenes, Surfactant-free emulsion polymerization of styrene using cross-linked seed particles. Colloid Polym. Sci., 1991, 269, 1086-1089.

36. K. S. Jeong, J. Tang, H. Liu, J. Kim, A. W. Schaefer, K. Kemp, L. Levina, X. Wang, S. Hoogland, R. Debnath, L. Brzozowski, E. H. Sargent, J. B. Asbury, Enhanced Mobility-Lifetime Products in PbS Collodial Quantum Dot Photovoltaics. ACS Nano, 2012, 6, 89-99.

37. R. C. Laible, Allyl Polymerizations. Chem. Rev., 1958, 58, 807-843.

38. Odian, G.G. *Principles of Polymerization*, 3rd Ed.; John Wiley and Sons, Inc.: New York, 1991; 1-374.

39. Rudin, A. *The Elements of Polymer Science and Engineering*, 2nd Ed.; Academic Press: San Diego, 1999; 1-522.

40. M. A. Dubé**,** E. Saldivar-Guerra, I. Zapata-Gonzalez, Handbook of Polymer Synthesis, Characterization and Processing, Chapter 6: Copolymerization NJ, USA 2013, p. 105-125.

41. P. W. Tidwell, G. A. Mortimer J. Polym. Sci., 1965, 3, 369-387.

42. M. A. Dubé**,** J. B. P. Soares, A. Penlidis, A. E. Hamielec, Mathematical modelling of multicomponent chain-growth polymerizations in batch, semi-batch and continuous reactors: A Review. Ind. Eng. Chem. Res., 1997, 36, 966-1015.

43. I. Benedek, L. J. Heymans, Pressure-Sensitive Adhesives Technology, Marcel Dekker Inc., New York, 1997.

44. L. Qie, M. A. Dubé, Manipulation of chain transfer agent and cross-linker Polym. J., 2010, 1225-1236.

45. S. Roberge, M. A. Dubé, The effect of particle size and composition on the performance of styrene/butyl acrylate miniemulsion-based PSAs. Polymer, 2006, 47, 799-807.

46. R. Jovanovic, K. Ouzineb, T. F. McKenna, M. A. Dubé, Butyl acrylate/methyl methacrylate latexes: Adhesive properties. Macromolecular Symposia. 2004, 206, 43-56.

47. Dubé, M.A.; Soares, J.B.P.; Penlidis, A. Mathematical Modeling of Multicomponent Chain-Growth Polymerizations in Batch, Semibatch, and Continuous Reactors: A Review. Ind. Eng. Chem. Res. 1997, 36, 966-1015.

48. Barclay, B.R.; Penlidis, A.; Gao, J. Modelling and simulation of complex aspects of multicomponent emulsion polymerization. Polymer Reaction Engineering. 2003, 11, 737-814.

49. Plessis, C.; Arzamendi, G.; Leiza, J.R.; Alberdi, J.M.; Schoonbrood, H.A.S.; Charmot, D.; Asua, J.M. Seeded semibatch emulsion polymerization of butyl acrylate: Effect of the chain-transfer agent on the kinetics and structural properties. J. Polym. Sci.: Part A: Polym. Chem. 2001, 39, 1106-1119.

50. Plessis, C.; Arzamendi, G.; Leiza, J.R.; Schoonbrood, H.A.S.; Charmot, D.; Asua, J.M. Kinetics and polymer microstructure of the seeded semibatch emulsion copolymerization of n-butyl acrylate and styrene. Macromolecules. 2001, 34, 5147-5157.

51. Tobing, S.D.; Klein, A. Molecular parameters and their relation to the adhesive performance of acrylic pressure-sensitive adhesives. Journal of Applied Polymer Science. 2001, 79(12), 2230-2244.

52. D. Satas, Tailoring pressure sensitive adhesive polymers. Adhes. Age. 1972, 15, 19-23.

53. M. A. Dubé, S. Salehpour, Applying the Principles of Green Chemistry to Polymer Production Industries. Macromol. React. Eng., 8, 7-28.

54. H. Hua, M. A. Dubé, Terpolymerization monitoring with ATR-FTIR spectroscopy. J. Polym. Sci., Part A: Polym. Chem., 2001, 39, 1860-1876.

55. H. Hua, M. A. Dubé, In-line monitoring of emulsion homo- and copolymerizations using ATF-FTIR spectroscopy. Polym. React. Eng., 2002, 10, 21-39.

56. S. Roberge, M. A. Dubé, In-line monitoring of styrene/butyl acrylate miniemulsion polymerization with attenuated total reflectance/Fourier transform infrared spectroscopy. J. Appl. Polym. Sci., 2007, 103, 46-52.

57. H. Gunzler, H. U. Gremlich, IR Spectroscopy an Introduction, Wiley-VCH, Weinheim, 2002.

58. N. B. Colthup, L. H. Daly, S. E. Wiberley, Introduction to Infrared and Raman Spectroscopy, 3rd Edition, Academic Press, San Diego, 1990, p. 1-547.

Chapter 2 – Paper on Bulk Copolymerization of CLA

J. Macromol. Sci., Pure Appl. Chem., 2015, 52, 961-970.

Bulk Copolymerization of Conjugated Linoleic Acid with Styrene and Butyl Acrylate Reactivity Ratio Estimation

Stéphane Roberge and Marc A. Dubé*

Department of Chemical and Biological Engineering,

Centre for Catalysis Research and Innovation, University of Ottawa

161 Louis Pasteur Pvt., Ottawa, ON, K1N 6N5 Canada

* *Marc.Dube@uOttawa.ca*

Abstract

Free radical bulk copolymerizations of conjugated linoleic acid (CLA)/styrene (Sty) and CLA/butyl acrylate (BA) were performed at 80^{o}C. Copolymers were characterized for composition, conversion, molecular weights and glass transition temperature (T_g). A pseudo-kinetic model was developed and validated with experimental data. Reactivity ratios estimations were performed and one impurity commonly found in CLA, oleic acid, influenced the reaction kinetics significantly. The T_g of CLA homopolymer was predicted to be 5^{o}C.

2.1 Introduction

One important way to achieve a more sustainable polymerization process is to replace petroleum-based feedstock with bio-based, renewable materials[1]. Renewable materials often offer built-in degradability, if cross-linking is not overly excessive, as well as lower product toxicity[2]. Plant oils hold considerable promise as renewable materials given their lower gross energy requirement of 20 GJ/ton compared to that of fossil fuels such as propylene oxide at 104 GJ/ton[2]. Plant oils can be less energy intensive to produce than alcohols or sugars because they do not require solvent extraction or intensive heat input. Even if pressing can produce lower yields, the biomass residue can be used elsewhere. The replacement of a monomer will inevitably alter the polymer product properties. Our goal in the addition of a renewable monomer, therefore, will be to balance product performance with increased sustainability.

Plant oils are triglycerides comprising a glycerol backbone connected to three ester groups to which fatty acid chains are attached (see Figure 2.1). Plant oils have been used for decades in paint formulations, as flooring materials and for coating and resin applications[2]. A common flooring application, linoleum, is produced from the oxypolymerization of a drying oil (e.g., linseed oil). Oxypolymerized oils are not the only type of polymers prepared from plant oils: polyesters, polyurethanes, polyamides, acrylic resins, epoxy resins, and polyesteramides can also be produced[3]. Nowadays, plant oils are used as raw materials for surfactants, cosmetic products and lubricants[4]. In addition, they are used in the food and agro-chemical industries[5].

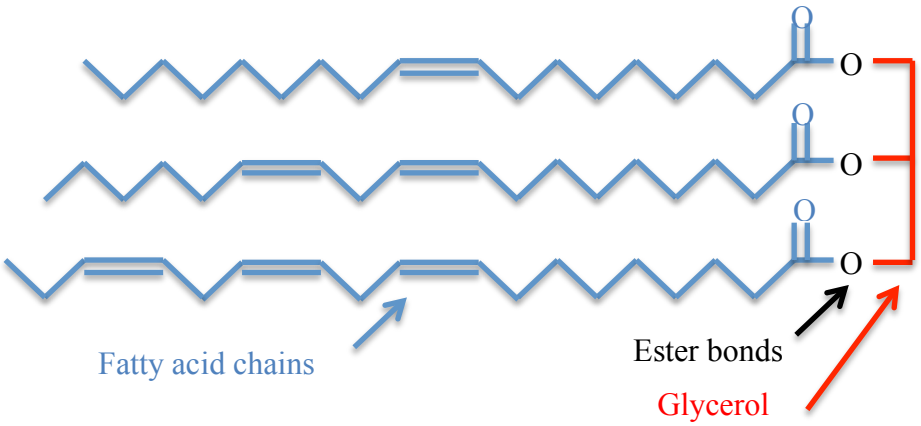

Figure 2.1: Triglyceride molecule

Plant oils are generally considered difficult to homopolymerize due to their lack of active functional groups[6]; their polymerization is difficult even cationically[7,8]. Attempts at copolymerization with styrene, to increase polymer molecular weight, have been reported[3]. The low reactivity of soybean oil is thought to be caused by its relatively high molecular weight and multiple chain structure[9]. It has been proposed that a steric effect could hinder the growth of the polymer chain in cases where only one of the three fatty acid chains on a triglyceride reacts through its double bonds. This condition would create dangling fatty acid chains which would act as plasticizers, thus, creating heterogeneity in the polymer matrix and reducing the glass transition temperature (T_g)[10]. Nevertheless, fatty acid-based polymers have been shown to be biodegradable in soil[11,12], biocompatible to human tissue and blood cells[11,13] and non-toxic[13].

To overcome the steric effect of triglycerides, the fatty acid chains can be separated from the backbone and then polymerized. Soybean oil, for example, consists of 53% linoleic acid (see Figure 2.2). Linoleic acid has mainly been used as a dietary supplement [14,15]. Linoleic acid, with its two double bonds, appears to be a good

candidate for free radical polymerization. Given its high linoleic acid content, soybean oil could be a practical source for this material and several production methods already exist.[16-20] Conjugated linoleic acid (CLA) isomers can be produced simply and inexpensively from soybean oil photo-isomerization[21]. Linoleic acid has been auto-oxidized to produce polymeric materials[22,23] and macro-initiators[24] suitable for free radical polymerization. Functionalities have also been added to facilitate its polymerization[25]. To the best of our knowledge, the free radical copolymerization of non-modified CLA has never been reported.

Figure 2.2: Linoleic acid molecule

Non-conjugated double bonds, where at least two single bonds separate the double bonds, are not believed to be very reactive to radical polymerization due to the presence of allylic hydrogen and the methylene groups between the non-conjugated double bonds. The hydrogen molecules surrounding the double bonds (allylic hydrogen) could trap radicals[10]. A reaction mechanism for styrene and fatty acid chains has been proposed wherein the double bonds react with free radicals, conjugated oils copolymerize and non-conjugated oils invoke degradative chain transfer[26]. It has also been proposed that conjugated double bonds polymerize and oxidize more rapidly than non-conjugated double bonds[27]. A non-conjugated oil such as oleic acid has been used as a surfactant replacement in the emulsion homopolymerization of styrene without any signs of copolymerization[28]. Oleic acid is also known for its insulating property preventing the

movement of electrons from the valence band to the conduction band[29] and trapping them, over a long period of time, inside the oleic acid. In terms of polymerizations, oleic acid radicals were shown to be very stable by resonance[30]. CLA would therefore be preferred for free radical polymerization. With the goal of producing for example, binding agents, it would be interesting to copolymerize CLA with styrene or butyl acrylate. An important first step would be the estimation of copolymer reactivity ratios.

Reactivity ratios[31] are important parameters used to predict copolymer composition via the Mayo-Lewis equation (see Equation 2.1):

$$\frac{d[M_1]}{d[M_2]} = \frac{[M_1](r_1[M_1]+[M_2])}{[M_2](r_2[M_2]+[M_1])} \tag{2.1}$$

where r_1 and r_2 are the reactivity ratios associated with the concentrations of monomers 1 ($[M_1]$) and 2 ($[M_2]$), respectively. The reactivity ratios for the copolymerization propagation step are related to the propagation rate constant as follows (see Equations 2.2 and 2.3):

$$r_1 = \frac{k_{p,11}}{k_{p,12}} \tag{2.2}$$

$$r_2 = \frac{k_{p,22}}{k_{p,21}} \tag{2.3}$$

where $k_{p,ij}$ is the propagation rate constant of a growing radical chain ending in monomer i adding a monomer j unit.

Low conversion copolymerizations (<10 wt.%) are typically required to minimize reactivity ratio estimation errors due to composition drift. A first set of experiments is used to provide preliminary reactivity ratio estimates. These preliminary estimates are then used along with the Tidwell-Mortimer criterion[32] to establish monomer feed compositions for a subsequent set of experiments (see Equations 2.4 and 2.5). Each feed composition from Eqns. 2.4 and 2.5 is replicated four times.

$$f_1^{'} = \frac{2}{2+r_1^*} \tag{2.4}$$

$$f_1^{''} = \frac{r_2^*}{2+r_2^*} \tag{2.5}$$

where r_1* is the preliminary reactivity ratio estimate of monomer 1 and r_2* is the preliminary reactivity ratio estimate of monomer 2. Equation 2.1 can also be expressed in terms of mole fractions instead of concentrations (see Equation 2.6).

$$F_1 = 1 - F_2 = \frac{r_1 f_1^2 + f_1 f_2}{r_1 f_1^2 + 2 f_1 f_2 + r_2 f_2^2} \tag{2.6}$$

where F_i is the instantaneous mole fraction of monomer *i* in the copolymer and f_i is the mole fraction of monomer *i* in the reaction mixture. The copolymer composition will drift

during the reaction if one reactivity ratio is significantly different than the other. Thus, knowledge of the reactivity ratios is important if one wishes to control copolymer composition using, for example, semi-batch feed policies[33]. Herein, the determination of the monomer reactivity ratios for the free radical copolymerization of CLA/Sty and CLA/BA is presented. Additional runs to higher conversion levels are also presented to validate the reactivity ratios and clarify the copolymerization kinetics.

2.2 Experimental

2.2.1 Materials

The reagents: conjugated linoleic acid (CLA, Penta, 74% CLA, 13% oleic acid, 13% saturated fatty acid), styrene (Sty, Sigma-Aldrich, 99%), butyl acrylate (BA, Sigma-Aldrich, 99%), benzoyl peroxide (BPO, Sigma-Aldrich, 100%) were used without further purification. In some instances, styrene and butyl acrylate were purified to remove the inhibitor, hydroquinone. All solvents used for sample work-up and characterizations (e.g., hexane (Fisher, 99.9%), methanol (Fisher, 99.9%) acetone (Fisher, 99%), tetrahydrofuran (THF, Fisher, 99.9%) and chloroform-d (Cambridge Isotope Laboratories, 99.8%) were also used as received.

The cost of pure CLA is prohibitive and a more affordable option (i.e., 74% purity) was chosen. This was done for practical considerations related to industrial application. As noted above, the additional components found in the CLA are oleic acid and saturated fatty acids.

2.2.2 Polymerizations

Bulk polymerizations were performed at 80 °C in glass ampoules with 1 cm outside diameter and 17 cm in length. The concentration of initiator, BPO, was 2 phm (parts per hundred parts monomer on a mass basis) for all experiments. To remove oxygen, three freeze-pump-thaw cycles were performed on each ampoule before flame-sealing them. The sealed ampoules were then submerged in a preheated oil bath for a known amount of time before being removed and quenched in an ice bath for 10 min. All samples were analyzed for monomer conversion and copolymer composition while selected samples were analyzed for molecular weight and T_g.

2.2.3 Characterization

Gravimetry

Mass conversion based on the total polymer in the reaction mixture was measured using gravimetry. The reaction mixture (~3 g) was first dissolved in acetone (~10 mL) then ~125 mL of methanol was used to precipitate the polymer. The soluble portion of the sample mixture was decanted and the polymer/methanol samples were left to dry in a fumehood for ~7 days, then under vacuum for ~7 days until a constant weight was reached. The composition from the polymer/methanol samples was used to perform a mass balance and correct the conversion calculation for any oligomeric species lost in the process.

^{1}H-NMR Spectroscopy

Proton nuclear magnetic resonance spectroscopy (^{1}H-NMR) was used to determine the cumulative copolymer composition. Analyses were carried out at room temperature in deuterated chloroform (~2% w/v) with a Bruker AVANCE III 400 Fourier transform ^{1}H-NMR spectrometer. The acquisition time was 4.6 seconds and 16 scans were performed per sample. A detailed presentation of peak assignments and calculation procedure for copolymer composition is shown in the Supplementary Information. Spectra for the poly(CLA/Sty) and poly(CLA/BA) are shown in Figures 2.3 and 2.4, respectively. Spectra for the monomers are available online in a supplementary information file.

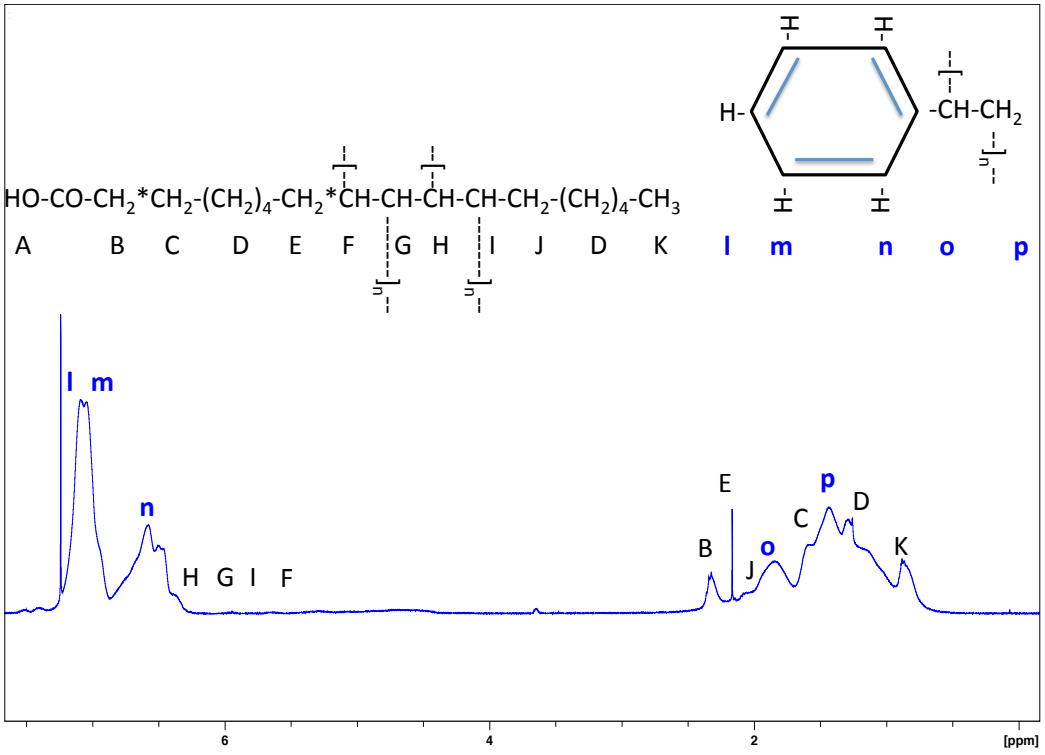

Figure 2.3: ^{1}H-NMR spectrum of CLA/Sty polymer in $CDCl_3$ with peak assignments.

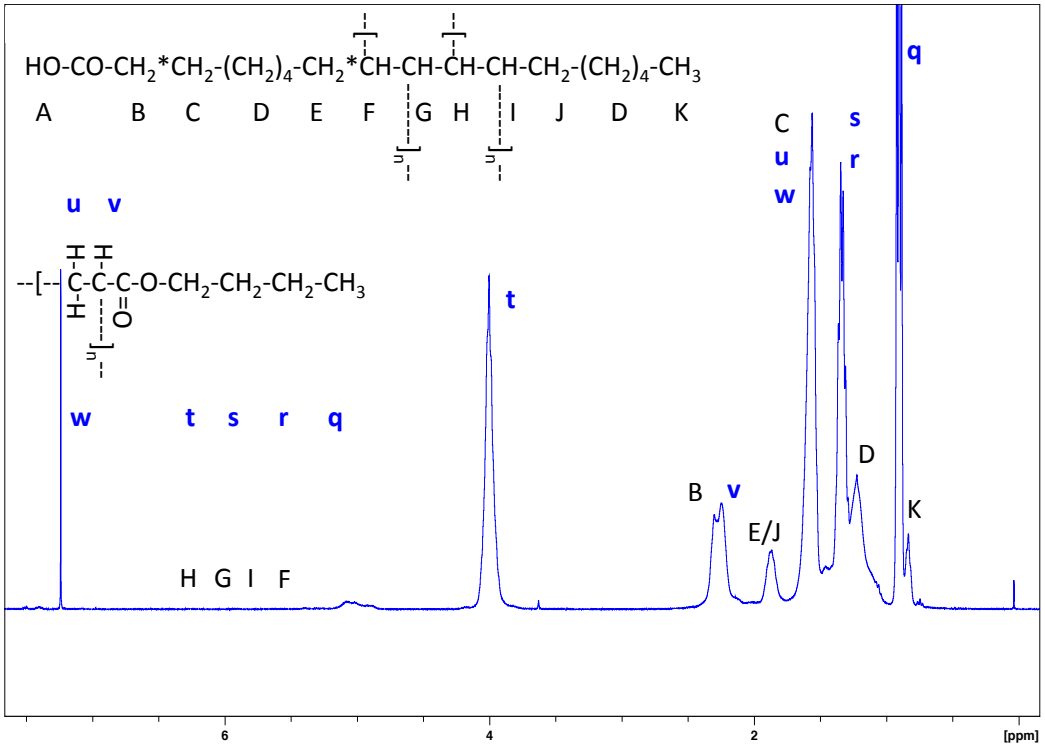

Figure 2.4: ^{1}H-NMR spectrum of CLA/BA polymer in $CDCl_3$ with peak assignments.

The relative mole fractions of each monomer bound in the copolymer were estimated (refer to Equations 2.7 to 2.14) from the areas under the appropriate absorption peaks of the spectra. In Figure 3, the phenyl group for the Sty bound in the polymer (peaks M-N) was located at ~6.2-7.2 ppm while the alkene hydrogen in CLA monomer (peak G) was located at ~5.9 ppm. Results were corrected for any traces of residual monomer. In Figure 4, the -OCH_2- group for BA bound in the polymer (peak T) was located at ~4.0 ppm while the alkene hydrogen in CLA monomer (peak G) was again located at ~5.9 ppm. For both cases, the isolated CLA monomer peak information was crucial for resolving the polymer composition because the methyl group in CLA polymer (peak K) was overlapped with peaks for all other components.

$$F_{CLA} = \frac{\text{mole CLA poly}}{\text{mole CLA poly+mole Sty (or BA) poly}} \quad (2.7)$$

where

$$Sty\ poly = \frac{\left(\text{peak @ 6.2−7.2 ppm} - \frac{\text{peak @ 7.3−7.5 ppm}}{4} * 2\right)}{5} \quad (2.8)$$

$$Sty = \frac{\text{peak @ 7.3−7.5 ppm}}{4} \quad (2.9)$$

$$BA\ poly = \frac{\text{peak @ 4.0 ppm}}{2} \quad (2.10)$$

$$BA = \frac{\text{peak @ 4.2 ppm}}{2} \quad (2.11)$$

$$CLA = \text{peak @ 5.9 ppm} \quad (2.12)$$

$$oleic\ acid = \frac{\text{peak @ 5.2 ppm} - \text{peak @ 5.9}}{2} \quad (2.13)$$

$$saturated + CLA\ poly = \frac{\text{peak @ 0.9 ppm}}{3} - BA\ poly - BA - CLA - oleic\ acid \quad (2.14)$$

As noted, a mass balance was performed on the polymer/methanol samples (i.e., decanted material) to account for any oligomeric materials and also to convert the

calculated concentrations from mol% to wt%. The polymer composition and conversion could then be calculated as follows (see Equations 2.15 to 2.20):

$$mole\ CLA\ poly = \frac{CLA\ in\ feed\ sample\ (g) - CLA\ in\ reaction\ sample(g)}{280.5\ (\frac{g}{mol})} \quad (2.15)$$

$$CLA\ in\ feed\ sample\ (g) = sample\ mass(g) * wt\%\ CLA\ in\ feed \quad (2.16)$$

$$CLA\ in\ reaction\ sample\ (g) = \ sample\ mass\ (g) * wt\%\ CLA\ from\ NMR \quad (2.17)$$

$$Sty\ poly\ (mole) = \frac{sample\ mass\ (g) * wt\%\ Sty\ poly\ from\ NMR}{104.1\ (\frac{g}{mol})} \quad (2.18)$$

$$BA\ poly\ (mole) = \frac{sample\ mass\ (g) * wt\%\ BA\ poly\ from\ NMR}{128.17\ (\frac{g}{mol})} \quad (2.19)$$

$$Conversion = \frac{CLA\ poly\ (g) + Sty(or\ BA)poly(g)}{CLA\ feed\ (g) + Sty\ (or\ BA)feed(g)} \quad (2.20)$$

Gel Permeation Chromatography (GPC)

The cumulative number- and weight-average molecular weights of the polymers were measured using an Agilent/Wyatt GPC system equipped with fractionating columns installed in series, a multi-angle light scatterer (MALS), a viscometer (VISC) and a refractive index detector (DRI) at 25 ^{o}C. Tetrahydrofuran (THF) was the mobile phase and delivered at 1.0 mL/min. For the molecular weight analysis, the refractive index increment (dn/dc) values used were 0.187 for Sty [34] and 0.056 for BA[35].

Differential Scanning Calorimetry (DSC)

The T_g of the polymers was measured with a TA Instruments Model Q1000 DSC equipped with a refrigerated cooling system and a nitrogen purge. The sample (~7 mg of dry polymer) was cooled to -80 ^oC and then heated at a rate of 10^oC/min until the sample reached 110 ^oC. The T_g was calculated from the inflection point in the reversed heat flow curve.

2.3 Results and Discussion

A first, important observation was made by performing mass balances via the ^1H-NMR spectroscopy results. Neither the oleic acid nor the saturated fatty acids were incorporated into the copolymer chains. The alkene hydrogens from CLA and oleic acid were used to make this determination. As shown in the supplementary information, ^1H-NMR spectra confirmed that the saturated fatty acids did not contain any alkene hydrogens and their only role in the reaction was to impart some viscosity to the reaction environment.

2.3.1 Reactivity Ratio Estimation

Reactivity ratio estimation experiments were performed for each copolymer pair, Sty/CLA and BA/CLA. Initially, standard procedures using nine more-or-less equidistant experiments along the monomer feed composition axis were performed to calculate initial estimates of the reactivity ratios. This was followed by experiments using the initial

reactivity ratio estimates with the Tidwell-Mortimer criterion (see Eqns. 2.4 and 2.5) to calculate optimal feed compositions which were replicated four times each for a total of eight additional runs. For both cases, RREVM software version 2.3 (Reactivity Ratio Error in Variables Method) was used for the reactivity ratio estimation[33,36]. This software uses a non-linear technique with the Mayo-Lewis equation (see Equation 2.1) and has been shown to be statistically correct[31-38]. The reaction times were kept to 5 min to minimize composition drift, nonetheless, most conversions greatly exceeded 10 wt% (see Table 2.1). Therefore, reactivity ratio estimates using this technique coupled with these data would be incorrect. One would therefore have to resort to alternative methods using, for example, a Meyer-Lowry based approach[38]. This was attempted, but an additional effect due to the presence of oleic acid was uncovered during the analysis. Thus, it was decided to develop a reaction model that would incorporate the effect of oleic acid and its ability to trap electrons[10,26-30]. It is hypothesized that the long chains (9 carbons) on each side of the oleic acid double bond (see Figure 2.5) form a resonance stabilized molecule after electrons are trapped at the alkene and allylic hydrogens.

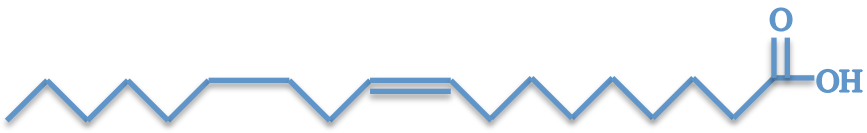

Figure 2.5: Oleic acid molecule

Table 2.1: Conversions from the initial experiments

	f_{CLA} (mol frac)	X (wt.%)	F_{CLA} (mol frac)
Sty	0.08	18	0.53
	0.16	30	0.73
	0.25	48	0.69
	0.34	51	0.75
	0.43	53	0.86
	0.53	65	0.87
	0.64	57	0.93
	0.75	60	0.94
	0.87	62	0.93
BA	0.08	19	0.45
	0.16	30	0.69
	0.25	38	0.78
	0.34	45	0.83
	0.43	50	0.71
	0.53	55	0.87
	0.64	55	0.83
	0.75	63	0.86
	0.87	56	0.79

2.3.2 Reaction Modeling with Oleic Acid

The following reaction model was developed:

1- Initiator thermal decomposition (refer to Equation 2.21)

$$I \xrightarrow{k_d} 2I \cdot \tag{2.21}$$

2- Initiation (refer to Equations 2.22 to 2.24)

$$I \cdot + A \xrightarrow{k_{iA}} R_A \cdot \tag{2.22}$$

$$I \cdot + B \xrightarrow{k_{iB}} R_B \cdot \tag{2.23}$$

$$I \cdot + O \xrightarrow{k_{iO}} R_O \cdot \tag{2.24}$$

Equation 2.21 depicts the initial decomposition of the initiator. In equations 2.22 and 2.23, the initiator, I, reacts with CLA (A) and Sty or BA (B) to form a reactive free radical, respectively. Equation 2.24 reflects the addition of the initiator to oleic acid (O), resulting in a resonance stabilized radical, R_O·. It should be noted that each oleic acid molecule has multiple sites for radical trapping via the alkene and allylic hydrogen atoms[10,26-30].

3- Propagation (refer to Equations 2.25 to 2.28)

$$R_A \cdot + A \xrightarrow{k_{pAA}} R_A \cdot \quad (2.25)$$

$$R_A \cdot + B \xrightarrow{k_{pAB}} R_B \cdot \quad (2.26)$$

$$R_B \cdot + A \xrightarrow{k_{pBA}} R_A \cdot \quad (2.27)$$

$$R_B \cdot + B \xrightarrow{k_{pBB}} R_B \cdot \quad (2.28)$$

Propagation is expected to occur normally and exclusively between CLA, Sty and BA. In this case, we are assuming terminal model copolymerization kinetics where R_A is a radical chain ending in A and R_B is a radical chain ending in B.

4- Termination (refer to Equations 2.29 to 2.32)

$$R_{m,A} \cdot + R_{n,A} \cdot \xrightarrow{k_{tAA}} P_{m+n} \quad (2.29)$$

$$R_{m,A} \cdot + R_{n,B} \cdot \xrightarrow{k_{tAB}} P_{m+n} \quad (2.30)$$

$$R_{m,B} \cdot + R_{n,A} \cdot \xrightarrow{k_{tBA}} P_{m+n} \quad (2.31)$$

$$R_{m,B}\cdot + R_{n,B}\cdot \xrightarrow{k_{tBB}} P_{m+n} \quad (2.32)$$

Termination is described via equations 2.29 through 2.32. The radicals, R, include a chain length (m and n) as well as the chain end (A and B). The equations depict termination by combination only, however it should be understood that termination by disproportionation is also included. Terminated polymer chains can also arise when oleic acid acts as a degradative chain transfer agent by abstracting/trapping electrons from the growing radical chains:

5- Oleic acid electron trapping (refer to Equations 2.33 and 2.34)

$$R_{m,A}\cdot + O \xrightarrow{k_{trAO}} P_m + R_O\cdot \quad (2.33)$$

$$R_{m,B}\cdot + O \xrightarrow{k_{trBO}} P_m + R_O\cdot \quad (2.34)$$

In equations 2.33 and 2.34, oleic acid abstracts/traps the electron from the growing polymer chain, R, resulting in a terminated polymer chain, P, and the oleic acid radical, $R_{O^{\cdot}}$. In equations 2.24, 2.33 and 2.34, above, the generated oleic acid radical, $R_{O^{\cdot}}$ is considered to be resonance stabilized. It therefore follows from the above mechanism that the following differential equations can be used to track the concentrations of CLA, Sty or BA, oleic acid, and polymer radical chains ending in A or B, over time (refer to Equations 2.35 to 2.40).

$$\frac{-d[A]}{dt} = k_{iA}[I\cdot][A] + k_{pAA}[R_A\cdot][A] + k_{pBA}[R_B\cdot][A] \quad (2.35)$$

$$\frac{-d[B]}{dt} = k_{iB}[I\cdot][B] + k_{pAB}[R_A\cdot][B] + k_{pBB}[R_B\cdot][B] \quad (2.36)$$

$$\frac{-d[O]}{dt} = k_{iO}[I\cdot][O] + k_{trAO}[R_A\cdot][O] + k_{trBO}[R_B\cdot][O] \quad (2.37)$$

$$\frac{-d[R_A\cdot]}{dt} = -k_{iA}[I\cdot][A] + k_{pAB}[R_A\cdot][B] - k_{pBA}[R_B\cdot][A] + k_{trAO}[R_A\cdot][O] + k_{tAA}[R_A\cdot]^2 + k_{tAB}[R_A\cdot][R_B\cdot] + k_{tBA}[R_B\cdot][R_A\cdot] \quad (2.38)$$

$$\frac{-d[R_B\cdot]}{dt} = -k_{iB}[I\cdot][B] - k_{pAB}[R_A\cdot][B] + k_{pBA}[R_B\cdot][A] + k_{trBO}[R_B\cdot][O] + k_{tBB}[R_B\cdot]^2 + k_{tAB}[R_A\cdot][R_B\cdot] + k_{tBA}[R_B\cdot][R_A\cdot] \quad (2.39)$$

$$[I\cdot] = [I]_0 e^{-k_d t} \quad (2.40)$$

An ordinary differential equation solver using a modified Runge Kutta method (ODE45) was run with Matlab. The Matlab file is included in the Supplementary Information. In order to simplify the model and decrease the computing time per simulation, the long chain hypothesis was invoked[39]. It is assumed that long polymer chains already exist after just a few seconds of reaction time. The CLA, oleic acid and saturated fatty acids also increased the viscosity of the reaction medium increasing the

mobility difference between small monomer molecules and polymer radical chains. In this scenario, the monomers are mainly consumed in the propagation reactions and the termination reactions can be neglected. It is usual practice to neglect the termination reactions for the purpose of copolymer composition predictions. Furthermore, preliminary simulations and parameter optimization led to the conclusion that those terms could be eliminated due to their negligible values compared to the propagation terms; this includes the initiation reactions for Sty, BA and oleic acid. It should be noted that the CLA initiation term, k_{iA}, was not negligible, suggesting that the CLA readily reacts with the initiator, more so than would Sty and BA. The rate constants of Sty and BA homopolymerization (k_{pBB}) were taken from the literature[40], all other rate constants were either negligible or were optimized. The optimized rate constants are shown in Table 2.2.

Table 2.2: Rate Constants (L/mol s) used with Matlab Model

	BA	**Sty**
k_{iA}	0.0003	0.0003
k_{pAA}	0.03	0.03
k_{pAB}	0.6	0.3
k_{pBA}	0.3	0.03
k_{pBB}	3024[40]	341[40]
k_{trAO}	1000	1000
k_{trBO}	2000	1000

The Matlab output was used to calculate copolymer composition and conversion. The copolymer composition is plotted versus conversion for 3 feeds with BA and 3 feeds with Sty in Figures 2.6 and 2.7, respectively.

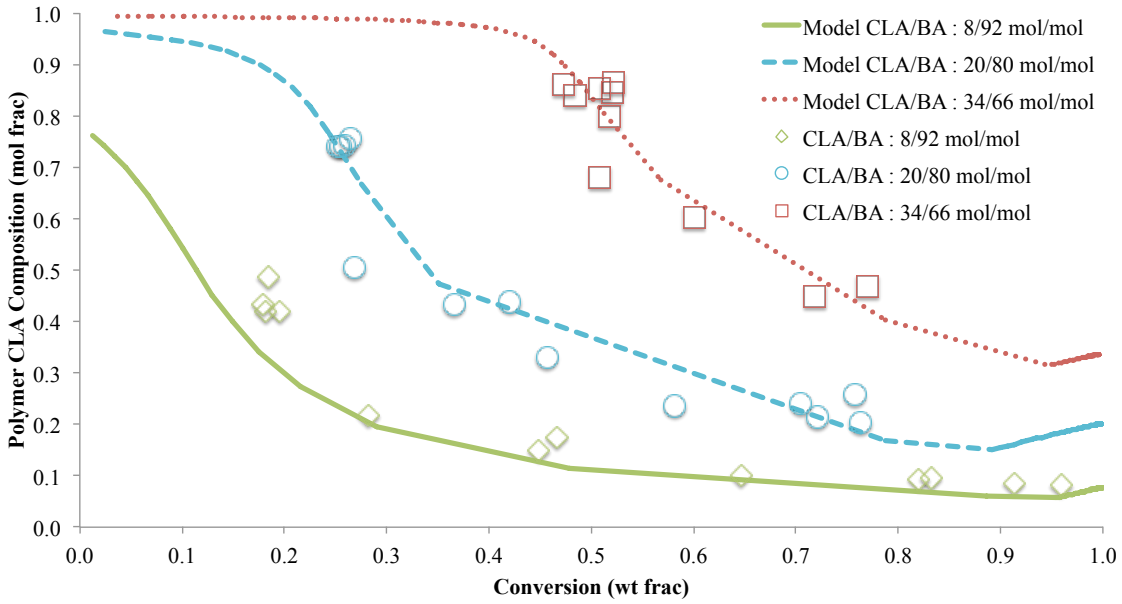

Figure 2.6: Copolymer composition versus conversion for CLA/BA copolymers

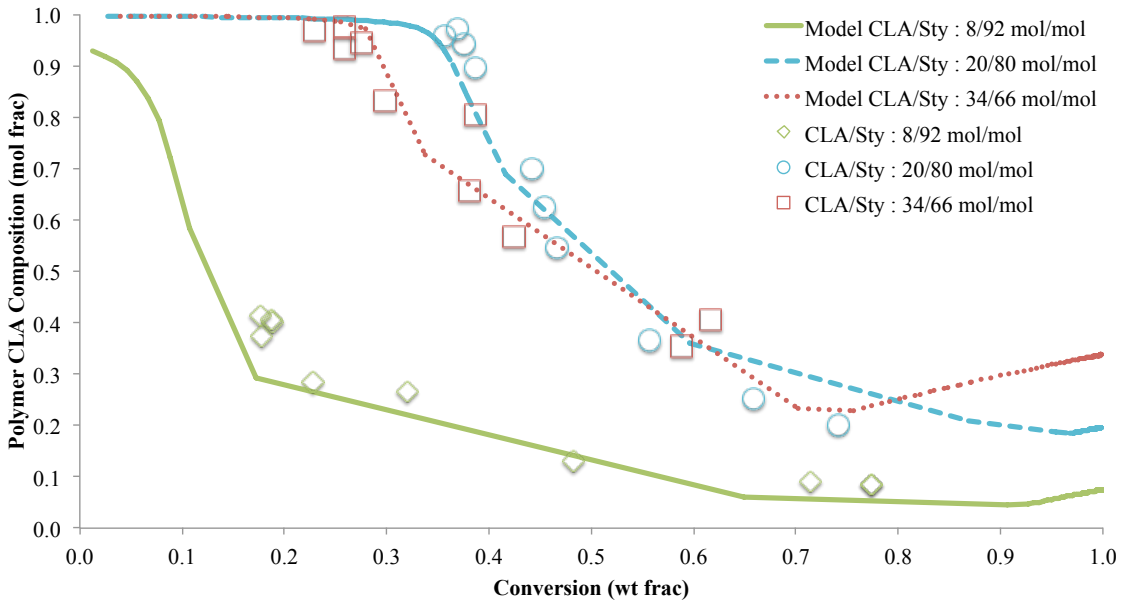

Figure 2.7: Copolymer composition versus conversion for CLA/Sty copolymers

In Figures 2.6 and 2.7, three distinct stages can be observed. In Stage 1, the dominant reaction is the production of CLA oligomers. This was confirmed with ^{1}H-NMR spectroscopy and GPC measurements. Stage 2 begins once the oleic acid has trapped a limited number of electrons. During Stage 2, Sty (or BA) dominate the propagation reactions over CLA, resulting in a sharp decrease in CLA content in the polymer, as observed in Figures 2.6 and 2.7. The beginning of Stage 3 is marked by the depletion of Sty (or BA) and the ongoing, yet slow, polymerization of CLA.

From each model (CLA/Sty and CLA/BA), the reactivity ratios were calculated. These are shown in Table 2.3 and were used to predict the copolymer composition as a function of CLA feed composition in the absence of impurities (see Figure 2.8). In both cases, when pure CLA is used, the model predicts very low CLA incorporation into the copolymer. In Figure 2.9, the copolymer composition as a function of CLA feed composition is shown when oleic acid is present in the reaction mixture. Thus, the

reactivity ratios indicate that CLA will not easily incorporate into the copolymer at a high rate. Rather, the presence of oleic acid allows for CLA homopolymerization at the beginning of the reaction. Only after the effect of oleic acid has abated, will "normal" copolymerization of the CLA and the co-monomer proceed. One can say that oleic acid was providing a beneficial CLA initiation or, on the other hand, a detrimental oligomer production, depending on the process needs. Finally, it should be noted that the alkene hydrogen of oleic acid was monitored with ^{1}H-NMR spectroscopy to ensure that oleic acid was not polymerizing; this was further confirmed using a mass balance approach.

Table 2.3: Reactivity ratios estimated from Matlab model

	Reactivity ratios
r_{CLA}	0.05
r_{BA}	10080
r_{CLA}	0.1
r_{Sty}	11367

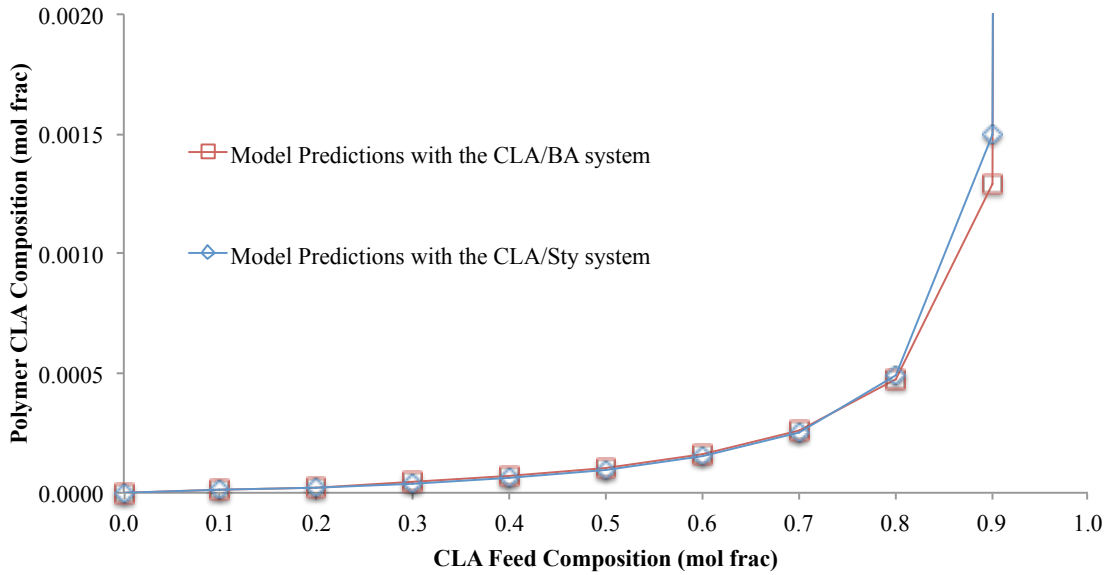

Figure 2.8: Prediction of Polymer CLA Composition from CLA feeds free of impurities

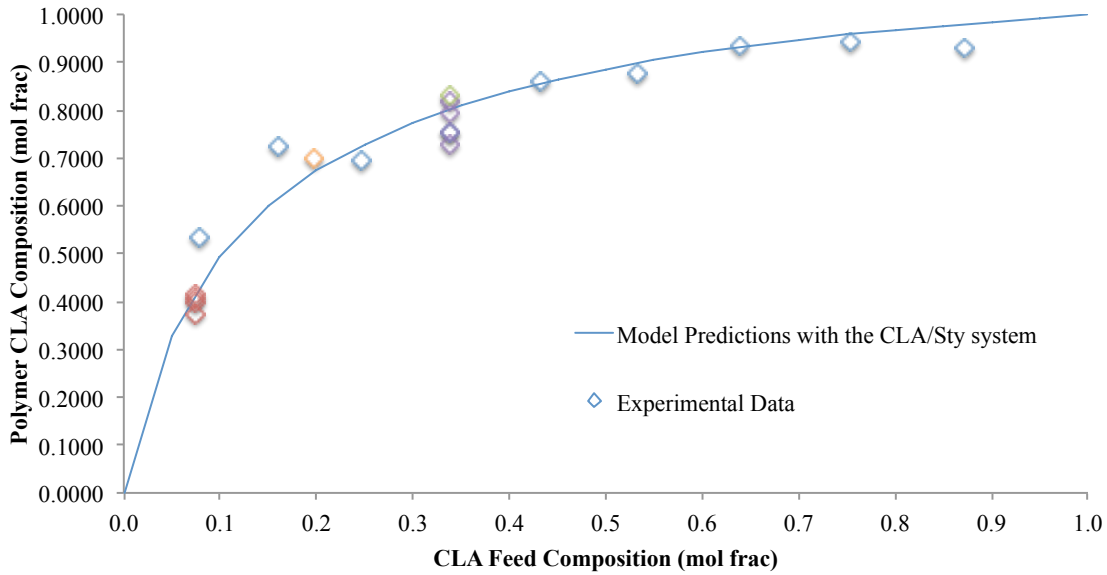

Figure 2.9: Predictions of Polymer CLA Composition from CLA feeds containing oleic acid

2.3.3 GPC Results

The CLA/Sty and CLA/BA copolymers were characterized for molecular weight and the results are shown in Figures 2.10 (CLA/Sty) and 2.11 (CLA/BA). In both figures, with an 8 mol% CLA feed concentration, relatively flat molecular weight profiles were observed. At higher CLA feed concentrations, the molecular weights are relatively quite low and show a steeply sloping increase with conversion. This is entirely consistent with the presence of greater amounts of oleic acid in the system. Only low molecular weight oligomers are formed at the early stages of the reaction, while the molecular weights increased significantly after the effect of oleic acid has abated. An increase in the oleic acid content in the feed produces more CLA-rich oligomers and reduces the overall molecular weight of the polymer while limiting the maximum conversion achieved after 24 h. It should be further noted that in Figure 2.10, for the CLA/Sty 20/80 mol/mol case, a larger concentration of oleic acid was noted in the feed due to a different lot (i.e., different supply bottle of CLA).

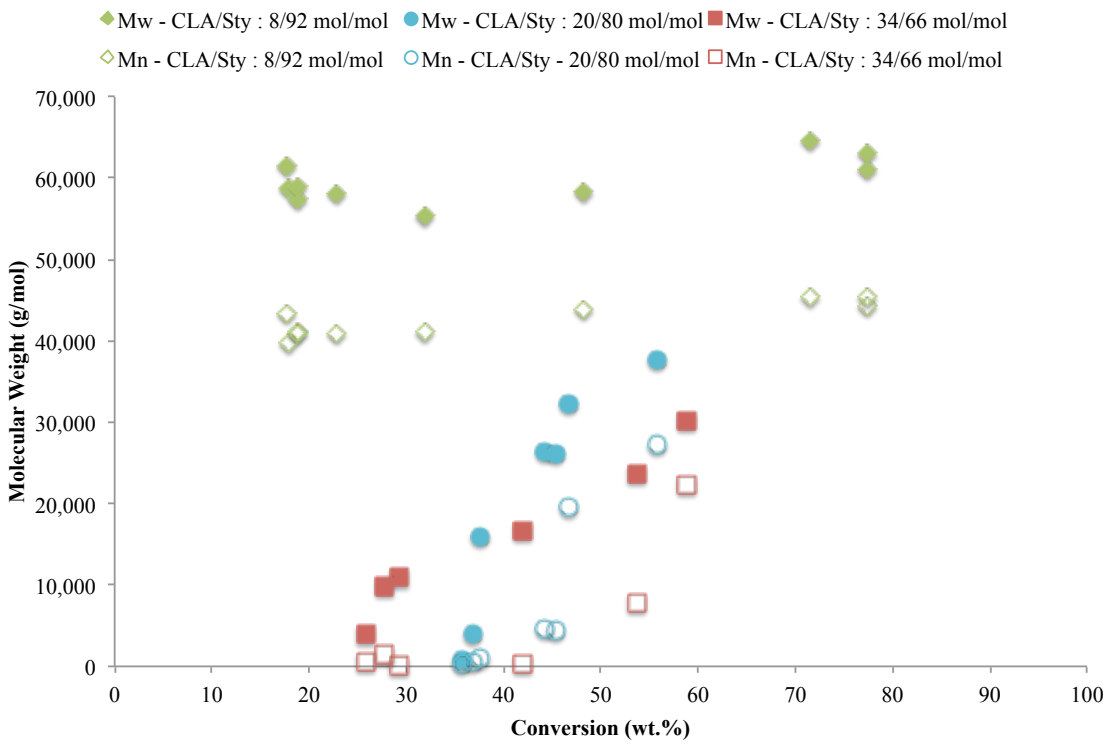

Figure 2.10: Weight-average molecular weight versus conversion for CLA-Sty polymer systems

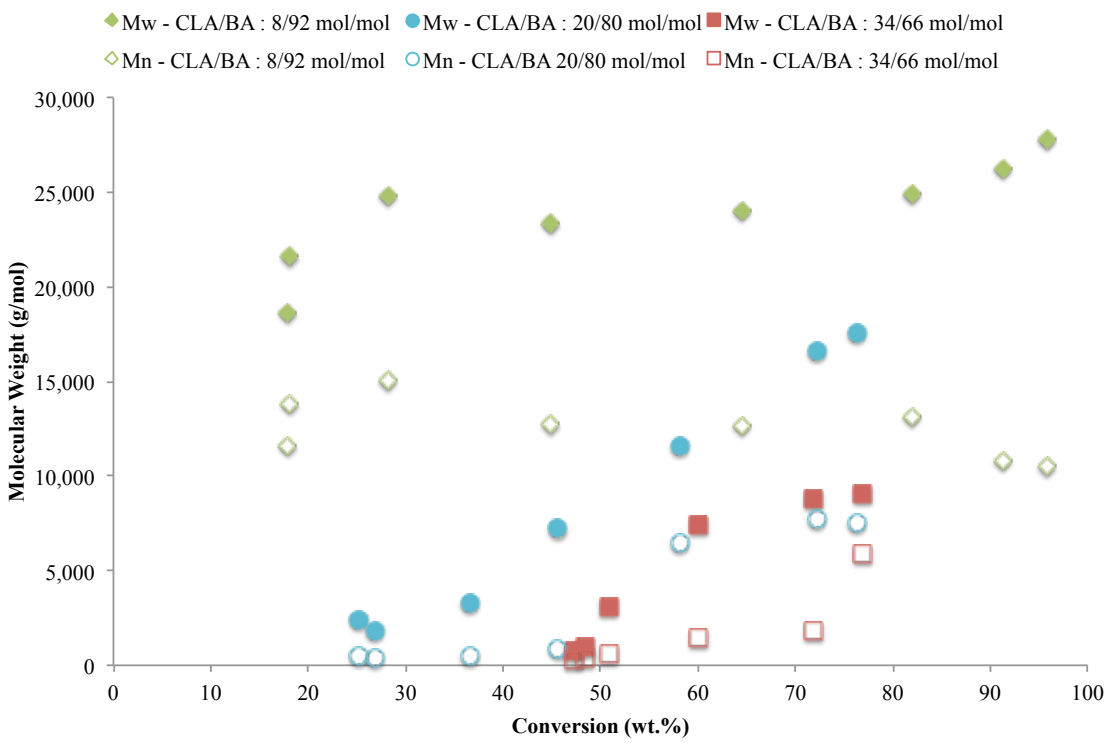

Figure 2.11: Weight-average molecular weight versus conversion for CLA-BA polymer systems

2.3.4 DSC Results

The CLA/Sty and CLA/BA copolymers were characterized for T_g. In all cases, only one inflexion point was found indicating a homogeneous distribution of the monomers bound inside the polymer matrix (see Supplementary information for example of DSC results). The DSC results for different copolymers are shown in Figure 2.12. A line was fitted through the experimental results for the CLA/Sty and CLA/BA systems, respectively. Both systems converge at high CLA copolymer composition at what can arguably be referred to as, a T_g of the CLA homopolymer of 5 ± 2°C.

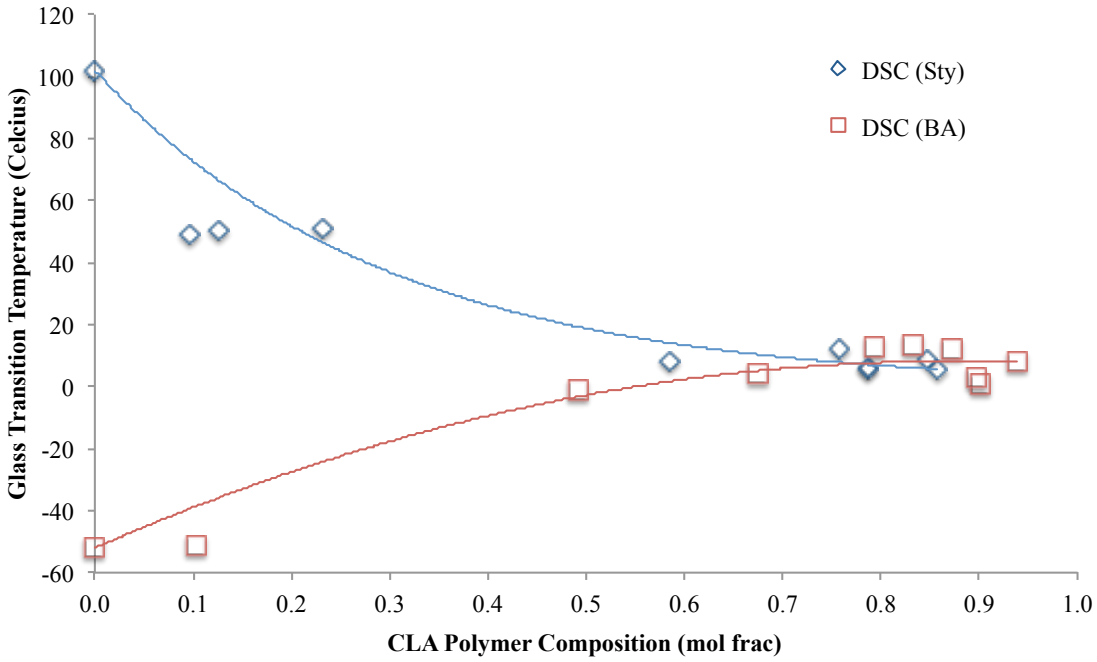

Figure 2.12: DSC results with line fitting for CLA/Sty and CLA/BA copolymers

2.4 Conclusions

High purity CLA is prohibitively expensive compared to monomers such as Sty and BA. However, a less costly version is available which contains a significant quantity of saturated fatty acids and oleic acid; this makes the CLA only moderately more expensive than Sty and BA. The saturated fatty acid does not react with any other components in the reaction mixture but the oleic acid plays a significant role in reaction kinetics without being incorporated into the copolymer.

In this work, CLA/Sty and CLA/BA bulk copolymerization reactivity ratios were estimated at 80°C and were shown to strongly favor the polymerization of Sty (or BA) during copolymerization. The strong effect on the reaction kinetics arose from the oleic

acid which abstracted freshly initiated radicals from the oligomers, followed by a resonance stabilized oleic acid radical. The reactions therefore undergo three reaction stages: first, oligomeric radical species containing primarily CLA (as opposed to Sty or BA) are deactivated by oleic acid, followed by the dominant polymerization of the co-monomer (i.e., Sty or BA), and ending with additional CLA consumption. Attempts at homopolymerizing CLA resulted only in the production of small oligomers.

Based on these findings, despite its interference with the polymerization kinetics, some oleic acid in the feed could be favourable towards the incorporation of CLA into the copolymer and could be used to adjust polymer molecular weight. In any case, the removal of oleic acid would make the cost of CLA copolymer production prohibitive. Finally, it should be noted that a relatively high incorporation of CLA into the copolymers was achieved; these were reported on a molar basis but because of its high molecular mass, the resulting copolymers contain a significant mass fraction of CLA.

2.5 Acknowledgements

The authors wish to gratefully acknowledge the financial support from the Natural Science and Engineering Research Council (NSERC) of Canada and Omnova Solutions (USA). Some GPC results were provided by Ms. Liana Martel.

2.6 References

1. M. A. Dubé, S. Salehpour, Applying the Principles of Green Chemistry to Polymer Production Industries. Macromol. React. Eng., first published online August 29th, 2013.
2. M. A. R. Meier, J. O. Metzger, U. S. Schubert, Plant oil renewable resources as green alternatives in polymer science. Chem. Soc. Rev., 2007, 36, 1788-1802.
3. F. S. Guner, Y. Yagci, A. T. Erciyes, Polymers from triglyceride oils. Prog. Polym. Sci., 2006, 31, 633-670.
4. German Federal Ministry of Food, Agriculture and Consumer Protection, Agency of Renewable Resources, http://www.fnr.de (last checked on September 20, 2013).
5. V. Sharma, P. P. Kundu, Addition polymers from natural oils – A review. Prog. Polym. Sci., 2006, 31, 983-1008.
6. Z. Liu, B. K. Sharma, S. Z. Erhan, From oligomers to molecular giants of soybean oil in supercritical carbon medium: 1. Preparation of polymers with lower molecular weight from soybean oil. Biomacromolecules, 2007, 8, 233-239.
7. B. Hazer, S. I. Demirel, M. Borcakli, M. S. Eroglu, M. Cakmak, B. Erman, Free radical crosslinking of unsaturated bacterial polyesters obtained from soybean oily acids. Polym. Bull., 2001, 46, 389-394.
8. F. Li, R. C. Larock, New Soybean oil – styrene – divinylbenzene thermosetting copolymers I. Synthesis and characterization. J. Appl. Polym. Sci., 2001, 80, 658-670.

9. F. Li, M. V. Hanson, R. C. Larock, Soybean oil – divinylbenzene thermosetting polymers: synthesis, structure, properties and their relationships. Polymer, 2001, 42, 1567-1579.

10. Z. S. Petrovic, Polyurethanes from vegetable oils. Polym. Rev., 2008, 48, 109-155.

11. R. P. Wool, S. P. Bunker, Polymer-solid interface connectivity and adhesion: Design of a bio-based pressure sensitive adhesive. J. Adhes., 2007, 83, 907-926.

12. C. M. Klapperich, R. P. Wool, L. Zhu, L. M. Bonnaillie, Proc. Biomater. Annu. Meeting, Pittsburgh, PA, 2006.

13. L. Zhu, R. P. Wool, Nanoclay reinforced bio-based elastomers: Synthesis and characterization. Polymer, 2006, 47, 8106-8115.

14. S. Cunnane, M. Anderson, Pure linoleate deficiency in the rat: influence of growth, accumulation of n-6 polyunsaturates, and (1-^{14}C) linoleate oxidation. J. Lipid Res., 1997, 38, 805-812.

15. D. J. Ruthig, K. A. Meckling-Gill, Both (n-3) and (n-6) fatty acids stimulate wound healing in the rat intestinal epithelial cell line. J. Nutr., 1999, 129, 1791-1798.

16. M. S. Manic, V. Najdanovic-Visak, M. Nunes da Ponte, Z. P. Visak, Extraction of free fatty acids from soybean oil using ionic liquids or poly(ethyleneglycol)s. AIChE J., 2011, 57, 1344-1355

17. J. Ogawa, s. Kishino, A. Ando, S. Sugimoto, K. Mihara, S. Shimizu, Production of Conjugated Fatty Acids by Lactic Acid Bacteria. J. Biosci. Bioeng., 2005, 100, 355-364.

18. G. L. Jin, S. H. Choi, H. G. Lee, Y. J. Kim, M. K. Song, Effects of Monensin and Fish Oil on Conjugated Linoleic Acid Production by Rumen Microbes in Holstein Cows Fed Diets Supplemented with Soybean Oil and Sodium Bicarbonate. Asian-Aust. J. Anim. Sci., 2008, 21, 1728-1735.

19. V. P. Jain, T. Tokle, S. Kelkar, A., Proctor, Effect of the Degree of Processing on Soy Oil Conjugated Linoleic Acid Yields. J. Agric. Food Chem., 2008, 56, 8174-8178.

20. R. Gangidi, A. Proctor, Photochemical production of conjugated linoleic acid from soybean oil. Lipids, 2004, 39, 577-582.

21. R. Gangidi, A. Proctor, Photochemical production of conjugated linoleic acid from soybean oil. Lipids, 2004, 39, 577-582.

22. N.F.L. Machado, L.A.E. Batista de Carvalho, J.C. Otero, M.P.M. Marques, The auto-oxidation process in linoleic acid screened by Raman spectroscopy. J. Raman. Spectrosc., 2012, 43, 1991-2000.

23. E. Keles, B. Hazer, Auto-oxidized Polyunsaturated Oils/Oily Acids: Post-it Applications and Reactions with Fe(III) and Adhesion Properties. Macromol. Symp., 2008, 269, 154-160.

24. B. Cakmakli, B. Hazer, S. Acikgoz, M. Can, F.B. Comert, PMMA-Multigraft Copolymers Derived from Linseed Oil, Soybean Oil, and Linoleic Acid: Protein Adsorption and Bacterial Adherence. J. Appl. Polym. Sci., 2007, 105, 3448-3457.

25. C. Vilela, R. Rua, A.J.D. Silvestre, A. Gandini, Polymers and copolymers from fatty-acid-based monomers. Ind. Crops. Products, 2010, 32, 97-104.

26. D. H. Hewitt, F. Armitage, Styrene copolymers in surface coatings. J. Oil Colour Chem. Assoc., 1946, 29, 109-128.

27. S. S. Narine, X. Kong, Bailey's Industrial Oil and Fat Products, 6th Edition, 6th Volume Set, Chapter 8: Vegetable Oils in the Production of Polymers and Plastics, John Wiley and Sons Inc., Edmonton 2005, p. 279-306.

28. A. Eshuis, H. J. Leendertse, D. thoenes, Surfactant-free emulsion polymerization of styrene using cross-linked seed particles. Colloid Polym. Sci., 1991, 269, 1086-1089.

29. K. S. Jeong et al., Enhanced Mobility-Lifetime Products in PbS Collodial Quantum Dot Photovoltaics. ACS Nano, 2012, 6, 89-99.

30. R. C. Laible, Allyl Polymerizations. Chem. Rev., 1958, 58, 807-843.

31. M. A. Dubé**,** E. Saldivar-Guerra, I. Zapata-Gonzalez, Handbook of Polymer Synthesis, Characterization and Processing,_ Chapter 6: Copolymerization (eds E. Vivaldo-Lima and E. Saldivar-Guerra), John Wiley and Sons Inc., Hoboken NJ, USA 2013, p. 105-125.

32. P. W. Tidwell, G. A. Mortimer J. Polym. Sci., 1965, 3, 369-387.

33. M. A. Dubé**,** J. B. P. Soares, A. Penlidis, A. E. Hamielec, Mathematical modelling of multicomponent chain-growth polymerizations in batch, semi-batch and continuous reactors: A Review. Ind. Eng. Chem. Res., 1997, 36, 966-1015.

34. R. R. Chance, S. P. Baniukiewicz, D. Mintz, G. Ver Strate, N. Hadjichristidis, Characterization of Low-Molecular-Weight Polymers: Failure of Universal Calibration in Size Exclusion Chromatography. Int. J. Polymer Analysis & Characterization, 1995, 1, 3-

35. K. Antolin, J-P Lamps, P. Rempp, Y. Gnanou, Synthesis of poly9t-butyl acrylate) macromonomers. Polymer, 1990, 31, 967-970.

36. L. A. Polic, T. A. Duever, A. Penlidis, Case studies and literature review on the estimation of copolymerization reactivity ratios. J. Polym. Sci., Part A: Polym. Chem., 1998, 36, 813-822.

37. N. Kazemi, T. A. Duever, A. Penlidis, A powerful estimations scheme with error-in-variable-model for nonlinear cases: Reactivity ratio estimation examples. Comput. Chem. Eng., 2013, 48, 200-208.

38. N. Kazemi, T. A. Duever, A. Penlidis, Design of Experiments for Reactivity Ratio Estimation in Multicomponent Polymerizations Using the Error-In-Variables Approach. Macromol. Theory Simul., 2013, 22, 261-272.

39. N. A. Dotson, R. Galvan, R. L. Laurence, M. Tirrell, Polymerization Process Modeling, John Wiley and Sons Inc., New York NY, USA 1996, p. 134-135.

40. J. Gao, A. Pendilis, Mathematical modeling and computer simulator/database for emulsion polymerizations. Prog. Polym. Sci., 2002, 27, 403-535.

Chapter 3 – Paper on Bulk Terpolymerization of CLA

Sust. Chem. Eng., 2015, DOI: 10.102/acssuschemeng.5b01106.

Bulk Terpolymerization of Conjugated Linoleic Acid with Styrene and Butyl Acrylate

Stéphane Roberge and Marc A. Dubé*

Department of Chemical and Biological Engineering,

Centre for Catalysis Research and Innovation, University of Ottawa

161 Louis Pasteur Pvt., Ottawa, ON, K1N 6N5 Canada

* *Marc.Dube@uOttawa.ca*

Abstract

Free radical bulk terpolymerizations of conjugated linoleic acid (CLA), styrene (Sty) and butyl acrylate (BA) were performed at 80°C. Terpolymers were characterized for composition, conversion, molecular weight and glass transition temperature. A pseudo-kinetic model was developed for the prediction of terpolymer composition and validated with experimental data. One impurity commonly found in CLA, oleic acid, was shown to influence the reaction kinetics significantly. The ability of oleic acid to trap electrons results in the formation of oligomeric species at the beginning of the reaction; after the oleic acid is consumed, the reaction kinetics proceed normally.

3.1 Introduction

A major principle in green chemistry is the use of renewable and sustainable raw materials which could possibly introduce elements of degradability, reduced product toxicity and lower gross energy requirements in polymer production.[1,2] The substitution of fossil fuel based monomers with renewable monomers such as plant oils is one interesting option for sustainable polymer production. Plant oils consist of triglycerides with a glycerol backbone and three fatty acid chains The steric effect of triglyceride hinders its use as a polymer building block,[3,4] but the smaller, less bulky fatty acid chains making up its structure are suitable candidates for polymerization. Fatty acid-based polymers have been shown to be biodegradable in soil,[5,6] biocompatible to human tissue and blood cells[5,7] and non-toxic.[7] In their non-conjugated form, these fatty acids could suffer from degradative chain transfer whereas the conjugated forms could be copolymerized.[8] Since conjugated linoleic acid (CLA) isomers (see Figure 3.1) can be produced simply and inexpensively from soybean oil photo-isomerization,[9] they were chosen for free radical polymerizations. As previously reported,[10] the cost of pure CLA is prohibitive and an affordable alternative containing non-conjugated oleic acid (see Figure 3.1) and saturated fatty acid can be used. It is notable that oleic acid has been used as a surfactant replacement in the emulsion homopolymerization of styrene without any signs of copolymerization.[11] Oleic acid is also known for its electron trapping ability[12] where the oleic acid radicals are resonance stabilized.[13] The saturated fatty acid would also not be expected to polymerize as it does not contain any vinyl groups required for free-radical polymerization. Alternatively, one could functionalize the CLA but this may increase material costs.[14] In this study, low-cost CLA containing oleic acid and saturated

fatty acids was used to produce terpolymers with styrene (Sty) and butyl acrylate (BA), to gain a better understanding of the terpolymerization kinetics. Copolymers of Sty and BA are commonly used as binding agents in coatings as well as in adhesive formulations. The addition of CLA to the copolymer formulation serves to reduce the amount of non-renewable BA in the formulation, therefore resulting in a terpolymer with increased amounts of a renewable component. Our eventual goal is to produce an adhesive formulation with a significant percentage of bio-sourced material.

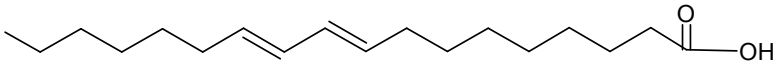

Conjugated linoleic acid

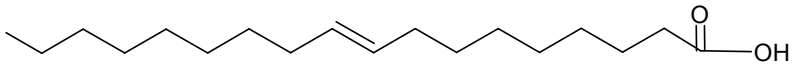

Oleic acid

Figure 3.1: Conjugated linoleic acid and oleic acid molecules

3.2 Experimental

3.2.1 Materials

CLA (Penta, 74% CLA, 13% oleic acid, 13% saturated fatty acid) was chosen for practical considerations related to industrial applications and was used without further purification. The other monomers, styrene (Sty, Sigma-Aldrich, 99%) and butyl acrylate (BA, Sigma-Aldrich, 99%) were purified to remove the inhibitor, hydroquinone. The

initiator, benzoyl peroxide (BPO, Sigma-Aldrich, 100%) was used without further purification. All solvents used for sample work-up and characterizations (e.g., methanol (Fisher, 99.9%), acetone (Fisher, 99%), tetrahydrofuran (THF, Fisher, 99.9%) and chloroform-d (Cambridge Isotope Laboratories, 99.8%) were also used as received.

3.2.2 Polymerizations.

Bulk polymerizations were performed at 80 °C in glass ampoules with 1 cm outside diameter and 17 cm in length. Roughly 2-3 grams of reaction mixture (monomers and initiator) were poured in each ampoule. The concentration of initiator, BPO, was 2 phm (parts per hundred parts monomer on a mass basis) for all experiments. To remove oxygen, three freeze-pump-thaw cycles were performed on each ampoule before flame-sealing them. The sealed ampoules were then submerged in a preheated oil bath for a known amount of time before being removed and quenched in an ice bath for 10 min. All samples were analyzed for conversion and copolymer composition while selected samples were analyzed for molecular weight and glass transition temperature (T_g). As shown in Table 1, eight different feed compositions were used in this study (f_i is mole fraction of monomer i in the feed). For the most part, Sty monomer feed concentrations were kept to about 10 mol% while varying the BA/CLA monomer ratio. This was done to achieve a particular T_g value for future adhesive applications. An additional run (i.e., Run 8) was added at a higher Sty content to provide a broader composition range.

Table 3.1. Feed composition, final polymer composition and glass transition temperature for bulk terpolymerizations

Run	Feed mole fraction			Polymer mole fraction			T_g
	f_{CLA}	f_{Sty}	f_{BA}	F_{CLA}	F_{Sty}	F_{BA}	(°C)
1	0.0767	0.103	0.822	0.26	0.13	0.61	-42
2	0.156	0.105	0.740	0.37	0.16	0.48	-40
3	0.234	0.108	0.652	0.42	0.18	0.40	-39
4	0.329	0.111	0.560	0.47	0.19	0.34	-44
5	0.424	0.116	0.461	0.52	0.20	0.28	-49
6	0.524	0.120	0.356	0.58	0.20	0.23	-49
7	0.746	0.127	0.127	0.68	0.22	0.11	-53
8	0.076	0.821	0.103	0.16	0.84	0.00	+55

3.2.3 Characterization

Gravimetry and ^{1}H-NMR Spectroscopy

The overall and individual monomer conversions were measured by combining both gravimetry (based on total polymer) and proton nuclear magnetic resonance ^{1}H-NMR spectroscopy. ^{1}H-NMR spectroscopy was used to subtract any unreacted components which were difficult to fully separate from the final product (e.g., saturated fatty acid, unreacted CLA). At the same time, gravimetry was necessary to account for the volatile components (i.e., Sty and BA) that would be separated from the reaction mixture prior to ^{1}H-NMR analysis. The reaction mixture (~3 g) was first dissolved in acetone (~10 mL) then ~125 mL of methanol was used to precipitate the polymer. The soluble portion of the sample mixture was decanted and the polymer/methanol samples

were left to dry in a fumehood for ~7 days, then under vacuum for ~7 days until a constant weight was reached. The composition from the polymer/methanol samples (via ^{1}H-NMR spectroscopy) was used to perform a mass balance and correct the conversion calculation for any oligomeric species lost in the process.

^{1}H-NMR was used to determine the cumulative terpolymer composition. Analyses were carried out at room temperature in deuterated chloroform (~2% w/v) with a Bruker AVANCE III 400 Fourier transform ^{1}H-NMR spectrometer. The acquisition time was 4.6 seconds and 16 scans were performed per sample. A detailed presentation of peak assignments and calculation procedure for polymer composition was reported previously[10] where the polymer composition was estimated from the areas under specific absorption peaks. A sample spectrum of poly(CLA/Sty/BA) is shown in Figure 3.2 where the phenyl groups of Sty units bound in the polymer (peaks m-n) are located at ~6.2-7.2 ppm, the -OCH_2- groups of BA units in the polymer (peak t) are located at ~4.0 ppm and the methyl groups of CLA units in the polymer are located at ~0.9 ppm (peak K). An isolated alkene hydrogen peak is located at ~5.9 ppm for CLA monomer (peak G). This information was crucial for calculating the polymer composition because the methyl group of CLA polymer (peak K) was overlapped by the peaks of most of the other components. Additionally, an alkene hydrogen peak (peak F) is located at ~5.4 ppm which represents both a single alkene in the CLA monomer and two alkene hydrogens surrounding the double bond in oleic acid (see Figure 3.1). Equations developed for copolymer composition estimation of CLA-containing copolymers[10] were extended for the estimation of terpolymer composition. These equations also served to provide a measure of conversion on a weight basis.

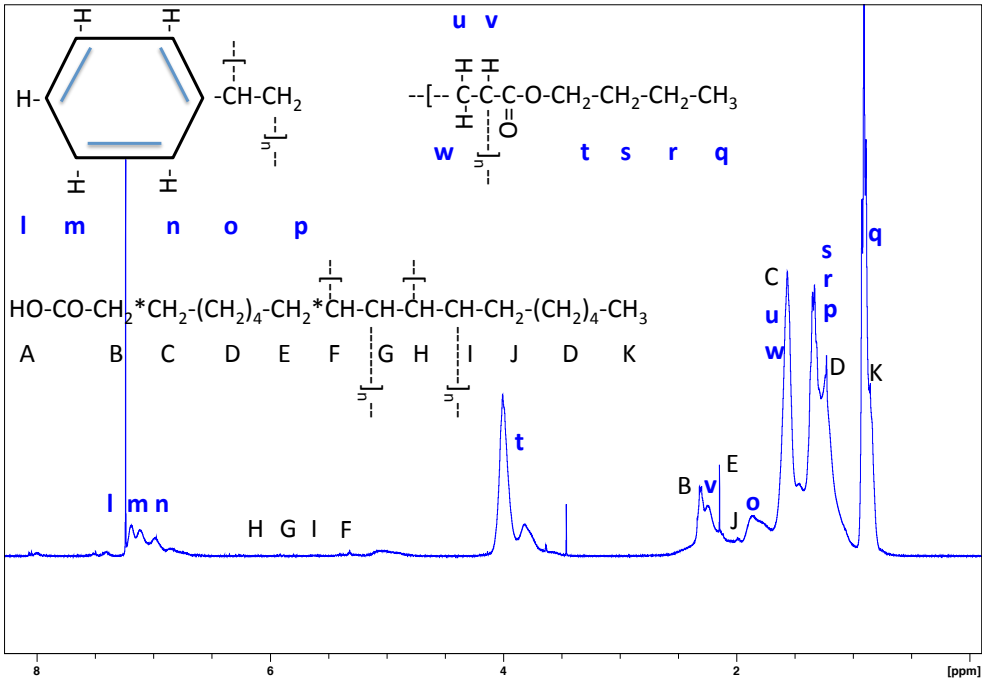

Figure 3.2: ^{1}H-NMR spectrum of CLA/Sty/BA: 26/13/61 mol/mol/mol terpolymer in $CDCl_3$.

Gel Permeation Chromatography (GPC)

The cumulative number- and weight-average molecular weights of the polymers were measured using an Agilent/Wyatt gel permeation chromatography (GPC) system equipped with fractionating columns installed in series (pore sizes of 10^4, 10^5 and 10^6 Angstroms covering molecular weight ranges of 4,000 to 500,000, 10,000 to 2,000,000 and 200,000 to 10,000,000, respectively), a multi-angle light scatterer (MALS), a viscometer (VISC) and a refractive index detector (DRI) at 25 ^{o}C. Tetrahydrofuran (THF) was the mobile phase and delivered at 1.0 mL/min. The MALS detector provides an absolute molecular weight measurement without the use of calibration. However, the

measurement is dependent on the refractive index increment (dn/dc) value used. The usual approach of using a weighted dn/dc value based on individual dn/dc values for the homopolymer of each component was employed. The dn/dc values used were 0.187 for poly(Sty)[15] and 0.056 for poly(BA).[16] Because of the lack of a dn/dc value for poly(CLA), a value was calculated from a terpolymer sample. The dn/dc of a CLA/Sty/BA = 26/13/61 mol/mol/mol terpolymer was measured as 0.070. From that value, the dn/dc of poly(CLA) was estimated to be 0.064, using a weighted average based on the terpolymer composition. The dn/dc was adjusted in this way for each terpolymer composition.

Differential Scanning Calorimetry (DSC)

The T_g of the polymers was measured with a TA Instruments Model Q1000 dynamic scanning calorimeter (DSC) equipped with a refrigerated cooling system and a nitrogen purge. The DSC was calibrated using empty cell, indium, sapphire and polystyrene standards. The sample (~7 mg of dry polymer) was cooled to -80 ^{o}C and then heated at a rate of 10^{o}C/min until the sample reached 110 ^{o}C. The T_g was calculated from the inflection point in the reversed heat flow curve.

3.3 Results and Discussion

As previously reported,[10] mass balances via ^{1}H-NMR spectroscopy demonstrated that the oleic acid and the saturated fatty acids were not incorporated into the polymer chains. The detected alkene hydrogens from CLA and oleic acid were used to make this determination. The oleic acid plays the role of an electron trap, thus deactivating free

radicals either from the initiator or oligomeric species in the reaction mixture.[10-13] It was hypothesized that the long chains (9 carbons) on each side of the oleic acid double bond (see Figure 3.1) formed a resonance stabilized molecule after electrons were trapped at the alkene and allylic hydrogens. However, the oleic acid has a limited capacity for electron trapping. Furthermore, the reactions appear to start with a fast production of CLA-rich oligomers until the effect of oleic acid has abated, followed by the dominant polymerization of the co-monomers (i.e., Sty or BA) and ending with a slow CLA consumption in an increasingly viscous reaction medium. The presence of oleic acid was shown to encourage CLA incorporation while lowering copolymer molecular weight.

Overall monomer conversions were calculated from gravimetry coupled with some ^{1}H-NMR spectroscopy analyses. The conversion results shown in Figures 3.3 and 3.4 demonstrate a rapid initial reaction rate consistent with a fast CLA-rich oligomer production; most conversions exceeded 10 wt.% after only 15 min of reaction time. This effect increased with increasing CLA in the feed. The inflection point (the time when the slope of the conversion vs. time curve started to decrease) indicates the moment when most of the oleic acid has been "consumed" or rather, deactivated, and a slower mechanism dominated by the consumption of Sty and BA takes place. Reactions were not conducted beyond 500 min for practical reasons and due to the likely approach of a dead-end polymerization due to depleting initiator concentration.

Evidence on the formation of oligomers was first obtained via the gravimetric measurement process, wherein a significant fraction of low molecular weight polymer (i.e., oligomer) was dissolved and decanted prior to sample drying. As discussed earlier, the decanted liquid was analyzed by ^{1}H-NMR spectroscopy and oligomers were

identified. Molecular weight analysis of the decanted liquid and the separated polymer, both showed significant low molecular weight oligomer fractions.

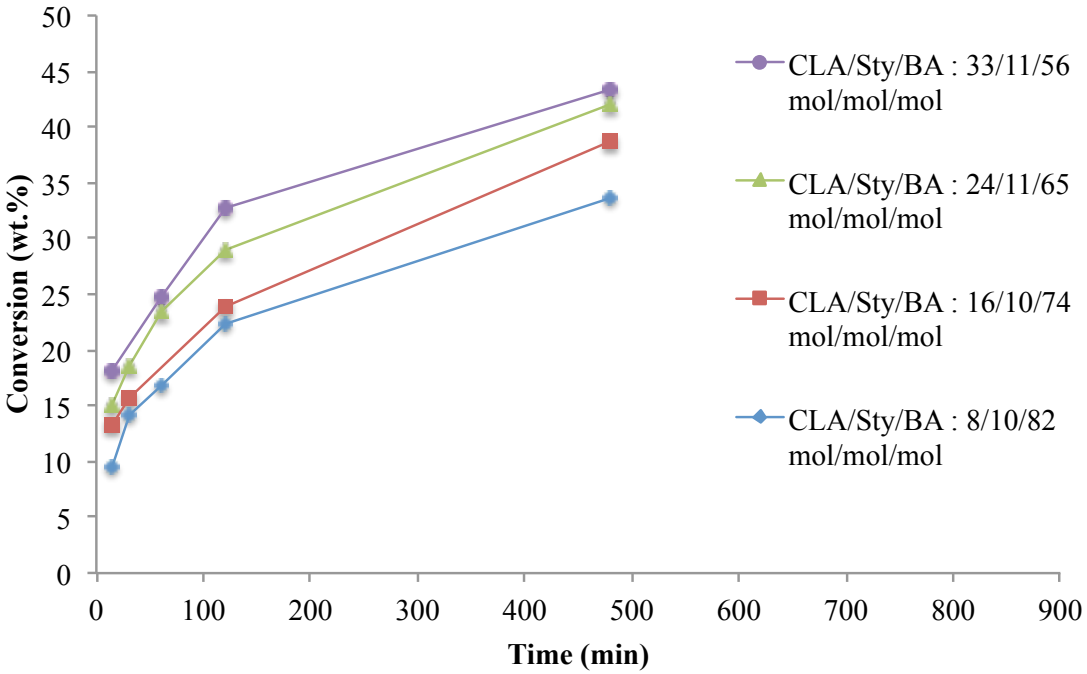

Figure 3.3: Terpolymer conversion versus time (higher BA concentration)

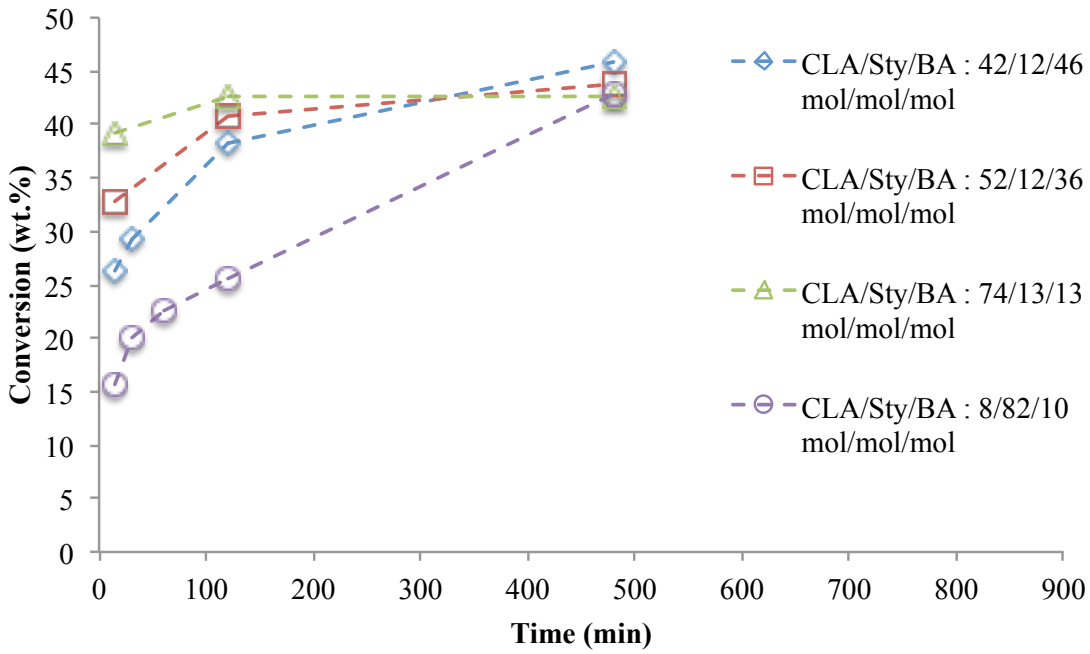

Figure 3.4: Terpolyer conversion versus time (lower BA concentration)

3.3.1 Reaction modeling with oleic acid

A reaction model was previously developed to incorporate the effect of oleic acid's ability to trap electrons for the copolymer systems CLA/BA and CLA/Sty.[10] Herein, we extend the model to the terpolymerization system. It should be noted that no further parameter estimation was necessary; all parameter values previously optimized for the copolymer systems were used as is. It should be further noted that the goal here is to model the terpolymer composition (vs. conversion) only and not the conversion vs. time or molecular weight profiles. This results in a number of simplifications to the model as discussed below.

Initiator thermal decomposition (refer to Equation 3.1)

$$I \xrightarrow{k_d} 2I \cdot \tag{3.1}$$

Initiation (refer to Equations 3.2 to 3.5)

$$I\cdot + 1 \xrightarrow{k_{i1}} R_1\cdot \quad (3.2)$$

$$I\cdot + 2 \xrightarrow{k_{i2}} R_2\cdot \quad (3.3)$$

$$I\cdot + 3 \xrightarrow{k_{i3}} R_3\cdot \quad (3.4)$$

$$I\cdot + O \xrightarrow{k_{iO}} R_O\cdot \quad (3.5)$$

Equation 3.1 depicts the initial decomposition of the initiator. In equations 3.2 to 3.4, the initiator, I, reacts with CLA (1), Sty (2) and BA (3) to form a reactive free radical, respectively. Equation 3.5 reflects the addition of the initiator to oleic acid (O), resulting in a resonance stabilized radical, R_{O}·. It should be noted that each oleic acid molecule has multiple sites for electron trapping via the alkene and allylic hydrogen atoms.[4,8,10-13,17]

Propagation (refer to Equations 3.6 to 3.14)

$$R_1\cdot + 1 \xrightarrow{k_{p11}} R_1\cdot \quad (3.6)$$

$$R_1\cdot + 2 \xrightarrow{k_{p12}} R_2\cdot \quad (3.7)$$

$$R_1\cdot + 3 \xrightarrow{k_{p13}} R_3\cdot \quad (3.8)$$

$$R_2\cdot + 1 \xrightarrow{k_{p21}} R_1\cdot \quad (3.9)$$

$$R_2\cdot + 2 \xrightarrow{k_{p22}} R_2\cdot \quad (3.10)$$

$$R_2\cdot + 3 \xrightarrow{k_{p23}} R_3\cdot \quad (3.11)$$

$$R_3\cdot + 1 \xrightarrow{k_{p31}} R_1\cdot \quad (3.12)$$

$$R_3\cdot + 2 \xrightarrow{k_{p32}} R_2\cdot \quad (3.13)$$

$$R_3\cdot + 3 \xrightarrow{k_{p33}} R_3\cdot \quad (3.14)$$

Propagation is expected to occur normally and exclusively between CLA, Sty and BA. In this case, we are assuming terminal model terpolymerization kinetics where R_1 is a radical chain ending in CLA, R_2 is a radical chain ending in Sty and R_3 is a radical chain ending in BA.

Termination (refer to Equations 3.15 to 3.23)

$$R_{m,1}\cdot + R_{n,1}\cdot \xrightarrow{k_{t11}} P_{m+n} \tag{3.15}$$

$$R_{m,1}\cdot + R_{n,2}\cdot \xrightarrow{k_{t12}} P_{m+n} \tag{3.16}$$

$$R_{m,1}\cdot + R_{n,3}\cdot \xrightarrow{k_{t13}} P_{m+n} \tag{3.17}$$

$$R_{m,2}\cdot + R_{n,1}\cdot \xrightarrow{k_{t21}} P_{m+n} \tag{3.18}$$

$$R_{m,2}\cdot + R_{n,2}\cdot \xrightarrow{k_{t22}} P_{m+n} \tag{3.19}$$

$$R_{m,2}\cdot + R_{n,3}\cdot \xrightarrow{k_{t23}} P_{m+n} \tag{3.20}$$

$$R_{m,3}\cdot + R_{n,1}\cdot \xrightarrow{k_{t31}} P_{m+n} \tag{3.21}$$

$$R_{m,3}\cdot + R_{n,2}\cdot \xrightarrow{k_{t32}} P_{m+n} \tag{3.22}$$

$$R_{m,3}\cdot + R_{n,3}\cdot \xrightarrow{k_{t33}} P_{m+n} \tag{3.23}$$

Termination is described via equations 3.15 through 3.23. The radicals, R, include a chain length (m and n) as well as the chain end (1, 2, and 3). The equations depict termination by combination only, however it should be understood that termination by disproportionation is also included. By invoking the long-chain hypothesis, the termination equations eventually become negligible compared to other terms in the

composition model. Terminated polymer chains can also arise when oleic acid acts as a degradative chain transfer agent by trapping electrons from the growing radical chains.

Oleic acid electron trapping (refer to Equations 3.24 and 3.26)

$$R_{m,1}\cdot + O \xrightarrow{k_{tr1O}} P_m + R_O\cdot \tag{3.24}$$

$$R_{m,2}\cdot + O \xrightarrow{k_{tr2O}} P_m + R_O\cdot \tag{3.25}$$

$$R_{m,3}\cdot + O \xrightarrow{k_{tr3O}} P_m + R_O\cdot \tag{3.26}$$

In equations 3.24 to 3.26, oleic acid traps the electron from the growing polymer chain, R, resulting in a terminated polymer chain, P, and the oleic acid radical, $R_O\cdot$. In equations 3.5, 3.24, 3.25, and 3.26 above, the generated oleic acid radical, $R_O\cdot$, is considered to be resonance stabilized. It therefore follows from the above mechanism that the following differential equations can be used to track the concentrations of CLA (1), Sty (2), BA (3), oleic acid (O), and polymer radical chains ending in 1, 2, and 3 over time (refer to Equations 3.27 to 3.34).

$$\frac{-d[1]}{dt} = k_{i1}[I\cdot][1] + k_{p11}[R_1\cdot][1] + k_{p21}[R_2\cdot][1] + k_{p31}[R_3\cdot][1] \tag{3.27}$$

$$\frac{-d[2]}{dt} = k_{i2}[I\cdot][2] + k_{p12}[R_1\cdot][2] + k_{p22}[R_2\cdot][2] + k_{p32}[R_3\cdot][2] \tag{3.28}$$

$$\frac{-d[3]}{dt} = k_{i3}[I\cdot][3] + k_{p13}[R_1\cdot][3] + k_{p23}[R_2\cdot][3] + k_{p33}[R_3\cdot][3] \tag{3.29}$$

$$\frac{-d[O]}{dt} = k_{iO}[I\cdot][O] + k_{tr1O}[R_1\cdot][O] + k_{tr2O}[R_2\cdot][O] + k_{tr3O}[R_3\cdot][O] \tag{3.30}$$

$$\frac{-d[R_1\cdot]}{dt} = -k_{i1}[I\cdot][1] + k_{p12}[R_1\cdot][2] + k_{p13}[R_1\cdot][3] - k_{p21}[R_2\cdot][1] - k_{p31}[R_3\cdot][1] + k_{t11}[R_1\cdot]^2 + k_{t12}[R_1\cdot][R_2\cdot] + k_{t13}[R_1\cdot][R_3\cdot] + k_{t21}[R_2\cdot][R_1\cdot] + k_{t31}[R_3\cdot][R_1\cdot] + k_{tr1O}[R_1\cdot][O] \quad (3.31)$$

$$\frac{-d[R_2\cdot]}{dt} = -k_{i2}[I\cdot][2] - k_{p12}[R_1\cdot][2] + k_{p21}[R_2\cdot][1] + k_{p23}[R_2\cdot][3] - k_{p32}[R_3\cdot][2] + k_{t12}[R_1\cdot][R_2\cdot] + k_{t21}[R_2\cdot][R_1\cdot] + k_{t22}[R_2\cdot]^2 + k_{t23}[R_2\cdot][R_3\cdot] + k_{t32}[R_3\cdot][R_2\cdot] + k_{tr2O}[R_2\cdot][O] \quad (3.32)$$

$$\frac{-d[R_3\cdot]}{dt} = -k_{i3}[I\cdot][3] - k_{p13}[R_1\cdot][3] - k_{p23}[R_2\cdot][3] + k_{p31}[R_3\cdot][1] + k_{p32}[R_3\cdot][2] + k_{t13}[R_1\cdot][R_3\cdot] + k_{t23}[R_2\cdot][R_3\cdot] + k_{t31}[R_3\cdot][R_1\cdot] + k_{t32}[R_3\cdot][R_2\cdot] + k_{t33}[R_3\cdot]^2 + k_{tr3O}[R_3\cdot][O] \quad (3.33)$$

$$[I\cdot] = [I]_0 e^{-k_d t} \quad (3.34)$$

An ordinary differential equation solver using a modified Runge Kutta method (ODE45) was run with Matlab and the code is available as supporting information on-line. In order to simplify the model and decrease the computing time per simulation, the long chain hypothesis was invoked.[18] As a result, the reaction terms containing termination parameters in equations 3.31-3.33 were eliminated. Previous simulations and parameter optimization for the copolymer systems CLA/BA and CLA/Sty led to the conclusion that the terms for Sty and BA initiation reactions were negligible compared to that of CLA. The significance of the CLA initiation term, k_{i1}, suggests that CLA readily reacts with initiator, more so than would Sty and BA. During the initial reaction stages, CLA-rich

oligomeric species are generated because oleic acid, which acts as an electron trap, quickly terminates any initiated polymer chains. As the reaction proceeds and the oleic acid is deactivated (i.e., space for electron trapping is filled), Sty and BA begin to dominate the polymerization due to their higher rates of propagation; this is due to their smaller size relative to CLA in the face of increasing reaction viscosity. In other words, the CLA propagation parameter reflects a viscosity impediment and is thus, an "effective" rate parameter (recall that we refer to this as a pseudo-kinetic model). This effect was further confirmed by the terpolymer composition and molecular weight results shown later and in any case is consistent with our previous reports on CLA/Sty and CLA/BA copolymerizations.[10]

The rate constants previously reported for CLA/Sty and CLA/BA were used in the development of this model.[10] The rate constants of Sty and BA homopolymerization and copolymerization (k_{p22}, k_{p23}, k_{p32}, k_{p33}) were taken from the literature.[19] The rate constants used in the model are shown in Table 3.2.

Table 3.2. Rate constants (L/mol s) used with Matlab Model

k_{i1}	0.0003
k_{p11}	0.03
k_{p12}	0.3
k_{p13}	0.6
k_{p21}	0.03
$k_{p22}^{(19)}$	341
$k_{p23}^{(19)}$	357
k_{p31}	0.3
$k_{p32}^{(19)}$	15205
$k_{p33}^{(19)}$	3024
k_{tr1O}	1000
k_{tr2O}	1000
k_{tr3O}	2000

The Matlab output was used to calculate terpolymer composition and conversion. Terpolymer composition vs. conversion plots for two example feed compositions are shown in Figures 3.5 and 3.6. The feed compositions selected were for a high BA feed (Figure 3.5) and a high Sty feed (Figure 3.6). The experimental compositions are well predicted by the model. The focus of this work being on renewable monomers, the terpolymer CLA composition is plotted versus conversion for 8 feeds in Figures 3.7 and 3.8.

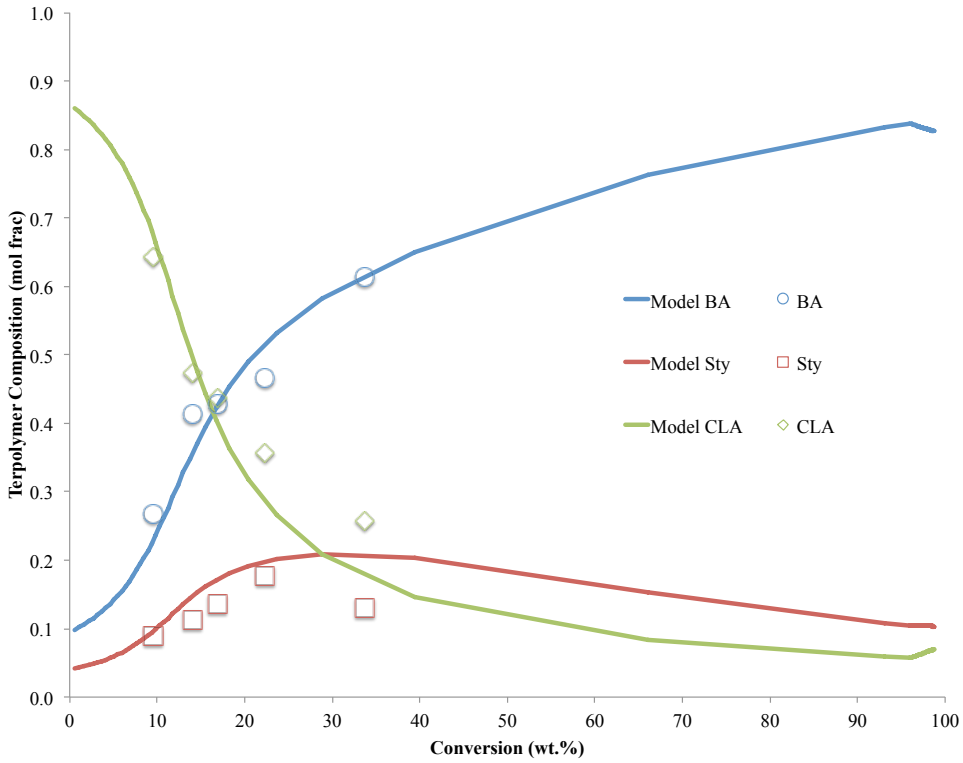

Figure 3.5: Terpolymer composition vs. conversion for high BA feed (CLA/Sty/BA: 8/10/82 mol/mol/mol).

In Figures 3.5 to 3.8, three distinct stages can be observed. In Stage 1, the dominant reaction is the production of CLA oligomers. This was confirmed with ^{1}H-NMR spectroscopy and GPC measurements. Stage 2 begins once the oleic acid has trapped a limited number of electrons. During Stage 2, Sty and BA dominate the propagation reactions over CLA, resulting in a sharp decrease in CLA content in the polymer, as observed in Figures 3.7 and 3.8. The beginning of Stage 3 is marked by the depletion of Sty and BA and the ongoing, yet slower, polymerization of CLA.

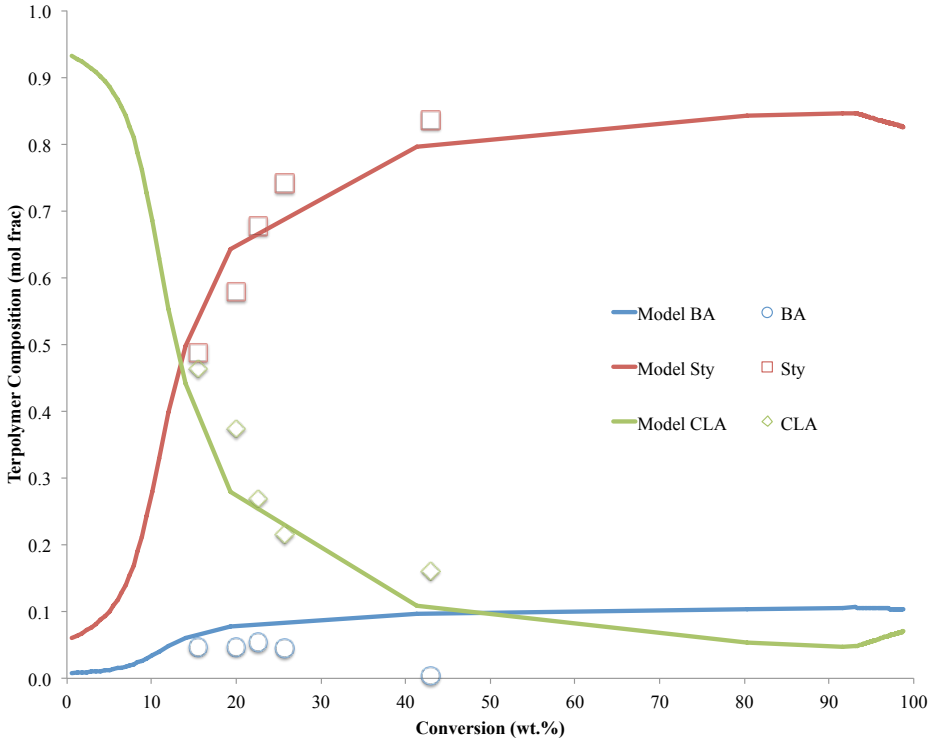

Figure 3.6: Terpolymer composition vs. conversion for high Sty feed (CLA/Sty/BA: 8/82/10 mol/mol/mol).

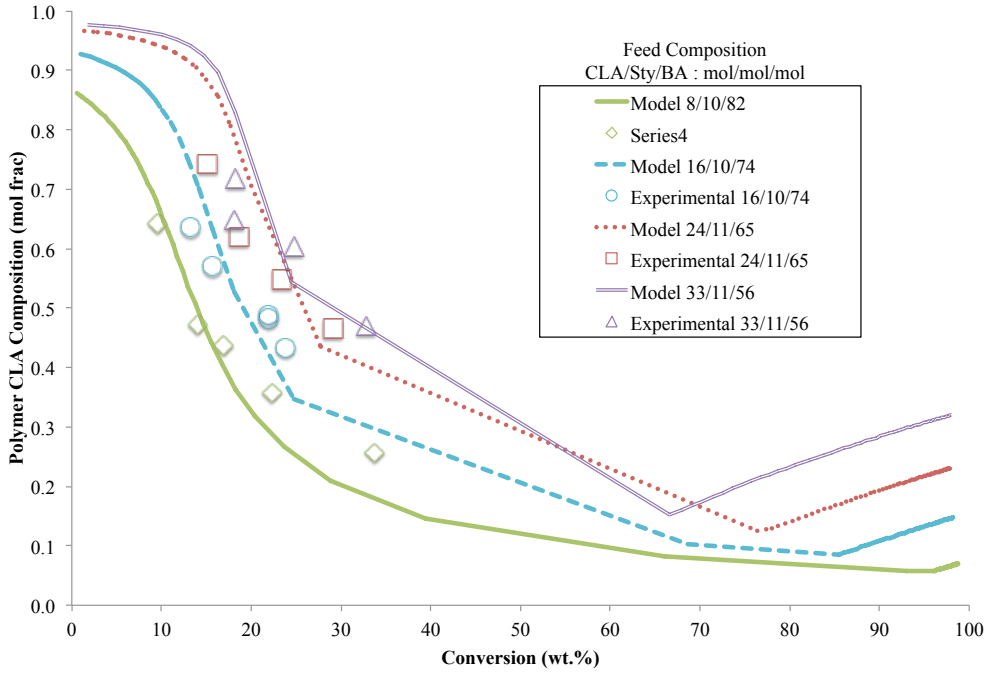

Figure 3.7: Terpolymer CLA composition versus conversion (higher BA feed concentration)

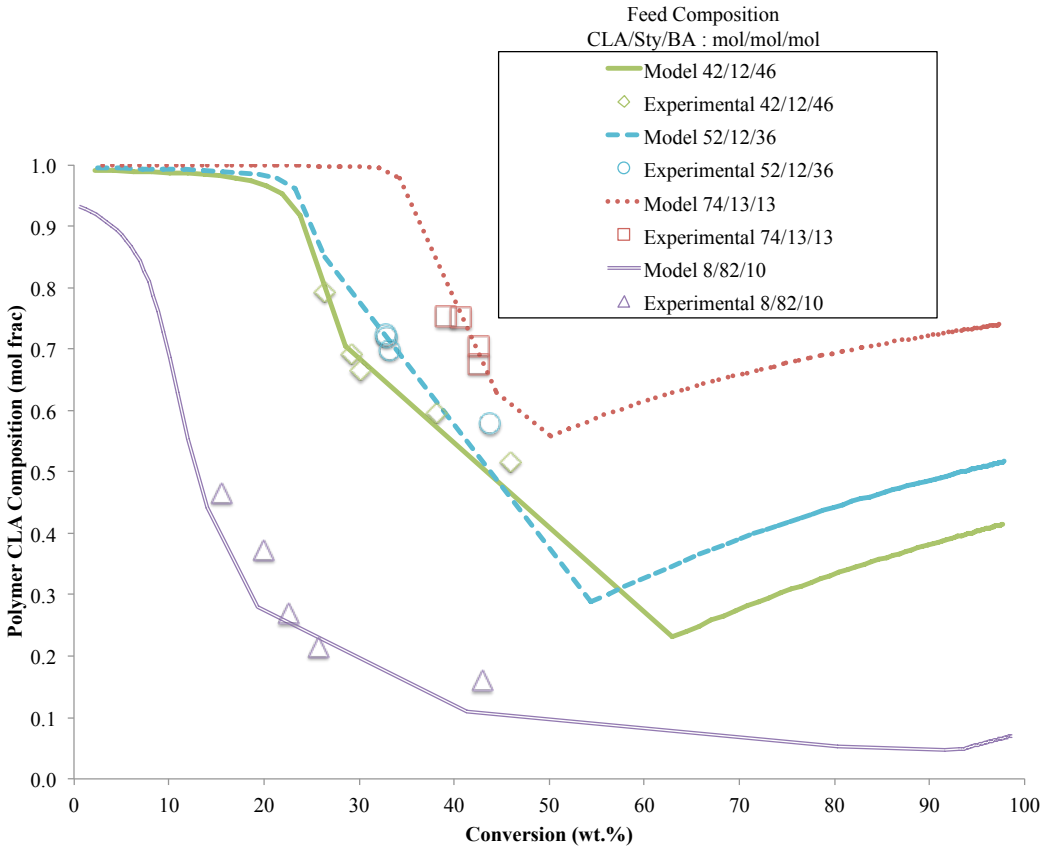

Figure 3.8: Terpolymer CLA composition versus conversion (lower BA feed concentration)

3.3.2 GPC Results

The CLA/Sty/BA terpolymers were characterized for molecular weight and the results are shown in Figure 3.9 for weight-average molecular weight versus conversion. Weight-average and number-average molecular weight results for high conversion terpolymer samples are shown in Table 3.3 where the polydispersity indicates a dominant termination by disproportionation. From Figure 3.9, with an 8 mol% CLA feed concentration, an increasing molecular weight profile was observed when the feed was rich in BA and a decreasing molecular weight profile was observed when the feed was

rich in Sty. With 16, 24, and 33 mol% CLA feed concentrations, a relatively flat molecular weight profile was observed with decreasing molecular weights when the CLA feed concentration was increased. At higher CLA feed concentrations, the molecular weights were relatively low and showed a steeply sloping increase with conversion. This is entirely consistent with the presence of greater amounts of oleic acid in the system. Only low molecular weight oligomers are formed at the early stages of the reaction, while the molecular weights increased significantly after the effect of oleic acid has abated. An increase in the oleic acid content in the feed produced more CLA-rich oligomers and reduced the overall molecular weight of the terpolymer. Similar results were reported previously where copolymers were evaluated.[10]

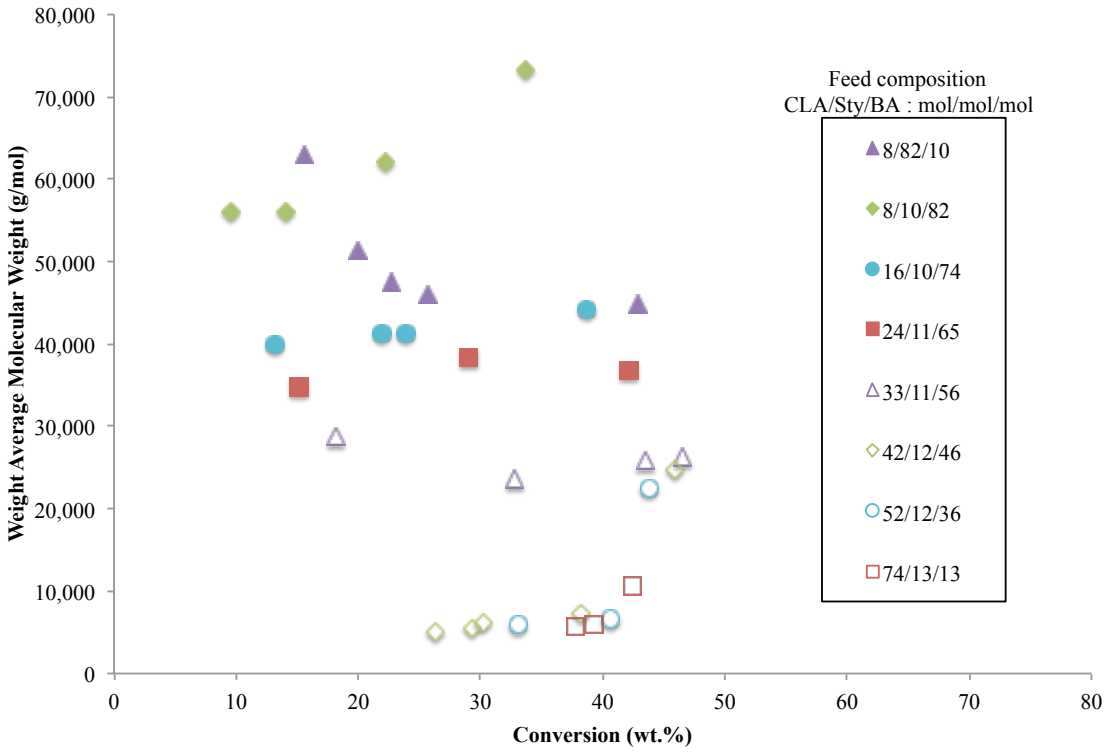

Figure 3.9: Weight-average molecular weight versus conversion for CLA/Sty/BA terpolymers.

Table 3.3. Number- and weight-average molecular weight for CLA/Sty/BA terpolymers

Run	M_n (g/mol)	M_w (g/mol)	Conversion (wt.%)	PDI
1	44,700	73,400	34	1.6
2	28,100	44,200	39	1.6
3	22,900	36,800	42	1.6
4	17,200	26,200	47	1.5
5	17,400	24,700	46	1.4
6	15,800	22,600	44	1.4
7	7,800	10,600	42	1.4
8	30,300	45,000	43	1.5

It should be clarified that molecular weight analysis was performed on both the decanted liquid and precipitate from the gravimetric process (described in the experimental section). The GPC analysis revealed that a significant portion of oligomers was extracted although some oligomers remained in the precipitated polymer. The data in Figure 3.9 and Table 3.3 represent only the precipitated polymer and not the extracted oligomers. The small fraction of oligomers excluded from the GPC analysis would not be expected to influence the average molecular weight values reported herein outside the range of expected analytical error.

All the terpolymers were characterized for their glass transition temperatures and only one inflection point was found indicating a homogeneous distribution of the monomers inside the polymer matrix. The DSC results for different terpolymers are shown in Table 3.1 (all results are reported within +/- 5 ^{o}C instrument error). Most of the T_g values were low, as expected due to their high BA and CLA content. Interestingly, the change in CLA content appeared to have little significant effect on T_g. For the reaction

producing a terpolymer with high Sty content (see Reaction 8 in Table 3.1), the measured T_g was, as expected, significantly higher (+55 ^oC).

3.4 Conclusions

CLA is a renewable monomer of high interest in potential for polymerization. However, high purity CLA is prohibitively expensive compared to monomers such as Sty and BA. A less costly version is available which contains a significant quantity of saturated fatty acids and oleic acid; this brings the CLA to a cost effective level in the range of most typical monomers. As previously reported,[10] the saturated fatty acid component in the CLA does not react with any other components in the reaction mixture. On the other hand, the oleic acid component does play a significant role in the polymerization reaction kinetics but does so without being incorporated into the polymer product. In this work, CLA/Sty/BA bulk terpolymerizations were performed at 80°C and were shown to strongly favour the polymerization of Sty and BA during terpolymerization. The strong effect on the reaction kinetics arose from the oleic acid which trapped electrons from freshly initiated radicals and oligomer radicals, followed by its resonance stabilization. The reactions therefore undergo three reaction stages: first, oligomeric radical species containing primarily CLA (as opposed to Sty and BA) are deactivated by oleic acid, followed by the dominant polymerization of the co-monomers (i.e., Sty and BA), and ending with additional, slow, CLA consumption. Despite its interference with the polymerization kinetics, the presence of oleic acid in the feed appears to encourage the incorporation of CLA into the terpolymer and modify the polymer molecular weight. The presence of oligomers would be expected to have an

effect on polymer properties. Of course, further study on particular polymer properties would be needed and one should be able to take corrective action to reduce (or increase) the amount of oligomers depending on specific needs.

It should be noted that conversions in this study were deliberately kept low due to the focus on composition analysis. Future applications of these terpolymers at higher conversions for adhesive and coatings applications are foreseen.

3.5 Acknowledgments

The authors gratefully acknowledge the financial support from the Natural Science and Engineering Research Council (NSERC) of Canada and Omnova Solutions (USA).

3.6 References

1. M.A. Dubé, S. Salehpour, Applying the Principles of Green Chemistry to Polymer Production Industries. Macromol. React. Eng., 2014, 8, 7-28.
2. M. A. R. Meier, J. O. Metzger, U. S. Schubert, Plant oil renewable resources as green alternatives in polymer science. Chem. Soc. Rev., 2007, 36, 1788-1802.
3. F. Li, M. V. Hanson, R. C. Larock, Soybean oil – divinylbenzene thermosetting polymers: synthesis, structure, properties and their relationships. Polymer, 2001, 42, 1567-1579.
4. Z. S. Petrovic, Polyurethanes from vegetable oils. Polym. Rev., 2008, 48, 109-155.
5. R. P. Wool, S. P. Bunker, Polymer-solid interface connectivity and adhesion: Design of a bio-based pressure sensitive adhesive. J. Adhes., 2007, 83, 907-926.

6. C. M. Klapperich, R. P. Wool, L. Zhu, L. M. Bonnaillie, Proc. Biomater. Annu. Meeting, Pittsburgh, PA, 2006.

7. L. Zhu, R. P. Wool, Nanoclay reinforced bio-based elastomers: Synthesis and characterization. Polymer, 2006, 47, 8106-8115.

8. D. H. Hewitt, F. Armitage, Styrene copolymers in surface coatings. J. Oil Colour Chem. Assoc., 1946, 29, 109-128.

9. R. Gangidi, A. Proctor, Photochemical production of conjugated linoleic acid from soybean oil. Lipids, 2004, 39, 577-582.

10. S. Roberge, M. A. Dubé, Bulk Copolymerization of Conjugated Linoleic Acid with Styrene and Butyl Acrylate: Reactivity Ratio Estimation. J. Macromol. Sci., Pure Appl. Chem., 2015, 52, 961-970.

11. A. Eshuis, H. J. Leendertse, D. Thoenes, Surfactant-free emulsion polymerization of styrene using cross-linked seed particles. Colloid Polym. Sci., 1991, 269, 1086-1089.

12. K. S. Jeong, J. Tang, H. Liu, J. Kim, A. W. Schaefer, K. Kemp, L. Levina, X. Wang, S. Hoogland, R. Debnath, L. Brzozowski, E. H. Sargent, J. B. Asbury, Enhanced Mobility-Lifetime Products in PbS Collodial Quantum Dot Photovoltaics. ACS Nano, 2012, 6, 89-99.

13. R. C. Laible, Allyl Polymerizations. Chem. Rev., 1958, 58, 807-843.

14. M. Moreno, J.L. Miranda, M. Goikoetxea, M.J. Barandiaran. Sustainable polymer latexes based on linoleic acid for coatings applications. Prog. Org. Coat., 2014, 77, 1709-1714.

15. R. R. Chance, S. P. Baniukiewicz, D. Mintz, G. Ver Strate, N. Hadjichristidis, Characterization of Low-Molecular-Weight Polymers: Failure of Universal Calibration in Size Exclusion Chromatography. Int. J. Polymer Analysis & Characterization, 1995, 1, 3.

16. K. Antolin, J-P Lamps, P. Rempp, Y. Gnanou, Synthesis of poly9t-butyl acrylate) macromonomers. Polymer, 1990, 31, 967-970.

17. S. S. Narine, X. Kong, Bailey's Industrial Oil and Fat Products, 6th Edition, 6th Volume Set, Chapter 8: Vegetable Oils in the Production of Polymers and Plastics, John Wiley and Sons Inc., Edmonton 2005, p. 279-306.

18. N. A. Dotson, R. Galvan, R. L. Laurence, M. Tirrell, Polymerization Process Modeling, John Wiley and Sons Inc., New York NY, USA 1996, p. 134-135.

19. J. Gao, A. Penlidis, Mathematical modeling and computer simulator/database for emulsion polymerizations. Prog. Polym. Sci., 2002, 27, 403-535.

17. Narine, S. S.; Kong, X. Bailey's Industrial Oil and Fat Products, 6th Edition, 6th Volume Set, Chapter 8: Vegetable Oils in the Production of Polymers and Plastics, John Wiley and Sons Inc., Edmonton 2005.

18. Dotson, N. A.; Galvan, R.; Laurence, R. L.; Tirrell, M. Polymerization Process Modeling, John Wiley and Sons Inc., New York NY, USA 1996.

19. Gao, J.; Penlidis, A. Mathematical modeling and computer simulator/database for emulsion polymerizations. Prog. Polym. Sci., 2002, 27, 403-535.

Chapter 4 – Paper on Emulsion Terpolymerization of CLA

Int. J. Adhes. Adhes. **submitted December 2015**

Emulsion Terpolymerization of Conjugated Linoleic Acid with Styrene and Butyl Acrylate

Stéphane Roberge, Marc A. Dubé*

Department of Chemical and Biological Engineering,

Centre for Catalysis Research and Innovation, University of Ottawa

161 Louis Pasteur Pvt., Ottawa, ON, K1N 6N5 Canada

* *Marc.Dube@uOttawa.ca*

Abstract

Free radical emulsion terpolymerizations of conjugated linoleic acid (CLA), styrene (Sty), and butyl acrylate (BA) were performed at 80^{o}C. Terpolymers were characterized for composition, conversion, molecular weight and glass transition temperature while latexes were characterized for viscosity, particle size, tack, peel strength, and shear strength. One impurity commonly found in CLA, oleic acid, was shown to influence the reaction kinetics significantly. Adhesive performance was tuned using divinylbenzene (DVB) crosslinker to keep the terpolymer molecular weight in a desired range. By using a constrained mixture design, the influence of terpolymer composition, chain transfer agent (CTA) concentration, DVB concentration, molecular weights, viscosity and particle size on tack, peel strength and shear strength was investigated. The final forms of the resulting empirical models allowed the creation of 3D response surfaces for pressure sensitive adhesive (PSA) performance optimization.

4.1 Introduction

Polymer production using renewable sources such as plant oils can address several green chemistry principles[1, 2]. Plant oils, or triglycerides, are made of three fatty acid chains bonded to a glycerol backbone (see Figure 4.1.a). The polymerization of plant oils is made difficult due to steric hindrance which can be overcome by the use of its component fatty acid chains such as linoleic acid (see Figure 4.1.b)[3, 4]. Because of the ability of conjugated oils to copolymerize[5], conjugated linoleic acid (CLA) was chosen for free radical polymerization (see Figure 4.1.c). With the prohibitive cost of high purity CLA[6, 7]. an affordable CLA containing impurities such as oleic acid (see Figure 4.1.d) and saturated fatty acids (see Figure 4.1.e) presents an interesting option for polymerization. Oleic acid has been used as a surfactant replacement in the emulsion homopolymerization of styrene without any signs of copolymerization[8]. Oleic acid is also known for its electron trapping ability[9] where the oleic acid radicals are resonance stabilized[10]. Oleic acid also was shown to influence the reaction kinetics significantly for bulk copolymerizations and terpolymerizations involving CLA, Styrene (Sty) and n-butyl acrylate (BA)[6, 7]. In this study, low-cost CLA containing oleic acid and saturated fatty acids was used to produce terpolymers with Sty and BA with the goal of producing pressure-sensitive adhesives (PSA) with a significant concentration of a renewable component.

PSA's are characterized by instantaneous adhesion upon application of light pressure[11]. They are soft and tacky with a low glass transition temperature within the -60 to 20 ^{o}C range. While an acrylic polymer such as poly(BA) can be soft and tacky, thus providing good tack and peel strength, it often lacks in shear strength. The addition of a

"hard" monomer such as Sty is useful to regulate tack, peel strength and shear strength[12, 13]. Monomers with functional groups such as acrylic acid (AA) can be added to improve peel strength, shear strength and film formation, but at the expense of reducing tack[14]. In this study, the effect of terpolymer composition, chain transfer agent (CTA) concentration, divinylbenzene (DVB) concentration, molecular weight, viscosity and particle size on tack, peel strength, and shear strength were evaluated for CLA/Sty/BA emulsion terpolymerization.

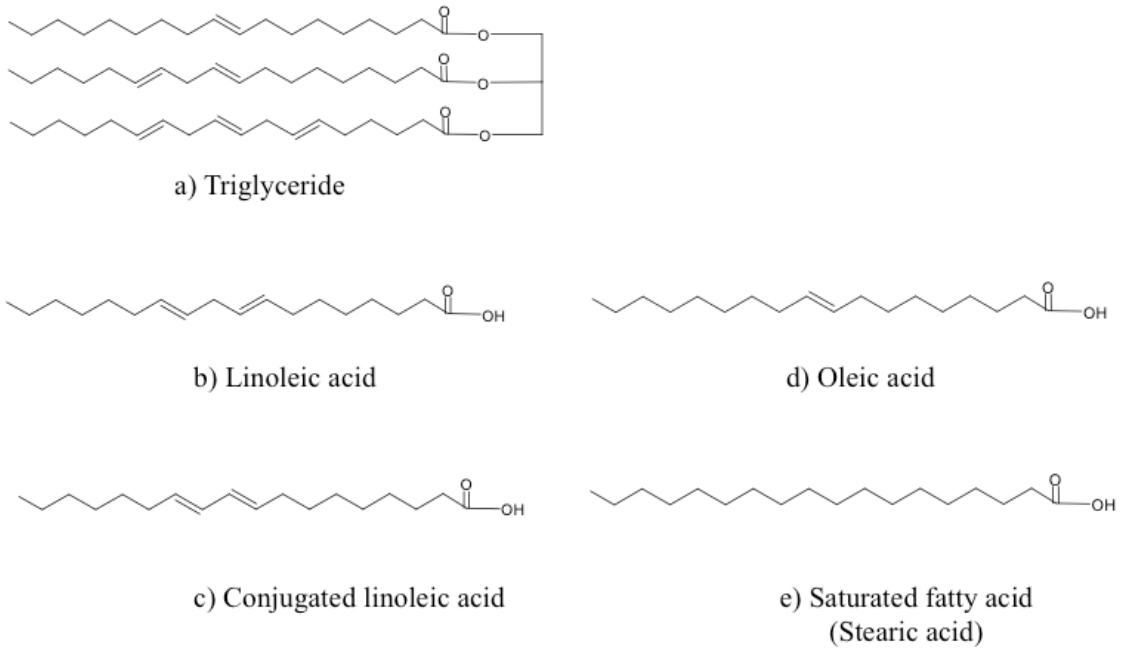

Figure 4.1: Molecule of a) Triglyceride, b) Linoleic acid, c) Conjugated linoleic acid, d) Oleic acid, and e) Saturated fatty acid.

4.2 Experimental

4.2.1 Materials

An affordable conjugated linoleic acid (CLA, Penta, 74% CLA, 13% oleic acid, 13% saturated fatty acid) was chosen for practical reasons and used without further purification. Sty (Sigma-Aldrich, 99%), BA (Sigma-Aldrich, 99%) and all solvents (e.g., acetone (Fisher, 99%), tetrahydrofuran (THF, Fisher, 99.9%) and chloroform-d (Cambridge Isotope Laboratories, 99.8%)) were used as received. The water soluble initiator, potassium persulfate (KPS, Fisher, 100%), and the emulsifier, sodium dodecyl sulphate (SDS, EM Science, 100%) also were used as received while the solvent phase was distilled deionized (DDI) water. In some instances, sodium bicarbonate ($NaHCO_3$, Fisher, 100%), n-dodecyl mercaptan (CTA, Sigma Aldrich, 98+%), acrylic acid (AA, Acros, 99.5%) and divinylbenzene (DVB, Sigma Aldrich, 80%) were added to modify the latex properties.

4.2.2 Polymerizations

Batch emulsion polymerizations were performed at 80 °C in a 1.2L, jacketed glass reactor (LabMax, Mettler-Toledo) and stirred at 200 rpm. The reactor was equipped with a nitrogen pressurizing line, a sampling line, a vent with reflux condenser, and a port for an IR probe. CLA, Sty, BA, CTA, AA, DVB were mixed for 15 min, while DDI water, SDS, and $NaHCO_3$ were also mixed for 15 min in separate beakers. The two solutions were then combined and mixed for 45 min before being poured into the reactor. Oxygen was purged from the reaction mixture with nitrogen for 45 min while the reaction temperature was raised. After the reaction mixture reached 80 °C, a deoxygenated

initiator solution was pumped into the reactor and this marked the beginning of the polymerization. Samples were taken regularly through the sampling line for offline analyses by gravimetry and ^{1}H-NMR spectroscopy. As shown in Table 4.1, three different feed compositions were used repeatedly in this study (f_i is mole fraction of monomer i in the feed). Based on previous knowledge[13], polymer compositions were selected to produce PSAs with acceptable adhesive performance. The Sty feed composition was set to 10 mol% while the CLA in the feed was added at the expense of the BA fraction normally used[6, 7]. It should be noted that due to its high molar mass, the mass fractions of CLA were quite elevated despite the relatively low mol fraction (see Table 4.1). All additional ingredient concentrations are listed in Table 4.2.

Table 4.1: Monomer feed composition for emulsion terpolymerization.

Feed formulation	f_{CLA} (wt. frac.)	f_{CLA} (mol frac.)	f_{Sty} (mol frac.)	f_{BA} (mol frac.)
A	0.16	0.08	0.10	0.82
B	0.23	0.12	0.10	0.78
C	0.30	0.16	0.10	0.74

Table 4.2: Emulsion formulations (phm = parts per hundred parts monomer on a weight basis).

Emulsion formulation	AA (phm)	KPS (phm)	SDS (phm)	CTA (phm)	DVB (phm)	Feed formulation (from Table 4.1)
1	0.0	0.5	0.5	0.0	0.0	A
2	0.0	0.2	1.0	0.0	0.0	A
3	0.0	1.0	1.0	0.0	0.0	A
4	0.0	0.5	1.0	0.0	0.0	A
5	4.0	0.5	1.0	1.0	0.0	A
6	4.0	0.5	1.0	1.0	0.1	A, B, C
7	4.0	0.5	1.0	1.0	0.2	A, B, C
8	4.0	0.5	1.0	1.0	0.3	A, B, C
9	4.0	0.5	1.0	0.5	0.2	A
10	4.0	0.5	1.0	0.3	0.2	C
11	4.0	0.5	1.0	0.0	0.2	C
12	4.0	0.5	1.0	0.0	0.4	C
13	4.0	0.5	1.0	0.0	0.6	A, B, C
14	4.0	0.5	1.0	0.0	0.8	A, B, C
15	4.0	0.5	1.0	0.0	1.0	A, B, C

4.2.3 Experimental design

A series of experiments (see Table 4.2) was designed to further our understanding of the CLA/Sty/BA emulsion terpolymerization kinetics while evaluating PSA performance. Some formulations were replicated more than once and all reactions were run at 80 °C and 50 wt.% solids content. The concentrations of water and $NaHCO_3$ were kept constant at 90 and 0.15 phm, respectively, where phm represents parts per hundred parts monomer on a weight basis. A set of preliminary screening experiments (formulations 1 to 5 in Table 4.2) were attempted prior to optimizing the formulation for PSA performance. In order to empirically model the relationships between CLA feed composition and DVB feed content with PSA performance, a 3-level factorial design for 2 variables was conducted (formulations 6 to 8 in Table 4.2). Based on the PSA performance obtained with this design, and with an additional round of screening experiments (formulations 9 to 12 in Table 4.2), a second 3^2 factorial design (formulations 13 to 15 from Table 4.2) was implemented to optimize the PSA performance.

4.2.4 Characterization

Samples of 3 to 10 g each were first cooled in an ice bath then dried as is for ~7 days in the fumehood and ~7 days in a vacuum oven, until a constant weight was achieved. The mass of any residual CLA monomer, oleic acid, and saturated fatty acid left in the dry sample was measured via ^{1}H-NMR spectroscopy and was subtracted from the measured dry sample mass to calculate monomer conversion based on the mass of the dried polymer[6, 7].

^{1}H-NMR spectroscopy was used to determine the cumulative terpolymer composition. Analyses were carried out at room temperature in deuterated chloroform (~2% w/v) with a Bruker AVANCE III 400 Fourier transform ^{1}H-NMR spectrometer. The acquisition time was 4.6 seconds and 16 scans were performed per sample. A detailed presentation of peak assignments and calculation procedure for polymer composition was reported previously[6, 7] where the polymer composition was estimated from the areas under specific absorption peaks. A sample spectrum of poly(CLA/Sty/BA) is shown in Figure 4.2 where the phenyl groups of Sty units bound in the polymer (peaks m-n) are located at ~6.2-7.2 ppm, the -OCH_2- groups of BA units in the polymer (peak t) are located at ~4.0 ppm and the methyl groups of CLA units in the polymer are located at ~0.9 ppm (peak K). An isolated alkene hydrogen peak is located at ~5.9 ppm for CLA monomer (peak G). This information was crucial for calculating the polymer composition because the methyl group of CLA polymer (peak K) was overlapped by the peaks of most of the other components. Additionally, an alkene hydrogen peak (peak F) is located at ~5.4 ppm which represents both a single alkene in the CLA monomer and two alkene hydrogens surrounding the double bond in oleic acid (see Figure 4.1). Equations developed previously for bulk terpolymer composition estimation[6, 7] were used for the estimation of emulsion terpolymer composition. The composition was also used with gravimetric data to calculate individual monomer conversions.

The cumulative number- and weight-average molecular weights of the polymers were measured using an Agilent/Wyatt gel permeation chromatography (GPC) system equipped with fractionating columns installed in series, a multi-angle light scatterer (MALS), a viscometer (VISC) and a refractive index detector (DRI) at 25 ^{o}C.

Tetrahydrofuran (THF) was the mobile phase and delivered at 1.0 mL/min. The MALS detector provides an absolute molecular weight measurement without the use of calibration. However, the measurement is dependent on the refractive index increment (dn/dc) value used. The usual approach of using a terpolymer composition weighted dn/dc value based on individual dn/dc values for the homopolymer of each component was employed. The dn/dc values used were 0.187 for poly(Sty)[15], 0.056 for poly(BA)[16], and 0.064 for poly(CLA)[7].

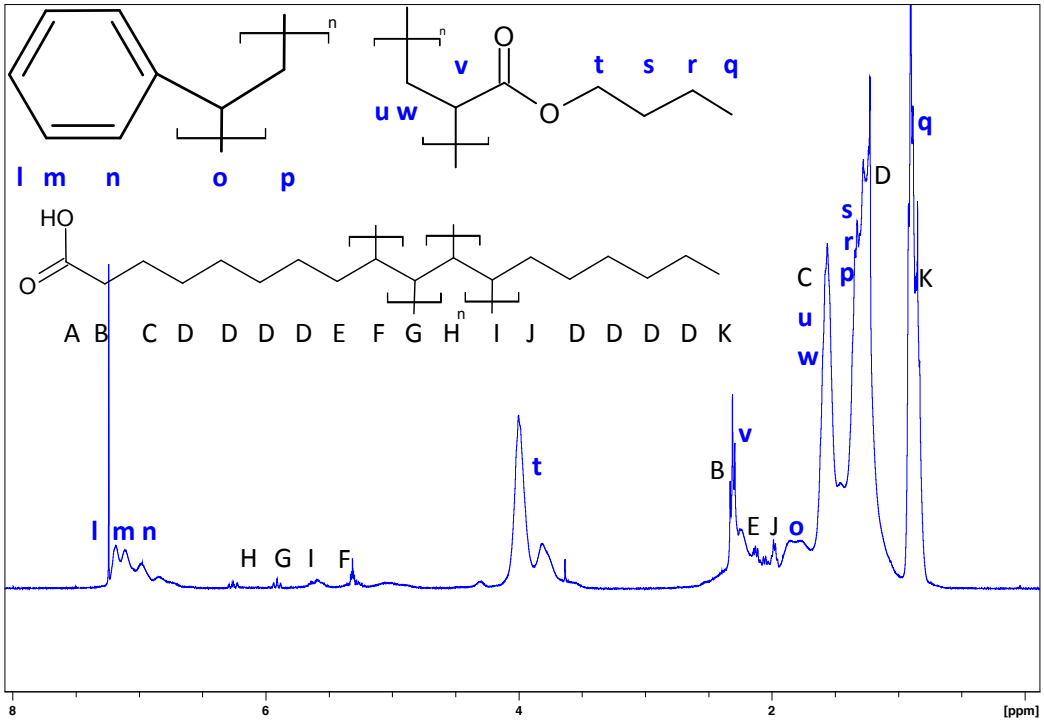

Figure 4.2: ^{1}H-NMR spectrum of CLA/Sty/BA: 8/19/73 mol/mol/mol terpolymer in $CDCl_3$.

The glass transition temperatures (T_g) of the polymers was measured with a TA Instruments Model Q1000 Dynamic Scanning Calorimeter (DSC) equipped with a refrigerated cooling system and a nitrogen purge. The sample (~7 mg of dry polymer) was cooled to -80 ^oC and then heated at a rate of 10^oC/min until the sample reached 110 ^oC. The T_g was calculated from the inflection point in the reversed heat flow curve.

The particle size of the latexes was determined with a Zetasizer Nano-S light scatterer from Malvern Instruments where a latex sample is diluted in DDI water and the z-average of 10 measurements is reported.

A small amount of acrylic acid (AA) was added to improve the peel strength and shear strength of the final PSA. It should be noted that the partitioning of AA in the water and oil phase will be strongly influenced by the pH of the reaction mixture[17]. In the St/BA/AA system, AA was found to be equally distributed between the water and oil phase when the pH was between 2 and 4. An increased pH of 6 and higher resulted in the presence of AA mainly in the water phase. Furthermore, at a pH of 6 to 7, the AA propagation rate decreased. With this in mind, the pH of the latexes in this study was maintained between 3.1 and 4.2. An Accumet Research AR50 pH meter was used to make the measurements.

Latexes were cast onto a 50 µm thick polyethylene terephthalate (PET) carrier with a size #30 Meyer rod to give a dry film thickness of ~30 µm. Prior to casting, latex agglomerates were removed with a sieve equipped with a size #30 mesh. The films were dried for 2 days before testing on a stainless steel substrate. Two films were cast per latex and two specimen per film were evaluated for tack, peel strength and shear strength. The average of four measurements was used in the analysis of adhesive performance.

Tack was measured using the PSTC-16 standard. A specimen of 25.4 mm x 177.8 mm was cut and one inch on both sides was masked with masking tape. A loop with the adhesive facing outside was formed and placed in the upper grip of an Instron E3000 universal tester (Instron, Inc.). The loop was then brought into contact with the substrate mounted onto a loop tack fixture inserted into the bottom grip. When the loop covered and area of 25.4 x 25.4 mm, the upper grip was brought up at a crosshead speed of 300 mm/min. The maximum force required to remove the specimen was recorded as the loop tack.

Peel strength was measure using the PSTC-101 standard. A specimen of 25.4 mm x 304.8 mm was cut and laminated onto the substrate using a 2040 g rubber coated roller. The average force per 10 mm to peel strength the specimen at a 180^{o} angle from the substrate was recorded and the testing speed was 300 mm/min.

Shear strength was measure using the PSTC-107 standard. A specimen of 25.4 mm x 152.4 mm was cut and an area of 25.4 mm x 25.4 mm was laminated onto the substrate using a 2040 g rubber coated roller. A 500 g weight was placed at the end of the specimen. Time to failure was recorded automatically using Labview™ software (National Instruments).

The storage modulus (G'), loss modulus (G'') and damping (tan delta) of the PSAs were measured with an RDA III rheometer (TA Instruments) equipped with 25 mm parallel plate geometry and liquid nitrogen cooling. Samples were casted into silicone release paper mould, dried in the fumehood for 7 days and dried under vacuum for 7 days at room temperature before being analyzed with frequency sweeps at different temperatures. Sample thickness was 1.7±0.2 mm. The frequencies included 0.1, 0.2, 0.5,

1, 2, 5, 10, 20, 50, 80 Hz and each frequency sweep was performed at -35, -23, 0, 23, 35, and 50 ^{o}C. A frequency master curve was built with this information by using the time-temperature superposition method and the frequency sweep at 23 ^{o}C as the reference[18]. TA Orchestrator version 7.2 was used to perform the computational analyses. A temperature sweep was also performed from -80 ^{o}C to 110 ^{o}C at a rate of 10 ^{o}C/min and frequency of 1.591 Hz. The maximum from the tan delta curve provided a glass transition temperature estimation.

4.3. Results and Discussion

Previously, mass balances via ^{1}H-NMR spectroscopy demonstrated that the oleic acid and saturated fatty acid components in the lower cost CLA were not incorporated into the polymer chains[6, 7]. The oleic acid plays the role of an electron trap resulting in the production of many oligomers in the reaction mixture[6-10]. It was hypothesized that the long chains (9 carbons) on each side of the oleic acid double bond (see Figure 4.1.d) formed a resonance stabilized molecule after electrons were trapped at the alkene and allylic hydrogens. However, the oleic acid has a limited capacity for electron trapping and eventually, this behaviour ends. Therefore, the reactions start with a fast production of CLA-rich oligomers until the effect of oleic acid has abated, followed by a dominant polymerization of the co-monomers (i.e., Sty or BA) and finally, ending with a slow CLA consumption. The presence of oleic acid was shown to encourage CLA incorporation[6, 7]. Thus, despite the fact that oleic acid acts as an impurity, its presence has a positive effect.

4.3.1 Gravimetric Results

Overall and individual monomer conversions were calculated from gravimetry coupled with ^{1}H-NMR spectroscopy analyses. The results from formulations 1 to 4 (see Table 4.2) are shown in Figure 4.3 and were chosen from the preliminary screening experiments. Two emulsifier (SDS) concentraton levels and three initiator (KPS) concentration levels were used to achieve a range of final latex particle sizes (see Table 4.2). The results in Figure 4.3 are consistent with welll-known effects of initiator and emulsifier concentrations on particle size and number, which eventually impacts the rate of polymerization[18]. The conversion results shown in Figure 4.4 for formulations 6 to 8 (see Table 4.2) demonstrate reaction rates for different CLA feed compositions and different DVB concentrations that are similar within experimental error. One should note that the CLA concentration was varied from 8 to 16 mol%, which is equivalent to a range of 16 to 30 wt.%. In Figure 4.3, an additional run at slightly differing Sty/BA ratio (20/80 mol/mol) with CTA (0.2 phm) but no DVB nor CLA is shown for comparison. It is clear that the presence of CLA causes a dramatic decrease in reaction rate after nucleation and limits the maximum conversion one can achieve.

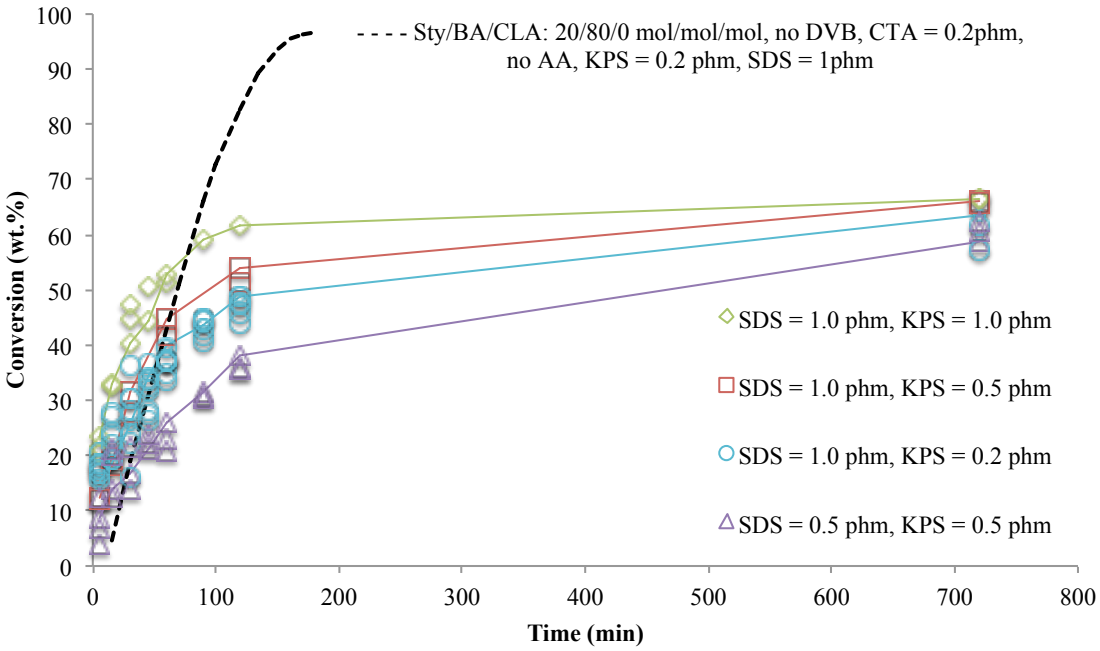

Figure 4.3: Conversion vs. time from preliminary screening experiments (Formulations 1 to 4, Table 4.2).

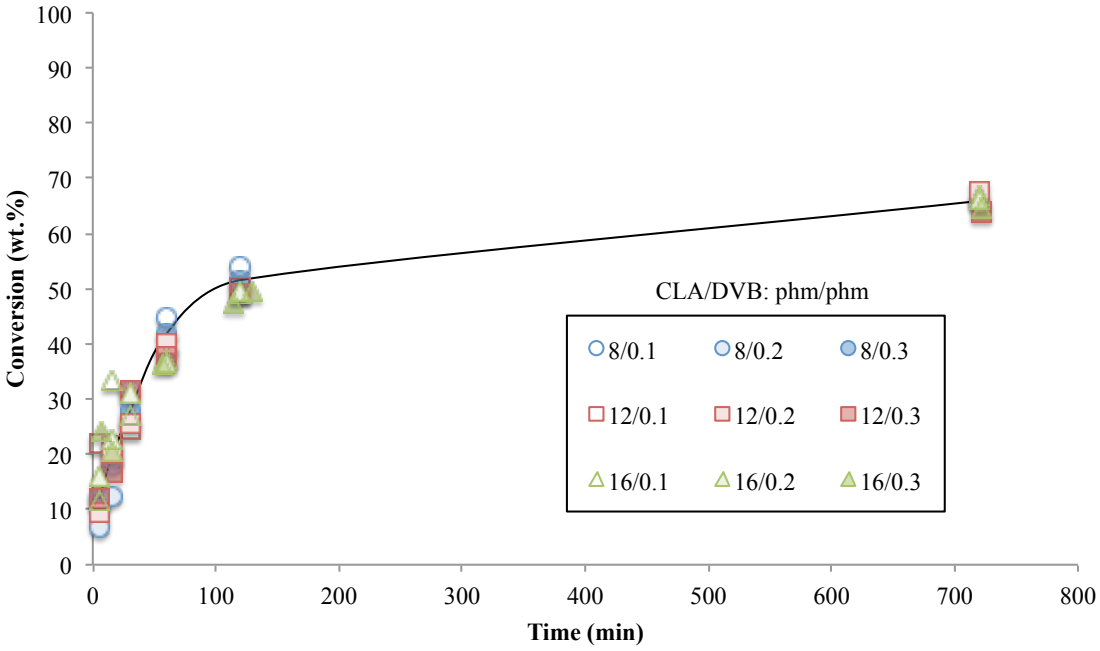

Figure 4.4: Conversion vs. time from 1st factorial design (formulations 6 to 8, Table 4.2).

4.3.2 ^{1}H-NMR Results

Terpolymer compositions were calculated from ^{1}H-NMR spectroscopy and are shown in Figure 4.5. Figure 4.5 displays results from a total of 8 distinct runs from formulations 1 to 4 (see Table 4.2). Initially, CLA-rich terpolymer production is observed; this is followed by the dominant consumption of the co-monomers Sty and BA. The Sty composition reaches a maximum at ~30 wt.% overall conversion which coincides more or less with the complete depletion of Sty monomer in the system; recall that Sty content in the formulation was 10 mol%. On the other hand, the BA composition increases throughout the polymerization. The polymer composition results from formulations 6 to 8 (see Table 4.2) are shown in Figure 4.6 and indicate an increased CLA incorporation into the polymer matrix with increasing CLA feed compositions. From Figure 4.6, as expected the changing DVB concentration had no significant effect on composition.

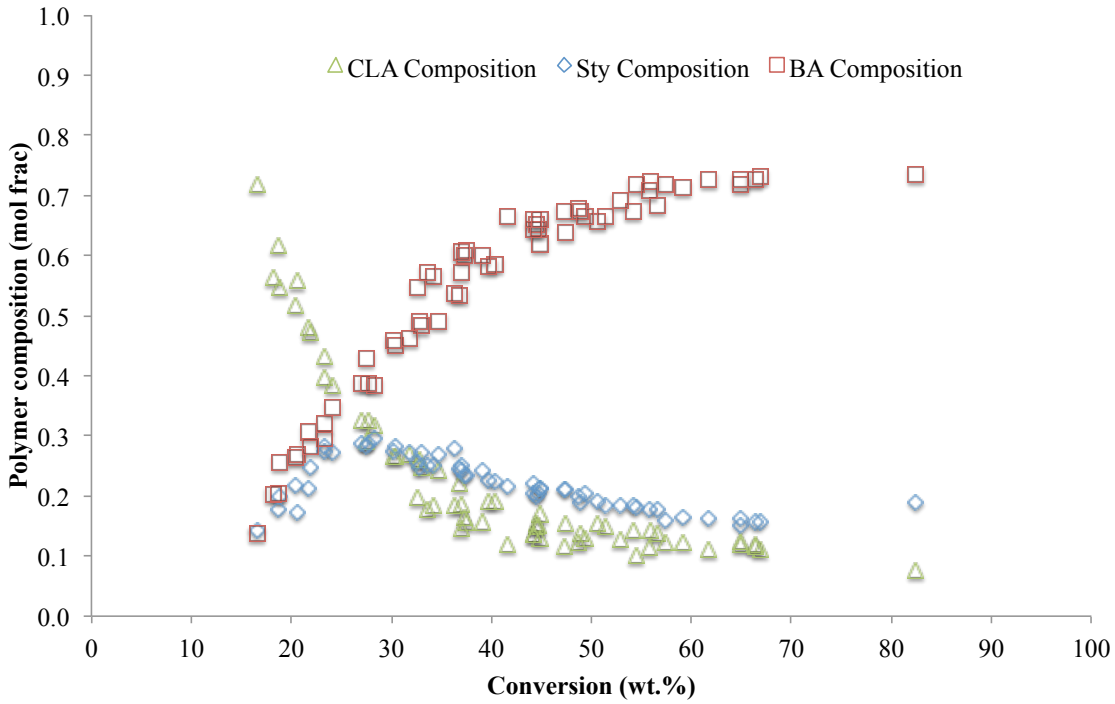

Figure 4.5: Terpolymer composition for preliminary screening experiments (formulations 1 to 4 in Table 4.2).

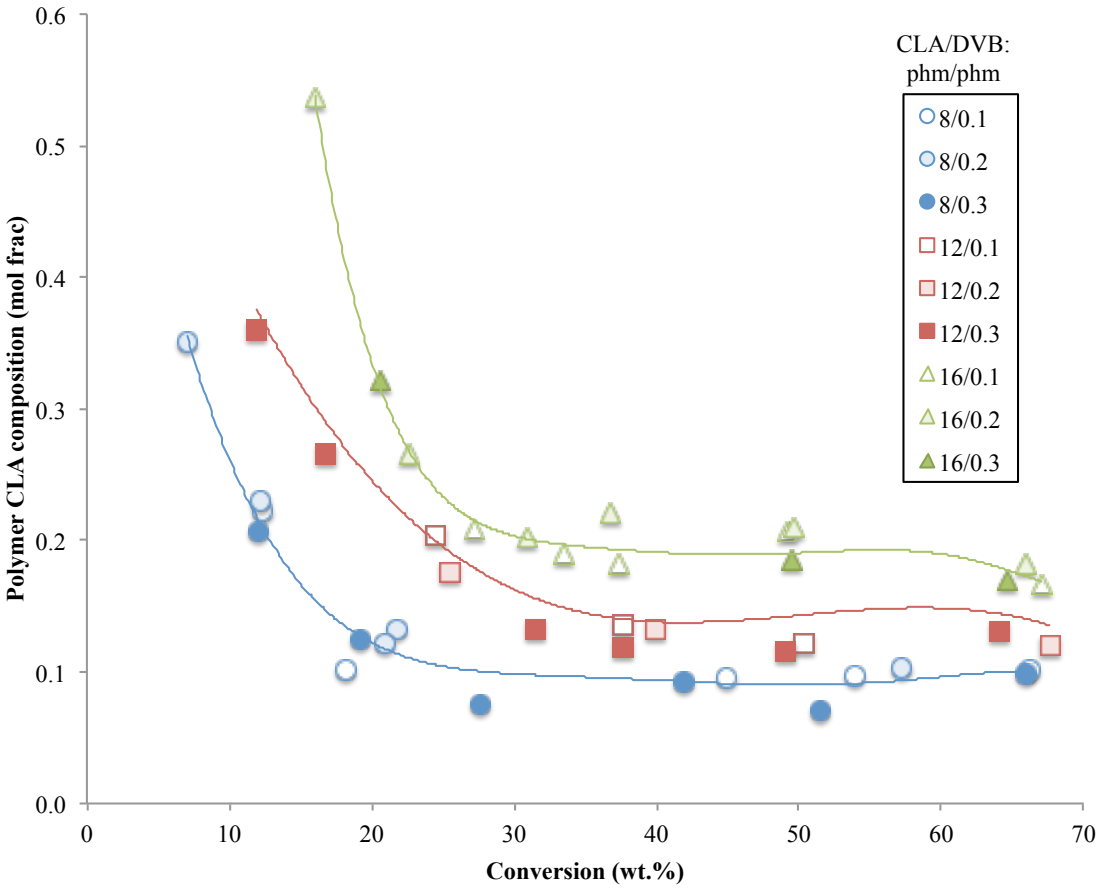

Figure 4.6: CLA content in terpolymers from 1st factorial design (formulations 6 to 8 in Table 4.2). Lines in figure are for visualisation only.

4.3.3 GPC Results

Weight-average molecular weight results for the CLA/Sty/BA terpolymers from formulations 6 to 8 (see Table 4.2) are shown in Figure 4.7. Due to the initial production of CLA-rich oligomers (see Figures 4.5 and 4.6), relatively low molecular weight polymers were produced during the early stages of the polymerizations. Increasing the CLA content resulted in lower molecular weight polymers (see Figure 4.7). At the same time, increasing DVB crosslinker concentration led to higher molecular weights, as

expected. These results provided a means to tune the molecular weight to achieve desired PSA properties in subsequent trials.

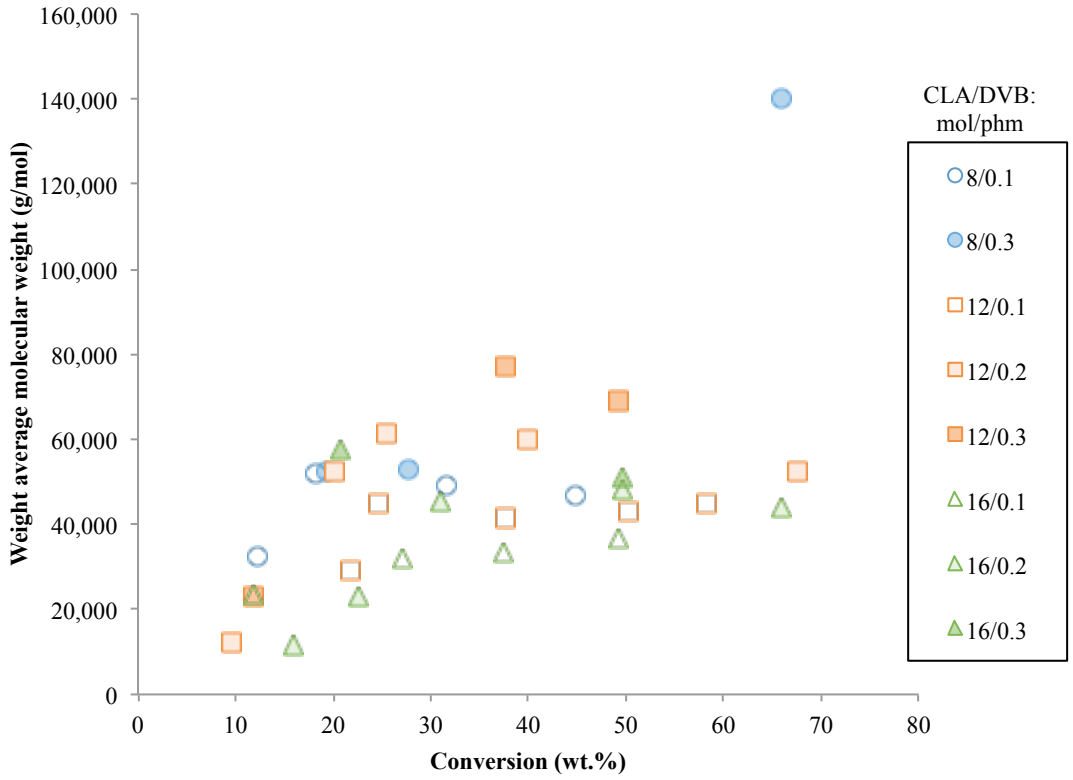

Figure 4.7: Molecular weight versus conversion from 1st factorial design (formulations 6 to 8 in Table 4.2).

Results in Figure 4.7 include reaction formulations containing 1 phm CTA (n-dodecyl mercaptan). Different polymer molecular weights were obtained by manipulating both the CTA and DVB concentrations. Initially, the CTA concentration was kept fairly high to prevent excessive cross-linking, thus keeping the polymer molecular weights relatively low (20,000 to 140,000). After analysis of data from the 1st factorial design for PSA performance, the molecular weights were progressively increased by decreasing CTA concentration to zero (see Figure 4.8.a) and subsequently increasing the DVB

concentration from 0.1 to 1 phm (see Figure 4.8.b). From these observations, CTA was not required to optimize PSA performance and three additional DVB concentration levels were evaluated (formulations 13 to 15 in Table 4.2). The formulations from the 2nd factorial design contained no CTA and varying concentrations of DVB. It is likely that the degradative chain transfer effect of CLA previously described[6, 7], is responsible for the lower demand for CTA in the formulation.

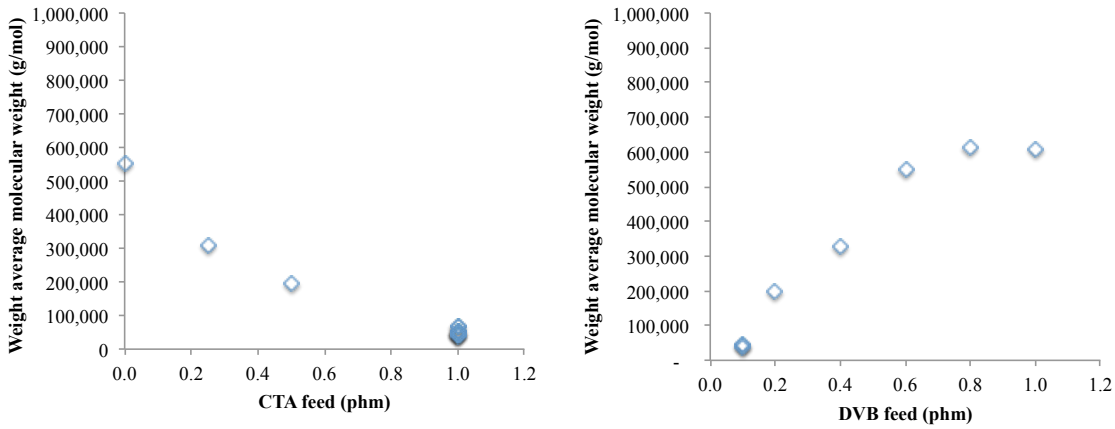

a) b)

Figure 4.8: a) Weight-average molecular weight versus CTA concentration (DVB concentration is constant at 2 phm), b) Weight-average molecular weight versus DVB concentration (CTA concentration is zero).

4.3.4 DSC Results

Terpolymers from formulations 5 to 15 (see Table 4.2) were characterized for their glass transition temperatures and, in most cases, one inflection point was found indicating a homogeneous distribution of the monomers inside the polymer matrix. In some cases, unreacted CLA monomer was included with the polymer sample and two

inflection points could be observed. All of the T_g values were low, in the range -49 to -36 ^oC, as expected due to their high BA and CLA content. After the T_g values were confirmed to be in an appropriate range for PSA formulations, the terpolymers from formulations 5 to 15 were evaluated for their adhesive properties.

4.3.5 PSA performance

Latexes from formulations 5 to 15 (see Table 4.2) were evaluated for tack, peel strength, and shear strength. Tack is defined as the strength of adhesion to a surface upon application of light pressure[11]. Peel strength represents the force to remove a PSA from a test panel at a controlled angle[11]. Shear strength represents the internal forces of an adhesive to resist displacement[11].

The results from the 1st factorial design, the second round of screening experiments and the 2nd factorial design were combined to enable the development of empirical models to describe PSA performance. These were used to manipulate reaction conditions and achieve an improved PSA performance. Independent variables used in the models included terpolymer composition, CTA concentration, DVB concentration, number- and weight-average molecular weight, viscosity, and particle size, while the dependent (or response) variables included tack, peel strength and shear strength. All variables were coded as follows (see Equation 4.1, *max* and *min* represent the maximum and minimum of each variable's value):

$$Coded\ value = \frac{actual\ value - \left(\frac{max + \min}{2}\right)}{\frac{|max - min|}{2}} \quad (4.1)$$

Because of correlation between the variables, a stepwise regression approach was used. To account for potential non-linear effects, second-order polynomials were also tested. Each of the three empirical models (for tack, peel strength and shear strength) were evaluated using residual plots, significance tests and lack-of-fit tests. The number of fitted parameters in the models was reduced by considering the p-statistic where the fitted parameter with the largest probability of including zero (p-statistic closest to 1) was removed before the remaining parameters were fit again. This process was repeated until all fitted parameters could reject the null hypothesis (p-statistic < 0.05) that a coefficient equals zero. For all models, there were no trends in the residuals, no lack of fit was found and the model explained a significant amount of variation in the data. The variables were then decoded to arrive at the final, non-coded model form. Despite some cohesive failure for some samples, these were included in the analysis only when their behaviour was consistent with the model, otherwise, these points were not included in the model development. Furthermore, in the interpretation of model results, one should recall that the models should be applied only to the experimental design space; extrapolation of results can only be done with caution.

The coded (Equation 4.2) and final decoded (Equation 4.3) forms for the tack model are:

$$tack\ coded = 0.23 - 0.28M_n + 0.08CTA \cdot d_p + 0.45CTA \cdot Visc$$
$$+1.16M_n \cdot F_{BA} - 0.84CTA^2 - 0.45M_n^2 - 0.01F_{BA}^2 + 0.64F_{CLA}^2$$
$$+1.47F_{BA} \cdot d_p - 0.17d_p^2 - 0.43F_{CLA} \cdot d_p \quad (4.2)$$

$$tack = 13.559 - 0.0001M_n + 0.1401CTA \cdot d_p + 0.0004CTA \cdot Visc$$
$$+0.0002M_n \cdot F_{BA} - 17.908CTA^2 - 2E^{-12}M_n^2 - 206.69F_{BA}^2 + 766.50F_{CLA}^2$$
$$+2.3656F_{BA} \cdot d_p - 0.0063d_p^2 - 1.9801F_{CLA} \cdot d_p \quad (4.3)$$

where M_n is the number-average molecular weight (g/mol), CTA is the CTA concentration (phm), d_p is the particle diameter (nm), Visc is the latex viscosity (mPa s), F_{BA} is the BA fraction bound in the polymer (mol fraction) and F_{CLA} is the CLA fraction bound in the polymer (mol fraction). From the model, one notes that many factors affect tack in a complex manner. It is most instructive to look at the coded version of the model to interpret the relative influence of a particular variable. As expected, tack was greatly influenced by the soft polymer component, BA. Particle size was another highly significant factor and its influence can be attributed to the packing of latex particles during film formation thus changing the surface area for adhesive contact with the substrate. The polymer molecular weight and CTA concentration (which affects molecular weight) were also expected to modify tack due to their influence on polymer flow. Normally, one sees an increase in tack with molecular weight up to a maximum followed by a decrease in tack[19-21]. This expected maximum is reflected by the significance of the second-order terms in the model related to both molecular weight and CTA concentration.

The coded (see Equation 4.4) and final decoded (see Equation 4.5) forms for the peel strength model are:

$$peel\ strength\ coded = 6.04 - 6.39CTA + 0.63Visc + 6.64CTA \cdot M_w + 0.77d_p \cdot M_w$$
$$-0.75Visc \cdot d_p - 0.29Visc^2 - 7.24M_w + 0.08M_w \cdot F_{Sty} \quad (4.4)$$

$$peel\ strength = 2.8424 - 3.7180CTA + 0.0113Visc + 3E^{-5}CTA \cdot M_w + 2E^{-7}d_p \cdot$$
$$M_w - 0.0001Visc \cdot d_p - 6E^{-8}Visc^2 - 2E^{-5}M_w + 2E^{-5}M_w \cdot F_{Sty} \quad (4.5)$$

where M_w is the weight-average molecular weight (g/mol) and F_{Sty} is the Sty fraction bound in the polymer (mol fraction). M_w and CTA (again, due to its effect on M_w) figured prominently in the peel strength model. These two factors should be considered together (and with their interaction effect, 4th term in the model). Overall, as M_w increases one observed the expected effect increased peel strength up to a maximum[19-22]. The influence of particle size and latex viscosity undoubtedly will affect the film formation process which will in turn be expressed as a modification of the peel strength.

The coded (see Equation 4.6) and final decoded (see Equation 4.7) forms for the shear strength model are:

$$shear\ strength\ coded = -0.96 - 0.92M_w + 0.01M_w \cdot CTA + 0.11M_w \cdot F_{CLA}$$
$$+0.65M_w \cdot DVB - 0.71M_n \cdot DVB + 0.15M_n \cdot F_{BA} + 0.14M_w \cdot d_p$$
$$+0.13M_w \cdot Visc + 0.23DVB^2 + 0.62M_n^2 \quad (4.6)$$

$$shear\ strength = -465.88 - 0.0289M_w + 0.0128M_w \cdot CTA + 0.0400M_w \cdot F_{CLA}$$
$$+0.0193M_w \cdot DVB - 0.0290M_n \cdot DVB + 0.0108M_n \cdot F_{BA} + 0.0001M_w \cdot d_p$$
$$+4E^{-7}M_w \cdot Visc + 1678.08DVB^2 + 3E^{-9}M_n^2 \quad (4.7)$$

where DVB is the divinylbenzene concentration (phm). Unlike tack and peel strength, shear strength relates primarily to the internal, cohesive strength of the polymer. According to the model, both molecular weight and crosslinker concentration have the strongest effect on shear strength, as expected[19, 20].

Selected experimental results for tack, peel strength and shear strength are compared to the model predictions in Figure 4.9. Because of the multi-factor influence on the responses, it is difficult to visualize the results in a graphical manner, but obvious and significant effects can be visualized in some cases. The results in Figure 4.9 illustrate only the effects of DVB and CLA concentration, thus other significant factors are being held constant for the model predictions whereas their experimental levels may differ from that used in the model. Nevertheless, the expected trends in the model predictions can be visualized.

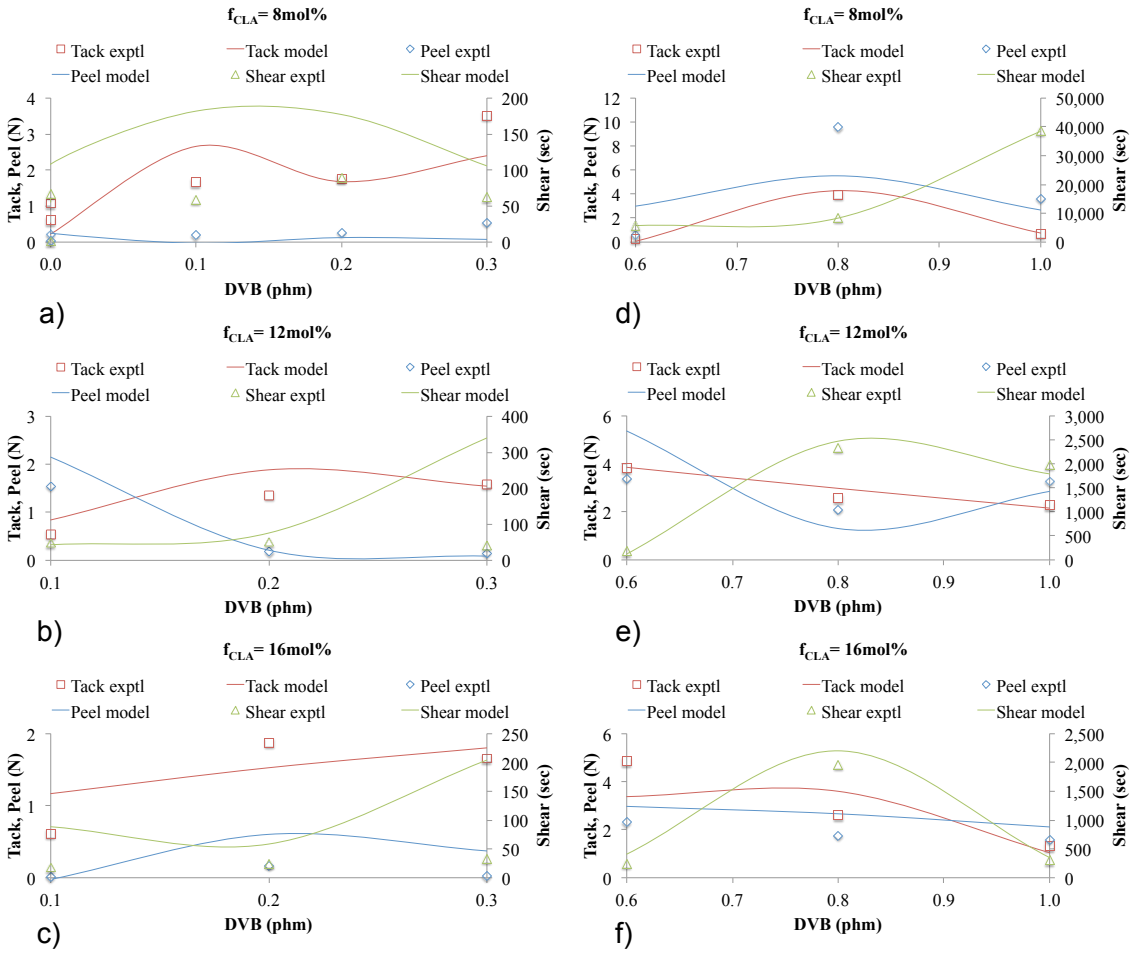

Figure 4.9: Experimental results versus models: a) 1st factorial design, f_{CLA} = 8 mol%; b) 1st factorial design, f_{CLA} = 12 mol%; c) 1st factorial design, f_{CLA} = 16 mol%; d) 2nd factorial design, f_{CLA} = 8 mol%; e) 2nd factorial design, f_{CLA} = 12 mol%; f) 2nd factorial design, f_{CLA} = 16 mol%.

Another approach for visualizing the models is via 3D response surfaces. From the models, 3D response surfaces were generated, as shown in Figures 4.10 to 4.12, for tack, peel strength and shear strength, in this case, as functions of particle size and molecular weight (M_n for tack, M_w for peel strength and shear strength). These figures illustrate regions where improvements to adhesive performance can be made. It is

interesting to note the usual conundrum facing adhesive design where conditions for optimum peel strength differ result in reduced shear strength (compare Figures 4.11 and 4.12). Of course, many 3D response surfaces can be constructed using the other significant variables to assist in visualizing adhesive performance.

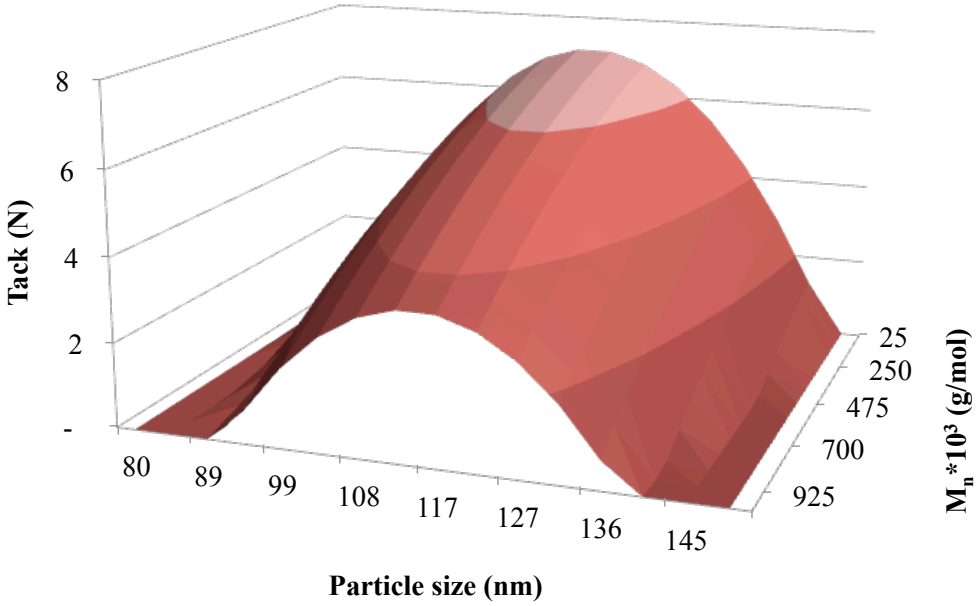

Figure 4.10: 3D response surface for tack model.

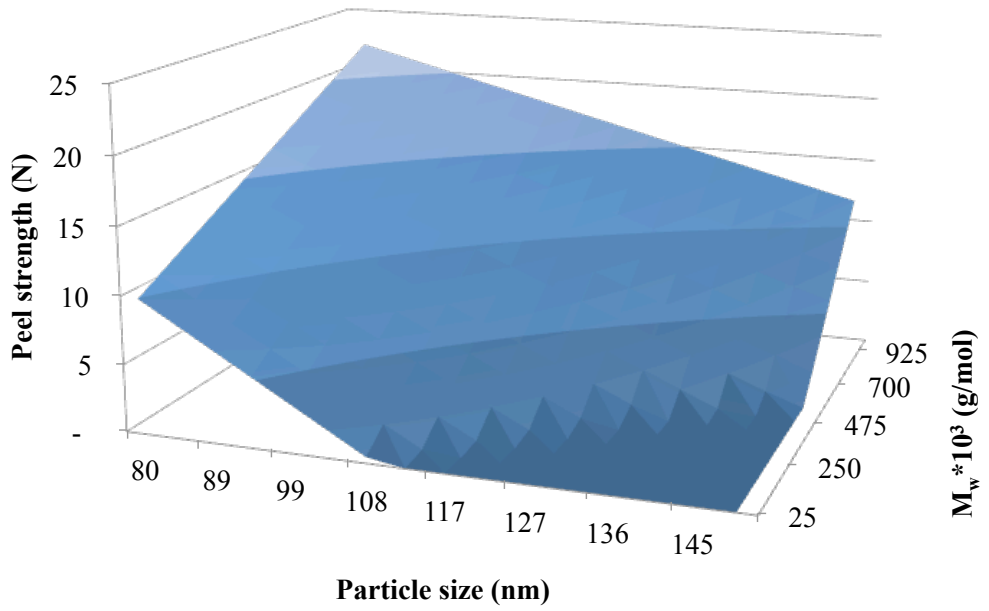

Figure 4.11: 3D response surface for peel strength model.

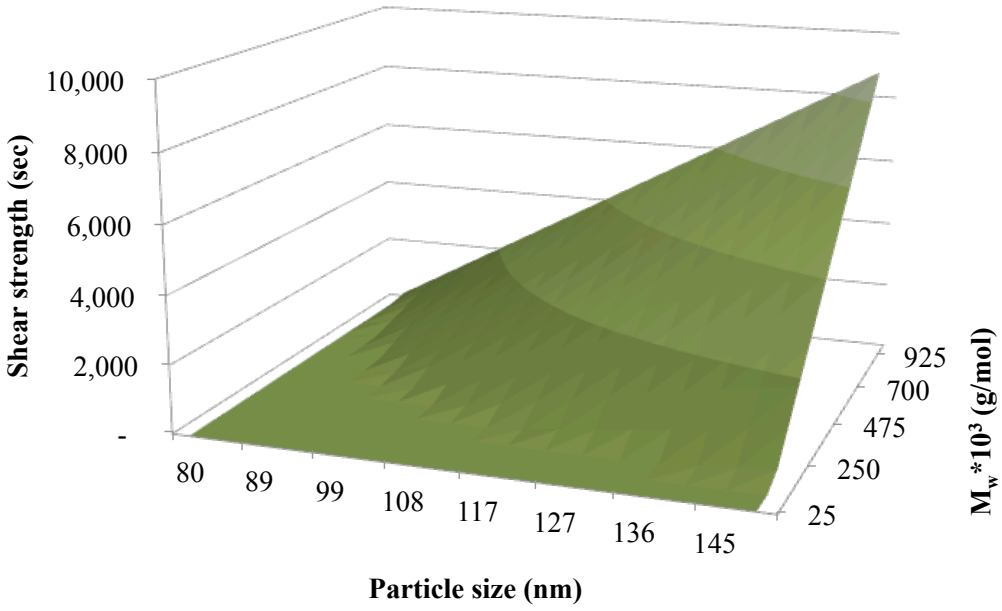

Figure 4.12: 3D response surface for shear strength model.

Latexes from formulations 14 and 15 (see Table 4.2) provided PSA performance in the optimum regions identified by the 3D response surfaces (see Figures 4.10 to 4.12). These adhesives are suitable for applications involving removable adhesives where low shear and low to medium tack and peel are required[23, 24]. Examples of removable adhesives include shelf marking, bus signage and premask. Typically, removable adhesives will have between 30 and 600 min of shear strength, between 1 and 4 N/cm^2 of tack and between 2 and 10 N/cm of peel strength[23, 24]. Latexes from formulations 14 and 15 (see Table 4.2) had between 33 and 39 min of shear strength, between 2.3 and 4.0 N/cm^2 of tack and between 2.1 and 9.5 N/cm of peel strength. The control over polymer particle size and molecular weight allowed the achievement of those targets.

4.3.6 DMA results

Latexes from formulations 14 and 15 (see Table 4.2) were analyzed for their viscoelastic properties. Their storage modulus and loss modulus are shown in Figures 4.13 and 4.14 respectively and were obtained with frequency sweeps at 23 ^{o}C. Similar polymer microstructures, represented in Figures 4.13 and 4.14 with parallel curves between different adhesives, allowed those adhesives to store (G') and dissipate (G") energy similarly under the testing conditions. As expected, the adhesive with the largest storage and loss modulus (Formulation 14, Feed A) had the largest molecular weight, thus providing improved cohesive strength. Consequently, this was also the adhesive with the best PSA performance. Temperature sweeps of the adhesives only produced a single peak on the tan delta curves indicating a homogeneous distribution inside the polymer matrix. These results are consistent with the results obtained with DSC analyses.

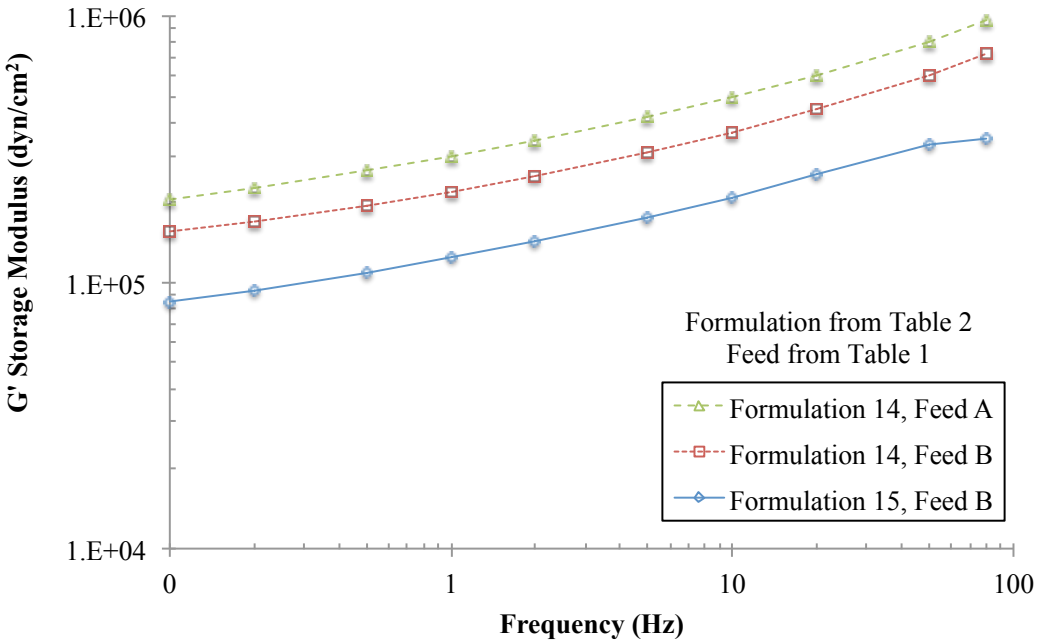

Figure 4.13: Storage modulus (G') versus frequency at 23 °C for three optimized PSAs.

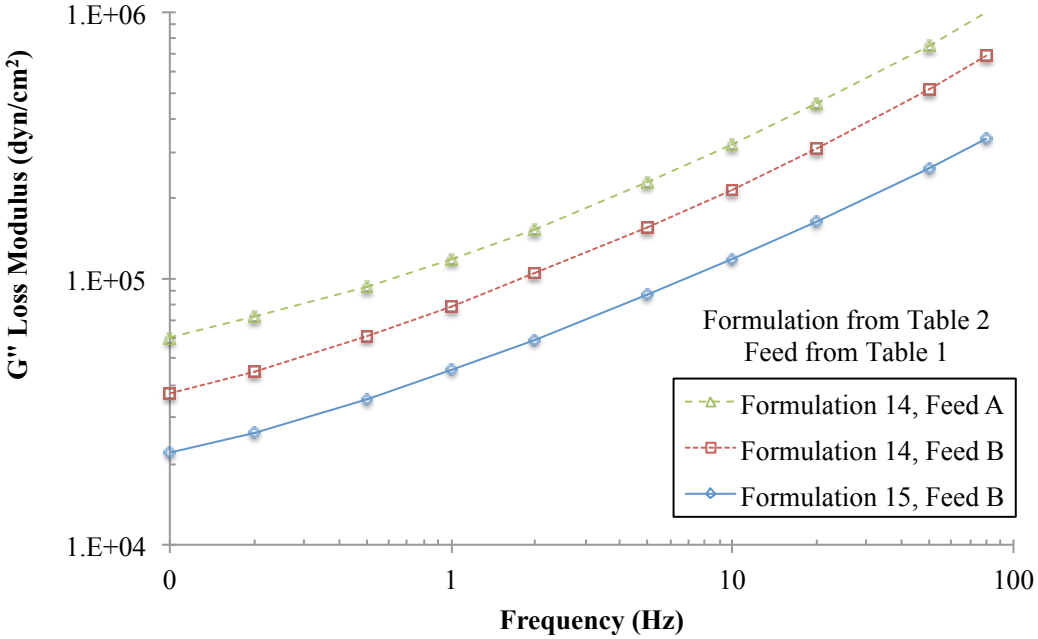

Figure 4.14: Loss modulus (G") versus frequency at 23 °C for .three optimized PSAs

4.4 Conclusions

CLA is a renewable monomer of high interest in potential for polymerization. However, high purity CLA is prohibitively expensive compared to monomers such as Sty and BA. A less costly version is available which contains a significant quantity of saturated fatty acids and oleic acid; this brings the CLA to a cost effective level in the range of most typical monomers. As previously reported[6, 7], the saturated fatty acid component in the CLA does not react with any other components in the reaction mixture. On the other hand, the oleic acid component does play a significant role in the polymerization reaction kinetics by trapping electrons to produce oligomers and subsequently stabilizing itself by resonance. In this work, CLA/Sty/BA emulsion terpolymerizations were performed at 80°C and were shown to strongly favour the polymerization of Sty and BA during terpolymerization. Despite its interference with the polymerization kinetics, the presence of oleic acid in the feed appears to encourage the incorporation of CLA into the terpolymer and modify the polymer molecular weight. The control over the polymer molecular weight, demonstrated by changing the CLA feed compositions, and CTA and DVB concentrations, allowed for improved PSA performance. By using a constrained mixture design, the influence of terpolymer composition, CTA concentration, DVB concentration, molecular weight, viscosity and particle size on PSA performance was investigated. All the models described a statistically significant amount of variation in the data, showed no trend in the residuals and showed no lack of fit. The final forms of the models enabled a path towards improved PSA performance. Further exploration into the optimal adhesive performance

region using the empirical models developed here is now possible. Ultimately, the goal of incorporating high amounts of a renewable monomer (i.e., CLA) into a practical application (i.e., PSA) has been achieved with 30 wt.% incorporation.

4.5 Acknowledgements

The authors gratefully acknowledge the financial support from the Natural Science and Engineering Research Council (NSERC) of Canada and Omnova Solutions (USA). Ms. Liana Martel is also acknowledged for her assistance with some of the polymer characterizations.

4.6 References

1. M.A. Dubé, S. Salehpour, Applying the Principles of Green Chemistry to Polymer Production Industries. Macromol. React. Eng., 2014, 8, 7-28.
2. M. A. R. Meier, J. O. Metzger, U. S. Schubert, Plant oil renewable resources as green alternatives in polymer science. Chem. Soc. Rev., 2007, 36, 1788-1802.
3. F. Li, M. V. Hanson, R. C. Larock, Soybean oil – divinylbenzene thermosetting polymers: synthesis, structure, properties and their relationships. Polymer, 2001, 42, 1567-1579.
4. Z. S. Petrovic, Polyurethanes from vegetable oils. Polym. Rev., 2008, 48, 109-155.
5. D. H. Hewitt, F. Armitage, Styrene copolymers in surface coatings. J. Oil Colour Chem. Assoc., 1946, 29, 109-128.

6. S. Roberge, M. A. Dubé, Bulk Copolymerization of Conjugated Linoleic Acid with Styrene and Butyl Acrylate: Reactivity Ratio Estimation. J. Macromol. Sci., Pure Appl. Chem., 2015, 52, 961-970.

7. S. Roberge, M. A. Dubé, Bulk Terpolymerization of Conjugated Linoleic Acid with Styrene and Butyl Acrylate. Sust. Chem. Eng., DOI: 10.102/acssuschemeng.5b01106

8. A. Eshuis, H. J. Leendertse, D. Thoenes, Surfactant-free emulsion polymerization of styrene using cross-linked seed particles. Colloid Polym. Sci., 1991, 269, 1086-1089.

9. K. S. Jeong, J. Tang, H. Liu, J. Kim, A. W. Schaefer, K. Kemp, L. Levina, X. Wang, S. Hoogland, R. Debnath, L. Brzozowski, E. H. Sargent, J. B. Asbury, Enhanced Mobility-Lifetime Products in PbS Collodial Quantum Dot Photovoltaics. ACS Nano, 2012, 6, 89-99.

10. R. C. Laible, Allyl Polymerizations. Chem. Rev., 1958, 58, 807-843.

11. I. Benedek, L. J. Heymans, Pressure-Sensitive Adhesives Technology, Marcel Dekker Inc., New York, 1997.

12. L. Qie, M. A. Dubé, Manipulation of chain transfer agent and cross-linker concentration to modify latex micro-structure for pressure-sensitive adhesives. Eur. Polym. J., 2010, 1225-1236.

13. S. Roberge, M. A. Dubé, The effect of particle size and composition on the performance of styrene/butyl acrylate miniemulsion-based PSAs. Polymer, 2006, 47, 799-807.

14. R. Jovanovic, K. Ouzineb, T. F. McKenna, M. A. Dubé, Butyl acrylate/methyl methacrylate latexes: Adhesive properties. Macromolecular Symposia. 2004, 206, 43-56.

15. R. R. Chance, S. P. Baniukiewicz, D. Mintz, G. Ver Strate, N. Hadjichristidis, Characterization of Low-Molecular-Weight Polymers: Failure of Universal Calibration in Size Exclusion Chromatography. Int. J. Polymer Analysis & Characterization, 1995, 1, 3.

16. K. Antolin, J-P Lamps, P. Rempp, Y. Gnanou, Synthesis of poly(t-butyl acrylate) macromonomers. Polymer, 1990, 31, 967-970.

17. A. M. Dos Santos, T. F. McKenna, J. Guillot, Emulsion copolymerization of styrene and n-butyl acrylate in presence of acrylic and methacrylic acids: Effect of pH on kinetics and carboxyl group distribution**.** J. of App. Polym. Sci., 1997, 65, 2343-2355.

18. G. Odian, Principles of polymerization, 4th Edition, Chapter 4: Emulsion polymerization, John Wiley and Sons Inc., New Jersey, 2004, p. 351-371.

19. D. Satas, Tailoring pressure sensitive adhesive polymers. Adhes. Age. 1972, 15, 19-23.

20. D. Satas, Handbook of Pressure Sensitive Adhesive Technology; Van Nostrand Reinhold, New York, 1989.

21. T. W. Brooks, R. M. Kell, L. G. Boss, D. E. Nordhaus, Analysis of Factors Important in Emulsion Acrylic Pressure Sensitive, Adhesive Design. TAPPI Proceedings. TAPPI Polymers, Laminations and Coating Conference, Boston, September, 1984, 469-476.

22. J. Y. Charmeau, P. A. Gerin, L. Vovelle, R. Schirer, Y. Holl, Adhesion of Latex Films. III. Surfactant Effects at Various Peel Rates. J. Adhes. Sci. Technol., 1999, 13, 203-215.

23. Technicote Inc., Pressure sensitive adhesive manufacturing, http://www.technicote.com/docs/ Adhesive%20Guide_2014%20SINGLES%20LOW.pdf (last checked December, 2015).

24. FLEXcon, Pressure sensitive adhesive manufacturing, https://www.flexcon.com/resources/tech-guides (last checked December, 2015).

Chapter 5 – Paper on IR Monitoring of CLA

J. Appl. Polym. Sci. **submitted December 2015**

Infrared Process Monitoring of Conjugated Linoleic Acid/Styrene/Butyl Acrylate Bulk and Emulsion Terpolymerization

Stéphane Roberge and Marc A. Dubé*

Department of Chemical and Biological Engineering,
Centre for Catalysis Research and Innovation, University of Ottawa
161 Louis Pasteur Pvt., Ottawa, ON, K1N 6N5 Canada
* *Marc.Dube@uOttawa.ca*

Abstract

Free radical bulk and emulsion co- and terpolymerizations of conjugated linoleic acid (CLA) with styrene (Sty) and butyl acrylate (BA) were performed at 80^{o}C. The polymerizations were monitored using an attenuated total reflectance Fourier transform infrared (ATR-FTIR) spectroscopic probe. Bulk polymerizations were monitored off-line while emulsion polymerizations were monitored in-line. Absorbance peaks related to the monomers and polymer were tracked to provide conversion and polymer composition data using a multivariate calibration method. Off-line measurements using gravimetry and ^{1}H-NMR spectroscopy were compared to the ATR-FTIR data and no significant differences were detected between the measurement methods.

5.1 Introduction

Significant effort is currently being made to replace petroleum-based monomers with more sustainable polymer building blocks. Plant oils offer built-in degradability if cross-linking is not excessive, lower product toxicity[1], and lower gross energy requirement[1] therefore satisfying several green chemistry principles[2]. Plant oils can be less energy intensive to produce than alcohols or sugars because they do not require solvent extraction or intensive heat input. Even if pressing can produce lower yields, the biomass residue called seedcake and comprised mainly of proteins, can be used elsewhere such as in animal feed[3]. Plant oils are made of triglycerides and they consist of a glycerol center with three fatty acid chains. The polymerization of smaller fatty acid chains such as linoleic acid should reduce the steric hindrance associated with the polymerization of the larger triglycerides[4]. Since it appears that conjugated oils copolymerize and non-conjugated oils invoke degradative chain transfer[5], conjugated linoleic acid (CLA) is preferred for free radical polymerizations. Several production methods exist for CLA[6-10] but it can also be produced simply and inexpensively from soybean oil photo-isomerization[11]. In previous work, we reported on the copolymerization and terpolymerization of CLA with styrene (Sty) and butyl acrylate (BA)[12-14] where oleic acid was shown to have a significant impact on the reaction kinetics for bulk and emulsion reactions.

An important principle of green chemistry involves the real-time monitoring of processes[2]. The inline monitoring of polymerizations using an attenuated total reflectance Fourier transform infrared (ATR-FTIR) spectroscopy would satisfy this green chemistry principle and has already been applied to monitoring conversion and polymer

composition in our laboratory[15-17]. In this technique, a sample is placed in contact with an internal reflection element (IRE) with a high refractive index and low infrared absorption in the region of interest. When the infrared beam enters the IRE at an angle just below the critical angle for total internal reflection, an evanescent wave is set up and is designed to penetrate 1-10 μm into the sample[18]. Since the infrared frequencies are similar to the vibrational movements of chemical bonds, the sample will only absorb infrared frequencies matching its own vibrational movements. The remaining infrared beam (or reflection spectra) can be detected to analyze which frequencies were absorbed. This remaining infrared beam intensity will not decrease significantly because the intensity of the evanescent wave decays exponentially with the distance from the IRE, thus allowing thick or strongly absorbing samples (e.g., water) to be analyzed[18]. The frequencies absorbed in the reflection spectra can be associated with functional groups in polymer chains[19]. A quantitative analysis is made possible by applying Beer's law, which stipulates that the absorbance intensity at a certain frequency is proportional to the concentration of the associated component[19]. For the measurement of the reflection spectra, an interferometer is used and a Fourier transform is applied to enhance the spectral resolution. Infrared spectroscopy includes three distinct spectral regions; namely near-infrared (NIR), mid-infrared (MIR) and far-infrared (FIR). The MIR spectral region encompasses the frequencies corresponding to the fundamental vibrations of virtually all functional groups of organic molecules[19]. In this article, we describe the application of ATR-FTIR spectroscopy to the monitoring of bulk and emulsion co- and terpolymerization of CLA, Sty and BA.

5.2 Experimental

5.2.1 Materials

Conjugated linoleic acid (CLA, Penta, 74% CLA, 13% oleic acid, 13% saturated fatty acid) was chosen for economical reasons and used without further purification. One should note that the saturated fatty acid portion of the CLA is non-reactive whereas the oleic acid portion plays the role of an impurity.[12-14] For bulk reactions, the reagents styrene (Sty, Sigma-Aldrich, 99%) and butyl acrylate (BA, Sigma-Aldrich, 99%) were purified to remove the inhibitor, hydroquinone. The initiator, benzoyl peroxide (BPO, Sigma-Aldrich, 100%), and all solvents (e.g., methanol (Fisher, 99.9%) and chloroform-d (Cambridge Isotope Laboratories, 99.8%)), were used as received.

For the emulsion polymerizations, the reagents Sty and BA were used as received. A water-soluble initiator, potassium persulfate (KPS, Fisher, 100%), was used along with the emulsifier, sodium dodecyl sulphate (SDS, EM Science, 100%), and distilled deionized (DDI) water as the suspending medium. In some instances, additives such as sodium bicarbonate ($NaHCO_3$, Fisher, 100%), n-dodecyl mercaptan (CTA, Sigma Aldrich, 98+%, acrylic acid (AA, Acros, 99.5%) and divinylbenzene (DVB, Sigma Aldrich, 80%) were added to modify the latex properties.

5.2.2 Polymerizations

Bulk polymerizations were performed at 80 °C in glass ampoules with 1 cm outside diameter and 17 cm in length (~2-3 g of monomer in each ampoule). The concentration of initiator, BPO, was 2 phm (parts per hundred parts monomer on a mass

basis) for all bulk experiments. To remove oxygen, three freeze-pump-thaw cycles were performed on each ampoule before flame-sealing them. The sealed ampoules were then submerged in a preheated oil bath for a known amount of time before being removed and quenched in an ice bath for 10 min. All samples were analyzed for conversion and polymer composition.

Emulsion polymerizations were performed at 80 °C in a 1.2L, jacketed glass reactor with a Labmax setup and stirred at 200 rpm. The reactor was equipped with a nitrogen pressurizing line, a sampling line, a vent with reflux condenser, and a port for an IR probe. CLA, Sty, BA, CTA, AA, DVB were mixed for 15 min while DDI water, SDS, and $NaHCO_3$ were also mixed for 15 min in a separate beaker. The two solutions were then combined and mixed for 45 min before being poured into the reactor. The oxygen was purged from the emulsion with nitrogen for 45 min while the reaction temperature was raised. After the reaction mixture reached 80 °C, a deoxygenated initiator solution was pumped into the reactor and this marked the beginning of the polymerization. Samples were taken regularly through the sampling line for offline analyses by gravimetry and ^{1}H-NMR spectroscopy.

5.2.3 Characterization

Gravimetry

For the bulk polymerizations, mass conversion based on the total polymer in the reaction mixture was measured using gravimetry. The reaction mixture (~3 g) was first dissolved in acetone (~10 mL) then ~125 mL of methanol was used to precipitate the polymer. The soluble portion of the sample mixture was decanted and the

polymer/methanol samples were left to dry in a fumehood for ~7 days, then under vacuum for ~7 days until a constant weight was reached. The composition from the polymer/methanol samples was used to perform a mass balance and calculate monomer conversion and polymer compositions.

For the emulsion polymerizations, samples of ~3-10 g were taken for off-line testing by gravimetry and ^{1}H-HMR spectroscopy. The samples were dried for ~7 days in the fumehood and ~7 days in a vacuum oven at room temperature, until a constant weight was achieved. The mass of CLA monomer, oleic acid, saturated fatty acid left in the dry sample were subtracted from the measured dry sample mass to calculate the dry polymer conversion[12-14].

^{1}H-NMR Spectroscopy

^{1}H-NMR spectroscopy was used to determine the cumulative copolymer composition. Analyses were carried out at room temperature in deuterated chloroform (~2% w/v) with a Bruker AVANCE III 400 Fourier transform ^{1}H-NMR spectrometer. The acquisition time was 4.6 seconds and 16 scans were performed per sample. A detailed presentation of peak assignments and calculation procedure for copolymer and terpolymer composition was reported previously [12-14].

ATF-FTIR spectroscopy

The bulk polymerizations were monitored offline with a ReactIR™ 45m (Mettler Toledo) reaction analysis system for collecting MIR spectra (4000-650 cm^{-1}) of the polymer/monomer mixture. The ReactIR 45m was equipped with fiber optic technology

for signal transmission from a stainless steel probe. The IRE element of the probe is a diamond composite (DiComp) material. The spectra were collected at a resolution of 8 cm^{-1} with a variable number of scans per sample, which were on average, 128 scans were per sample. For the emulsion polymerizations, spectra were collected in-line, every minute until the end of the reaction. An IR air background spectrum was collected from the empty reactor prior to adding the emulsion formulation.

5.3 Results and Discussion

In an attempt to validate the ATR-FTIR monitoring method for the bulk polymerizations, a series of CLA/Sty, CLA/BA and CLA/Sty/BA bulk experiments at several different compositions were performed at 80 ^{o}C. At the end of the reaction, an IR spectrum of the mixture was taken and the resulting polymer was characterized for polymer composition and conversion using ^{1}H-NMR spectroscopy and gravimetry. The ATR-FTIR monitoring method was then extended to a series of CLA/Sty/BA emulsion polymerizations where the reaction was monitored in-line. Occasional off-line sample characterization was performed using ^{1}H-NMR spectroscopy and gravimetry to validate the results. Both the bulk and emulsion polymerization off-line conversion and polymer composition results were reported previously[12-14].

Table 5.1 shows the feed compositions for the bulk and emulsion polymerizations. It should be noted that 32 different bulk formulations and 40 emulsion formulations were used. For the emulsion polymerizations, some runs contained small amounts of acrylic acid, CTA and DVB to modify latex properties.[14] The primary target application for the emulsion polymerizations was as a pressure-sensitive adhesive and as

such, the feed composition of Sty was kept to ~10 mol% while that of the CLA was kept below 16 mol%.

Table 5.1: Feed composition for bulk and emulsion experiments

Bulk reactions	f_{CLA} (mol frac)	f_{Sty} (mol frac)	f_{BA} (mol frac)
1	0.078	-	0.922
2	0.160	-	0.840
3	0.246	-	0.754
4	0.337	-	0.663
5	0.431	-	0.569
6	0.534	-	0.466
7	0.640	-	0.360
8	0.753	-	0.247
9	0.872	-	0.128
10	0.078	0.922	-
11	0.160	0.840	-
12	0.247	0.753	-
13	0.338	0.662	-
14	0.432	0.568	-
15	0.533	0.467	-
16	0.640	0.360	-
17	0.754	0.246	-
18	0.872	0.128	-
19	0.078	-	0.922
20	0.203	-	0.797
21	0.338	-	0.662
22	0.075	0.925	-
23	0.197	0.803	-
24	0.338	0.662	-
25	0.076	0.103	0.821
26	0.156	0.105	0.740
27	0.240	0.108	0.652
28	0.329	0.111	0.560
29	0.424	0.116	0.461
30	0.524	0.119	0.356
31	0.746	0.127	0.127
32	0.075	0.821	0.103

Emulsion reactions	f_{CLA} (mol frac)	f_{Sty} (mol frac)	f_{BA} (mol frac)
1-25	0.077	0.103	0.820
26-31	0.119	0.104	0.777
32-40	0.161	0.105	0.734

5.3.1 Peak Assignment

The univariate method is a straightforward calibration technique and because of its simplicity it should be attempted prior to the use of a multivariate method[15-17]. In the univariate approach to monitoring polymerizations, the absorbance of the different functional groups within the monomers or polymers are monitored. Each functional group is associated with a characteristic peak, and its concentration is assumed proportional to its absorbance according to Beer's law. This method was applied to a large population (107 spectra) of CLA/Sty, CLA/BA, and CLA/Sty/BA runs by tracking each characteristic peak height from each spectrum as a function of conversion. An example of such a spectrum is shown in Figure 5.1.

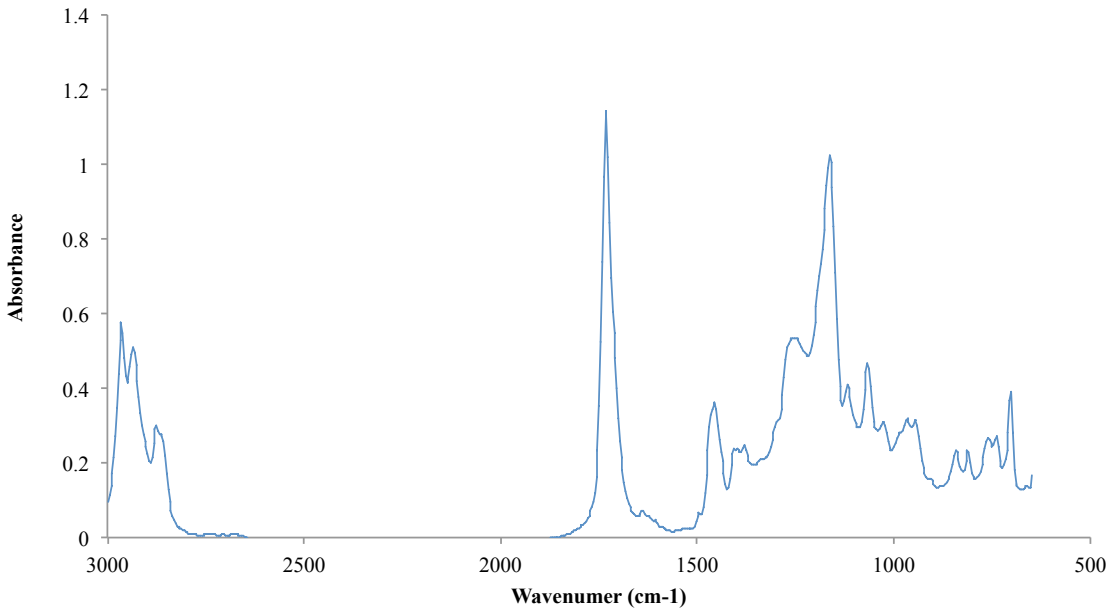

Figure 5.1: Example ATR-FTIR spectrum for bulk CLA/Sty/BA (26/13/61 mol/mol/mol) terpolymer.

Each characteristic peak was evaluated for correlation between the IR peak height and the off-line conversion measurements; some peaks were observed to be strongly correlated. All of the identified peaks were validated with the literature for correct assignment to either the monomer or polymer of CLA[20, 21], Sty[22] and BA[23]. The IR spectra of CLA, Sty, and BA monomers are shown, respectively, in Figures 5.2 to 5.4 and peak assignments are shown in Table 5.2.

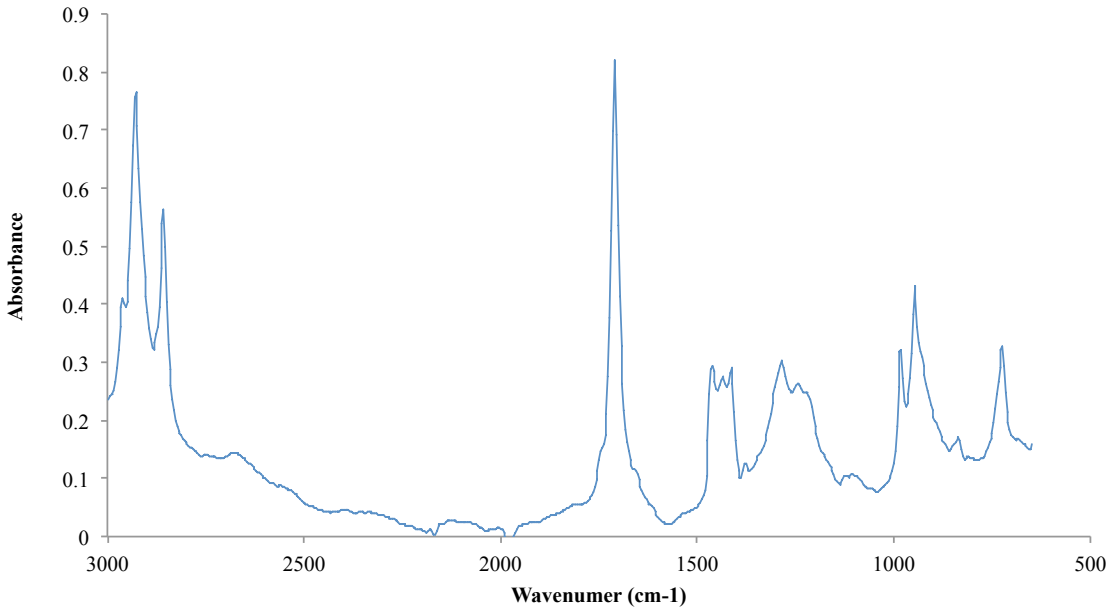

Figure 5.2: ATR-FTIR spectrum of CLA monomer

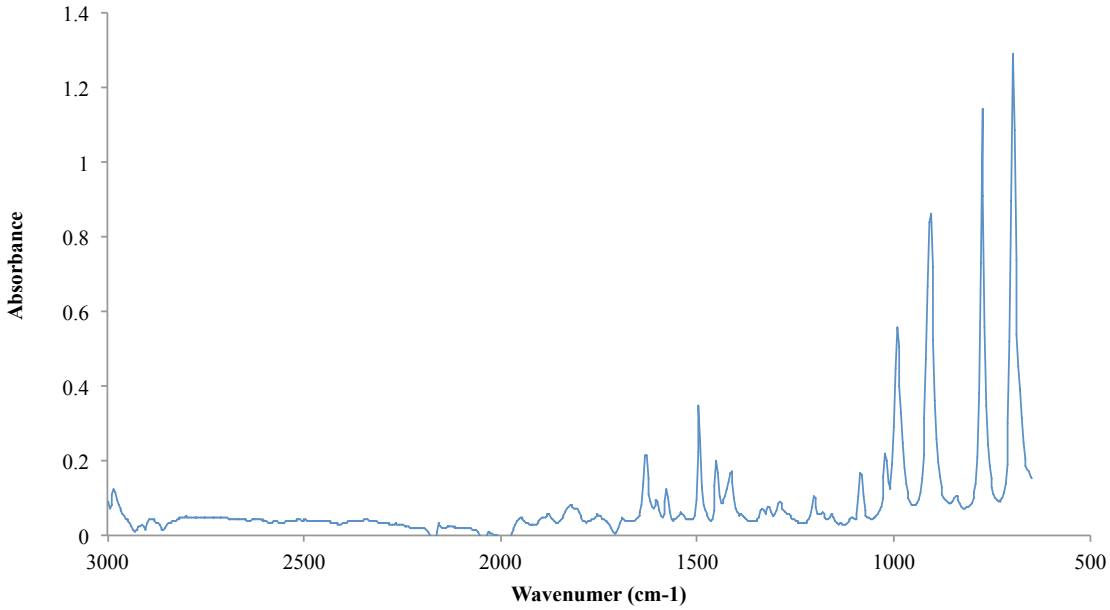

Figure 5.3: ATR-FTIR spectrum of Sty monomer

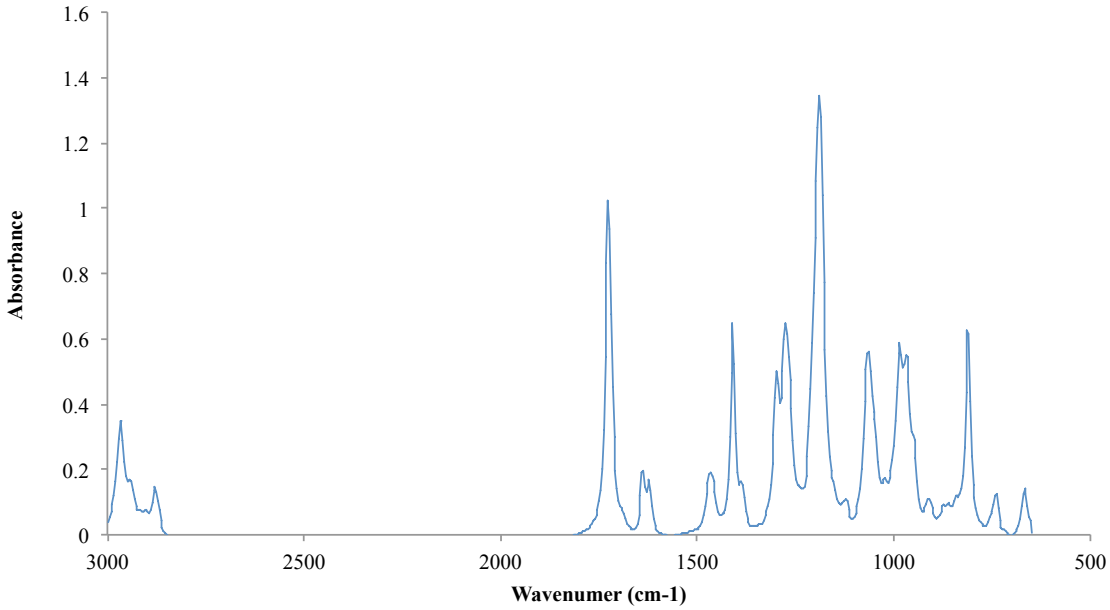

Figure 5.4: ATR-FTIR spectrum of BA monomer

Table 5.2: IR peak assignments for CLA, Sty, BA

Material	Wavenumber (cm^{-1})	Functional group	Comment
CLA	720	-(CH2)n-	aliphatic chains
	948	=C-H vibration	cis,trans dienes
	982	=C-H vibration	cis,trans dienes
	1160	C-O-C on ester group	
	1650	if non-conjugated	no peaks
	1745	-COOH groups	
	2930-2850	-CH2- groups	
	2960	methyl group end	shoulder
	3002	C-H stretching	cis,trans isomer
	3020	C-H stretching	cis,trans isomer
poly-CLA	1711	-COOH groups	
	2856	-CH2- groups	
	2927	-CH2- groups	
Sty	696.6	ring bending	
	773.7	ring C-H wag	
	906.9	-CH2 wag	
	991.8	-CH wag	
	1412	=CH2 deformation	
	1449	ring semi-circle stretching	
	1495	ring semi-circle stretching	
	1630	C=C stretching	
	3010	-CH stretching	
poly-Sty	1066	ring semi-circle stretching	
	1166	-CH-CH2 wag	
	1367	-CH-CH2 wag	
	2856	-CH3 asymmetric stretching	
	2927	-CH2 asymmetric stretching	
BA	668	C=O wagging	
	810	=CH2 twisting	
	1063	=CH2 rocking	
	1187	=C-(C=O)-O-CH2 stretching	aliphatic ester
	1273	=CH rocking	
	1409	C-H deformation in =CH2	
	1725	C=O stretching	
	2950-2850	aliphatic C-H stretching	
poly-BA	1470	C-H deformation	methyl band
	1740	C=O stretching	

As expected, the Sty and BA monomer peak heights trended down with conversion and the identified Sty and BA polymer peak heights trended up with conversion. When monitoring the CLA peaks, all the peak heights trended up with conversion indicating a probable overlap between monomer and polymer peaks. As a result of the above observations, a more complex multivariate calibration method was chosen for the IR monitoring of our reactions.

5.3.2 Multivariate Calibration Method for Bulk Polymerizations

A multivariate (partial least squares (PLS) regression) calibration was developed from 42 spectra selected from the bulk CLA/Sty, CLA/BA, and CLA/Sty/BA runs (see Table 5.1). QuantIR software from ReactIR 45m (Mettler Toledo) was used to perform the analysis. With the PLS approach, a set of calibration spectra are reduced to a smaller number of key spectra (called factors) taken in a linear combination to approximate the original spectral data. Each of those factors is composed of multiple peaks within the same spectral region. A predicted residual error sum of squares (PRESS) analysis is used to select the optimum number of factors for each component (composition or conversion). As factors that represent useful information are added to the analysis, the PRESS value decreases, indicating improvement in the PLS calibration error. At some point, the factors add unnecessary information and the PRESS value levels off or increases. The correct number of factors to select is associated to the initial levelling off point.

For the bulk polymerizations, the entire spectral region was chosen for the PRESS analyses performed on both conversion and polymer composition data. The optimum

number of factors was chosen (as suggested by the QuantIR software) as 8 for all four calibration models (i.e., overall conversion, and CLA, Sty and BA polymer compositions) and those results are shown in Figure 5.5.

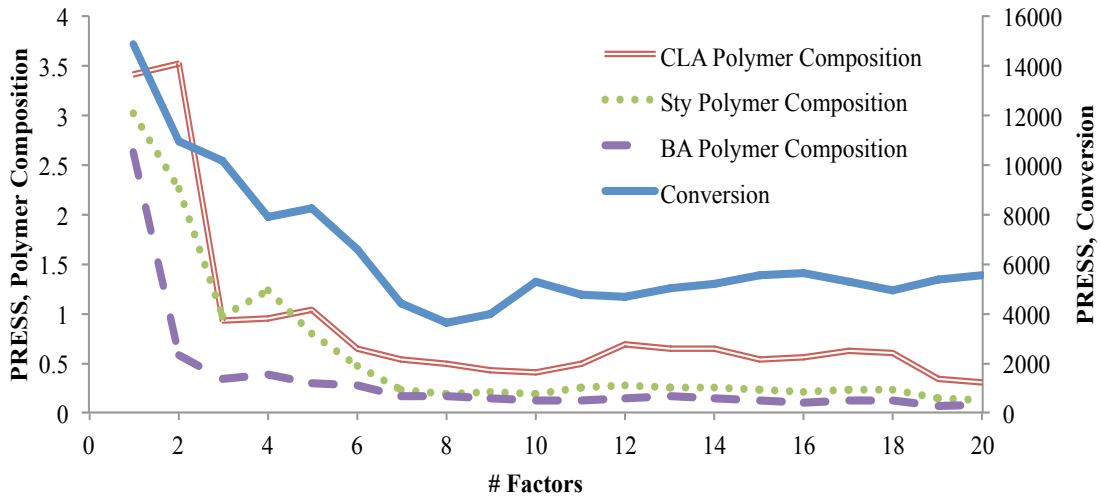

Figure 5.5: PRESS analyses for conversion and polymer compositions in bulk

The PLS models were built to establish a predictive relationship between the factors and the off-line gravimetric and ^{1}H-NMR measurements. Out of the 107 spectra available for these analyses, 42 were used for calibration (or training as it is referred to by the QuantIR software) and 65 were used for validation (or testing). Each of the four models was successfully calibrated and validated using the same set of spectra. Model predictions versus off-line data are shown in Figure 5.6 for conversion, and CLA, Sty and BA polymer compositions. All of the data used for calibration as well as for validation are included in Figure 5.6.

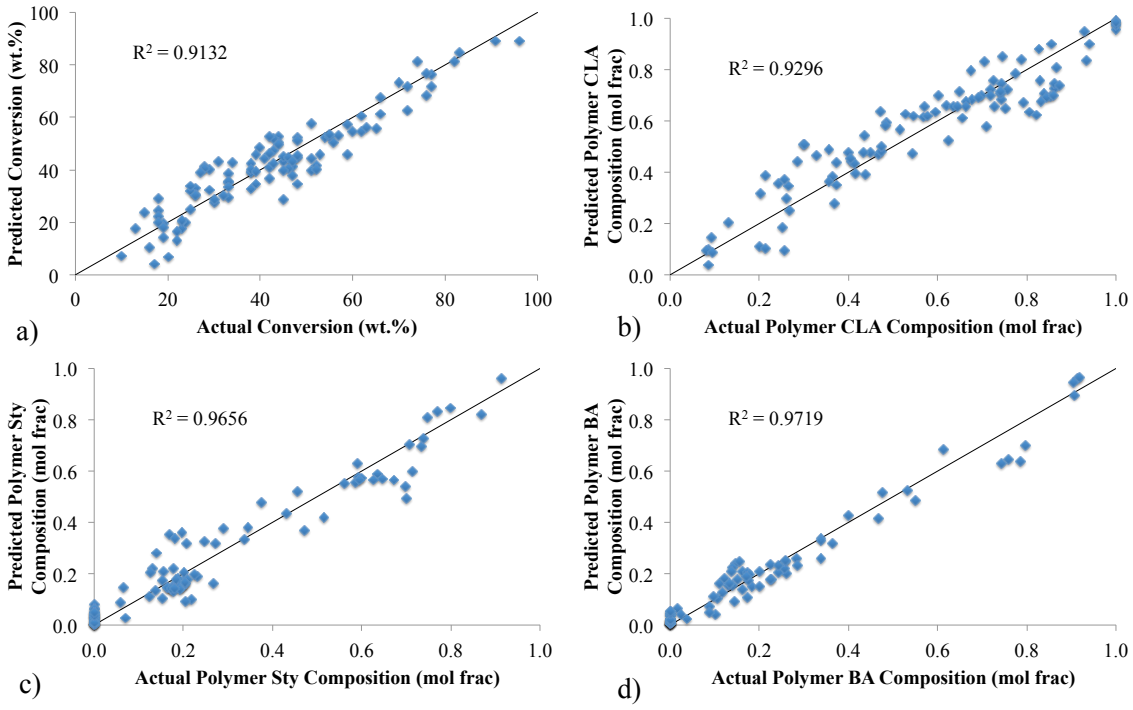

Figure 5.6: PLS predictions for bulk polymerizations: a) overall conversion, b) CLA polymer composition, c) Sty polymer composition, and d) BA polymer composition.

A paired comparison was carried out between the model predictions and the actual data. 95% confidence intervals for the difference between the off-line and ATR-FTIR data were found to include zero for all four models, indicating that no significant differences existed. The 95% confidence intervals were [-1.71, 0.80] (wt.%) for conversion, [-0.0125, 0.0208] (mole fraction) for CLA polymer composition, [-0.0116, 0.0132] (mole fraction) for Sty polymer composition, and [-0.0133, 0.0033] (mole fraction) for BA polymer composition.

5.3.3 Multivariate Calibration Method for Emulsion Polymerizations

As was the case for the bulk polymerizations, univariate calibration was attempted for the CLA/Sty/BA emulsion terpolymerizations and yielded similar results. Thus, the PLS calibration was applied to the emulsion polymerization runs (see Table 5.1). A total of 70 spectra were available for analysis. Figure 5.7 shows sample spectra for the duration of an emulsion terpolymerization. The PRESS analysis (see Figure 5.8) suggested the use of 9 factors for all four calibration models (i.e., overall conversion, and CLA, Sty and BA polymer compositions). Out of the 70 spectra used in these analyses, 55 were used for calibration (or training) and 15 were used for validation (or testing). All four models were successfully calibrated using the same set of spectra. Model predictions versus off-line data are shown in Figure 5.9 for conversion, and CLA, Sty and BA polymer compositions. It should be noted that all of the data used for both calibration and validation are included in Figure 5.9.

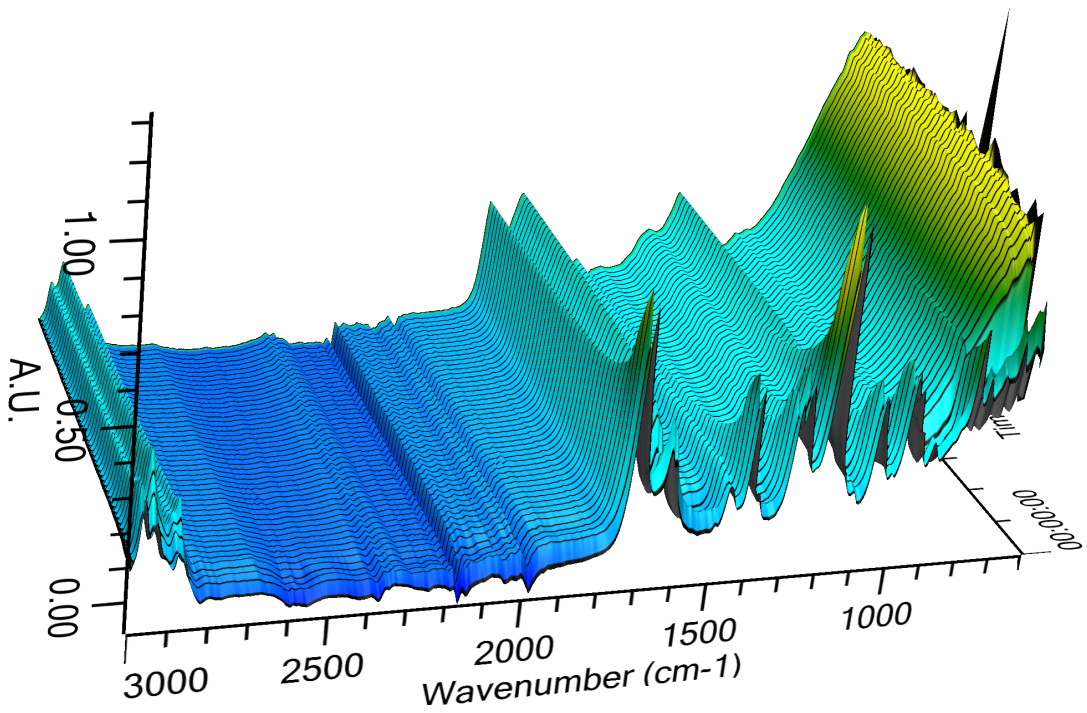

Figure 5.7: Example IR reaction spectra for CLA/Sty/BA: 8/10/82 mol/mol/mol feed composition

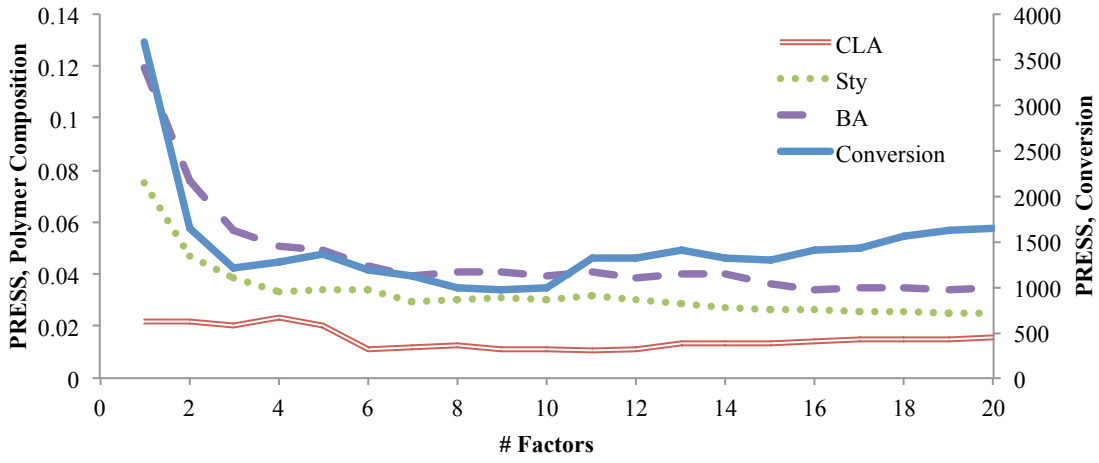

Figure 5.8: PRESS analyses for conversion and polymer composition in emulsion.

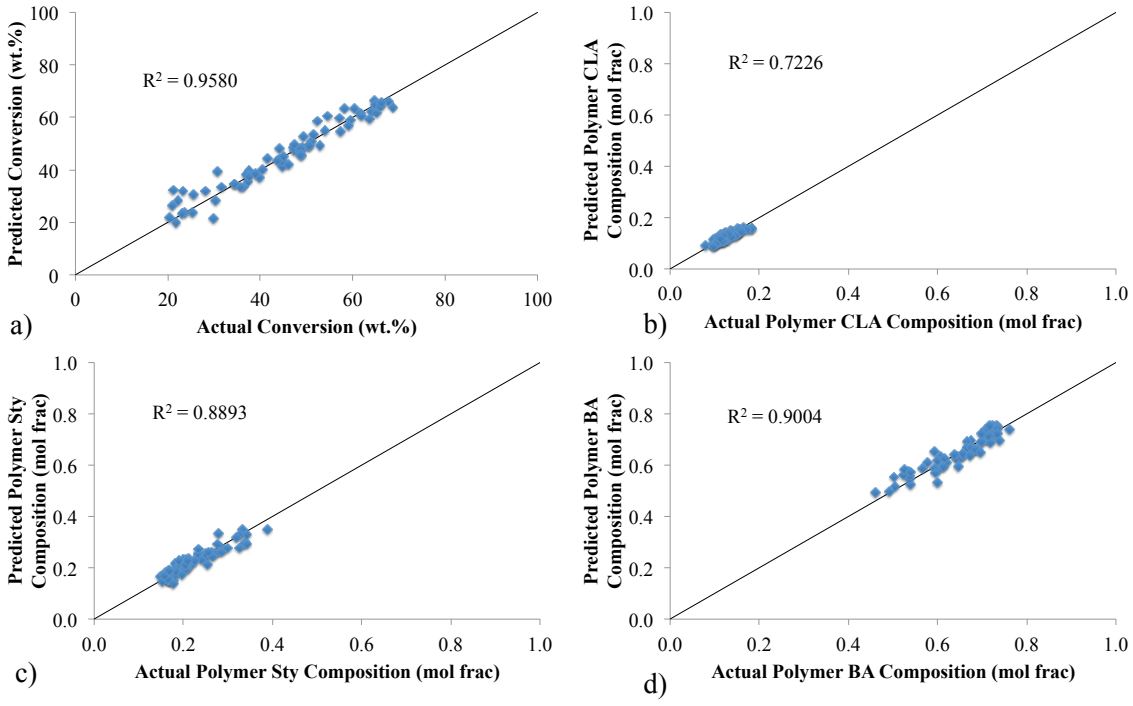

Figure 5.9: PLS predictions for emulsion polymerizations: a) overall conversion, b) CLA polymer composition, c) Sty polymer composition, and d) BA polymer composition.

As in the case for the bulk polymerizations, paired comparisons were carried out between the model predictions and the off-line data. 95% confidence intervals for the difference between the calibration model and the off-line data were found to include zero for all four models, indicating that no significant differences existed. The 95% confidence intervals are [-0.44, 1.18] (wt.%) for overall conversion, [-0.0028, 0.0030] (mole fraction) for CLA polymer composition, [-0.0063, 0.0041] (mole fraction) for Sty polymer composition, and [-0.0051, 0.0072] (mole fraction) and for BA polymer composition.

Another valuable consequence of in-line data collection is driven home in Figure 5.7. One notes that, in Figure 5.7, two large peaks at ~1190 cm^{-1} and at ~1730 cm^{-1}

increased quickly during the first 5-10 min of the reaction, and then decreased. These changes were rapid enough to make the monitoring of the true trajectory via off-line sampling difficult. According to our peak assignments, both of these peaks relate to both CLA polymer and BA monomer, i.e., the CLA polymer and BA monomer peaks overlap at both 1190 and 1730 cm^{-1} (refer to Table 5.2). This trajectory confirms earlier speculation on the behaviour of the oleic acid impurity found in the CLA.[12-14] An initial production of CLA-rich oligomers is reflected by the sharp increase in the two peaks for the first 5-10 min. When the effect of oleic acid, acting as an impurity, has abated, the consumption of BA monomer then causes the decrease of those same peaks due to their overlapping functional groups with that of the CLA polymer. Of course, if the peaks were strictly assigned to a monomer, one would expect the peaks to reach an absorbance near zero. In Figure 5.7, that is clearly not the case and the peaks level off due to the produced CLA polymer (oligomers). It should be added that the oleic acid and saturated fatty acid peak assignments overlap with that of the CLA. As the oleic acid and saturated fatty acid are not consumed, the peaks associated to these should not be affected.

5.4 Conclusions

The successful off-line and in-line monitoring of bulk and emulsion CLA/Sty/BA co- and terpolymerizations was achieved. The calibration models were validated using off-line data and no significant differences between the ATR-FTIR results and the off-line data were found. Beyond simply monitoring these polymerizations, the in-line monitoring method provided an interesting confirmation of the reaction kinetics. This kinetic observation demonstrates the value of a continuous in-line monitoring procedure

when fast kinetics precludes the ability to monitor a reaction using intermittent, costly and time-consuming off-line measurements.

5.5 Acknowledgements

The authors wish to gratefully acknowledge the financial support from the Natural Science and Engineering Research Council (NSERC) of Canada and Omnova Solutions (USA).

5.6 References

1. M. A. R. Meier, J. O. Metzger, U. S. Schubert, Plant oil renewable resources as green alternatives in polymer science. Chem. Soc. Rev., 2007, 36, 1788-1802.
2. M. A. Dubé, S. Salehpour, Applying the Principles of Green Chemistry to Polymer Production Industries. Macromol. React. Eng., first published online August 29th, 2013.
3. J. W. Lee, Advanced Biofuels and Bioproducts, Volume 1, Springer, New York, 2013, p. 1-1099.
4. Z. S. Petrovic, Polyurethanes from vegetable oils. Polym. Rev., 2008, 48, 109-155.
5. D. H. Hewitt, F. Armitage, Styrene copolymers in surface coatings. J. Oil Colour Chem. Assoc., 1946, 29, 109-128.
6. M. S. Manic, V. Najdanovic-Visak, M. Nunes da Ponte, Z. P. Visak, Extraction of free fatty acids from soybean oil using ionic liquids or poly(ethyleneglycol)s. AIChE J., 2011, 57, 1344-1355

7. J. Ogawa, s. Kishino, A. Ando, S. Sugimoto, K. Mihara, S. Shimizu, Production of Conjugated Fatty Acids by Lactic Acid Bacteria. J. Biosci. Bioeng., 2005, 100, 355-364.

8. G. L. Jin, S. H. Choi, H. G. Lee, Y. J. Kim, M. K. Song, Effects of Monensin and Fish Oil on Conjugated Linoleic Acid Production by Rumen Microbes in Holstein Cows Fed Diets Supplemented with Soybean Oil and Sodium Bicarbonate. Asian-Aust. J. Anim. Sci., 2008, 21, 1728-1735.

9. V. P. Jain, T. Tokle, S. Kelkar, A., Proctor, Effect of the Degree of Processing on Soy Oil Conjugated Linoleic Acid Yields. J. Agric. Food Chem., 2008, 56, 8174-8178.

10. R. Gangidi, A. Proctor, Photochemical production of conjugated linoleic acid from soybean oil. Lipids, 2004, 39, 577-582.

11. R. Gangidi, A. Proctor, Photochemical production of conjugated linoleic acid from soybean oil. Lipids, 2004, 39, 577-582.

12. S. Roberge, M. A. Dubé, Bulk Copolymerization of Conjugated Linoleic Acid with Styrene and Butyl Acrylate: Reactivity Ratio Estimation. J. Macromol. Sci., Pure Appl. Chem., 2015, 52, 961-970.

13. S. Roberge, M. A. Dubé, Bulk Terpolymerization of Conjugated Linoleic Acid with Styrene and Butyl Acrylate. Sust. Chem. Eng., 2015, DOI: 10.102/acssuschemeng.5b01106.

14. S. Roberge, M. A. Dubé, Emulsion Terpolymerization of Conjugated Linoleic Acid with Styrene and Butyl Acrylate. Int. J. Adhes. Adhes., **submitted December 2015**.

15. H. Hua, M. A. Dubé, Terpolymerization monitoring with ATR-FTIR spectroscopy. J. Polym. Sci., Part A: Polym. Chem., 2001, 39, 1860-1876.

16. H. Hua, M. A. Dubé, In-line monitoring of emulsion homo- and copolymerizations using ATF-FTIR spectroscopy. Polym. React. Eng., 2002, 10, 21-39.

17. S. Roberge, M. A. Dubé, In-line monitoring of styrene/butyl acrylate miniemulsion polymerization with attenuated total reflectance/Fourier transform infrared spectroscopy. J. Appl. Polym. Sci., 2007, 103, 46-52.

18. H. Gunzler, H. U. Gremlich, IR Spectroscopy an Introduction, Wiley-VCH, Weinheim, 2002.

19. N. B. Colthup, L. H. Daly, S. E. Wiberley, Introduction to Infrared and Raman Spectroscopy, 3rd Edition, Academic Press, San Diego, 1990, p. 1-547.

20. F. S. Guner, Y. Yagci, A. T. Erciyes, Polymers from triglyceride oils. Prog. Polym. Sci., 2006, 31, 633-670.

21. R. Kapoor, M. Reaney, N. D. Westcott, Bailey's Industrial Oil and Fat Products, Chapter 1: Conjugated Linoleic Acid Oils (eds. F. Shahidi), 6th Edition, 6 Volume Set, John Wiley and Sons Inc., New York, NY, USA, 2005, p. 1-35.

22. M. A. Dubé, L. Li, In-line monitoring of SBR emulsion polymerization using ATR-FTIR spectroscopy. Polym. Plast. Technol. Eng., 2010, 49, 648-656.

23. R. Jovanovic, M. A. Dubé, Off-line monitoring of butyl acrylate and vinyl acetate homopolymerization and copolymerization in toluene. J. Appl. Polym. Sci., 2001, 82,2958-2977.

Chapter 6 – General Discussion and Conclusion

The incorporation of renewable monomers into polymer applications will provide future generations with sustainable polymer production methods. With the ultimate goal focused on replacing 100% of petroleum monomers by renewable monomers, interim solutions should be provided to facilitate the shift to this new paradigm. The incorporation of 15-25% renewable monomers into polymer applications will attract the polymer production companies' interest and provide one such interim solution. CLA, being derived from plant oils, is considered a renewable monomer and this research project evaluated the hypothesis that CLA could be incorporated into polymer applications such as pressure-sensitive adhesives (PSAs).

6.1 Bulk copolymerizations with CLA/Sty and CLA/BA

This work was performed for the determination of the monomer reactivity ratios and to clarify the copolymerization kinetics. High purity CLA is prohibitively expensive compared to monomers such as Sty and BA. However, a less costly version is available which contains a significant quantity of saturated fatty acids and oleic acid; this makes the CLA only moderately more expensive than Sty and BA. Important observations were made by performing mass balances via the ^{1}H-NMR spectroscopy results. The saturated fatty acid does not react with any other components in the reaction mixture but the oleic acid plays a significant role in reaction kinetics without being incorporated into the copolymer. The strong effect on the reaction kinetics arose from the oleic acid which trapped electrons from freshly initiated radicals and oligomer radicals, followed by a

stabilization by resonance of the oleic acid radical. A pseudo-kinetic model was developed to include the oleic acid's ability at trapping electrons and was successful at predicting polymer composition when the conversion was known (see Figures 6.1 and 6.2). The reactions were shown to start with a fast production of CLA-rich oligomers until the effect of oleic acid has abated, followed by the dominant polymerization of the co-monomers (i.e., Sty or BA) and ending with a slow CLA consumption in an increasingly viscous reaction medium.

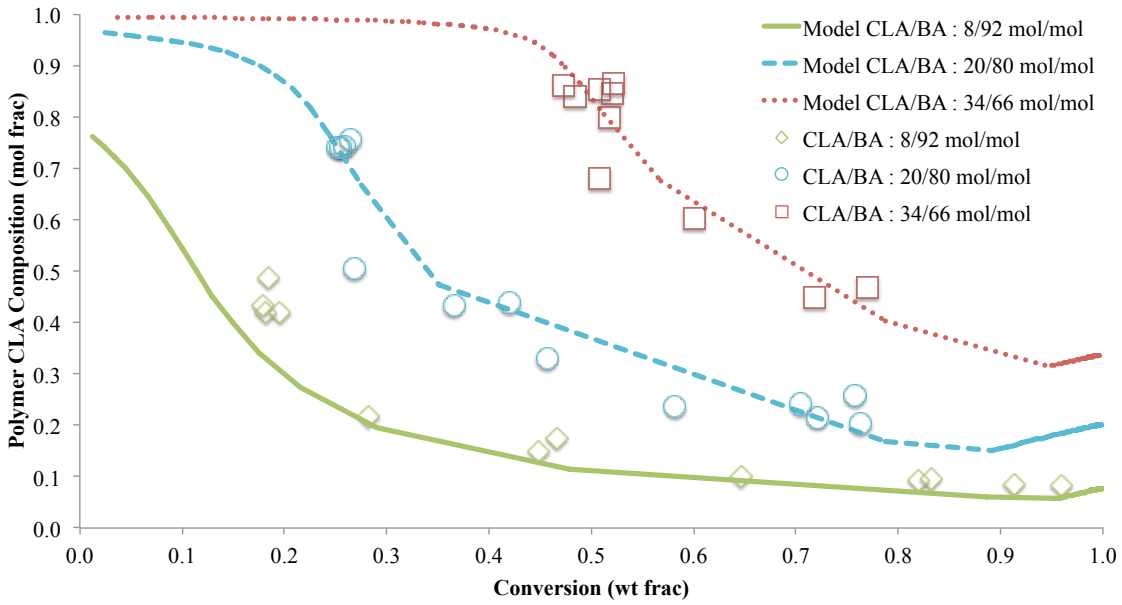

Figure 6.1: Copolymer composition versus conversion for CLA/BA copolymers

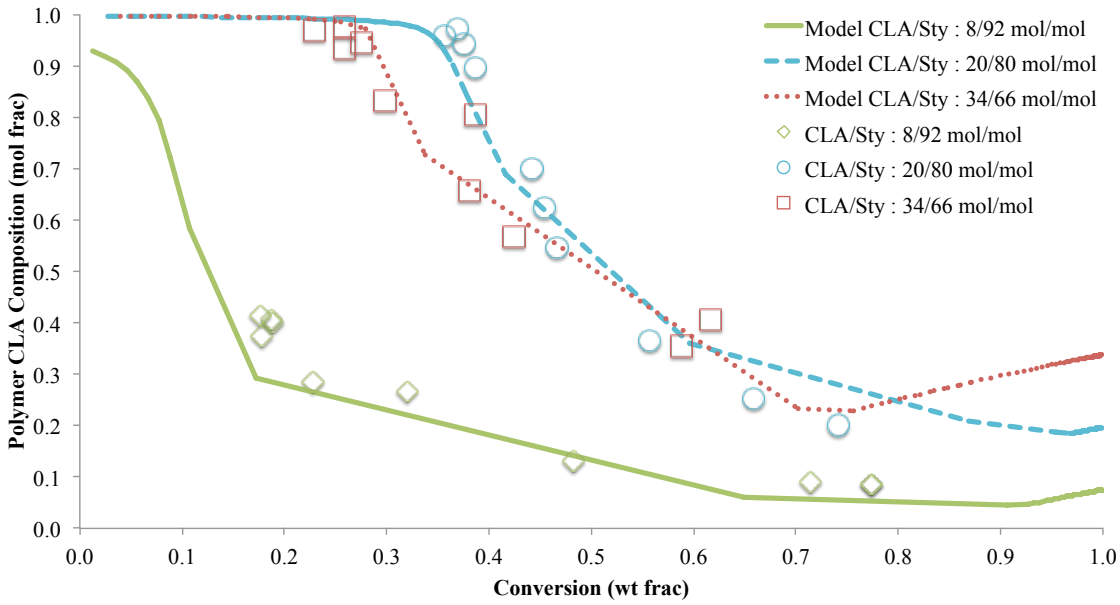

Figure 6.2: Copolymer composition versus conversion for CLA/Sty copolymers

The pseudo-kinetic models also allowed the estimation of reactivity ratios for the CLA/Sty and CLA/BA systems respectively (see Table 6.1). The reactivity ratios indicate that CLA will not easily incorporate into the copolymer at a high rate. Rather, the presence of oleic acid allows for a CLA-rich oligomer production at the beginning of the reaction.

Table 6.1: Reactivity ratios estimated from copolymer kinetic models

	Reactivity ratios
r_{CLA}	0.05
r_{BA}	10080
r_{CLA}	0.1
r_{Sty}	11367

Molecular weight results indicated relatively flat molecular weight profiles when the CLA feed concentration was 8 mol% (see Figures 6.3 and 6.4) At higher CLA feed concentrations, the molecular weights are relatively quite low and show a steeply sloping increase with conversion. This is entirely consistent with the presence of greater amounts of oleic acid in the system. Only low molecular weight oligomers are formed at the early stages of the reaction, while the molecular weights increased significantly after the effect of oleic acid has abated. Despite its interference with the polymerization kinetics, some oleic acid in the feed could be favourable towards the incorporation of CLA into the polymer and could be used to adjust polymer molecular weight. Attempts at homopolymerizing CLA resulted only in the production of small oligomers.

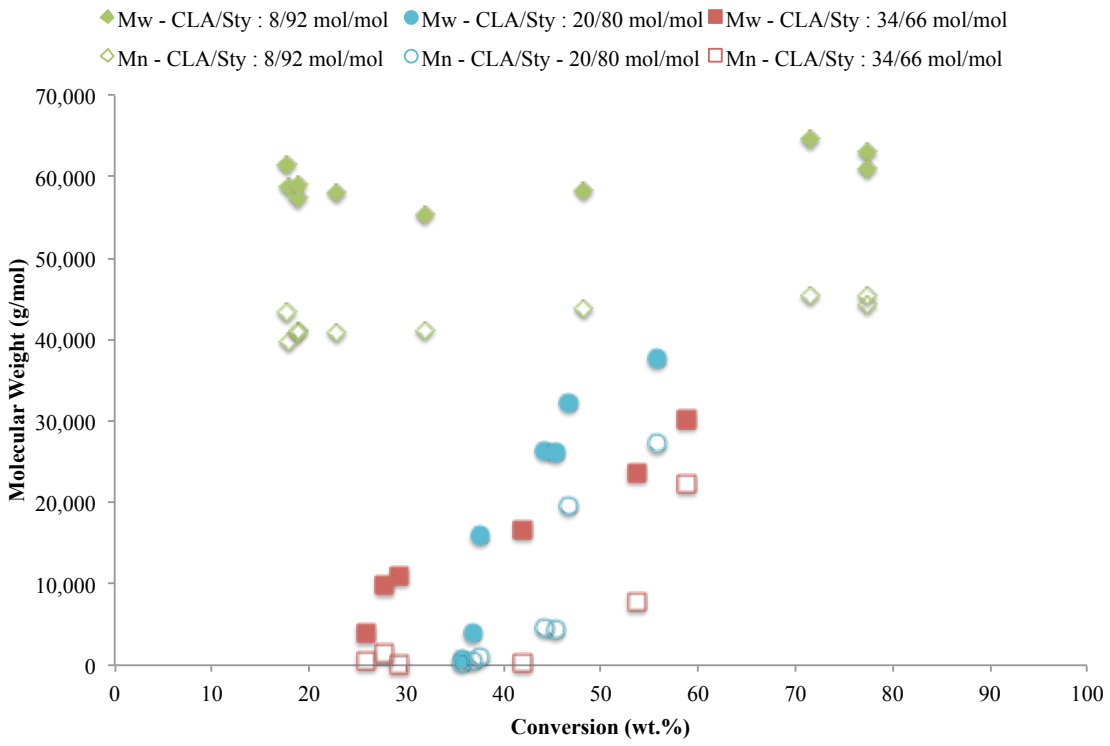

Figure 6.3: Weight-average molecular weight versus conversion for CLA-Sty polymer systems

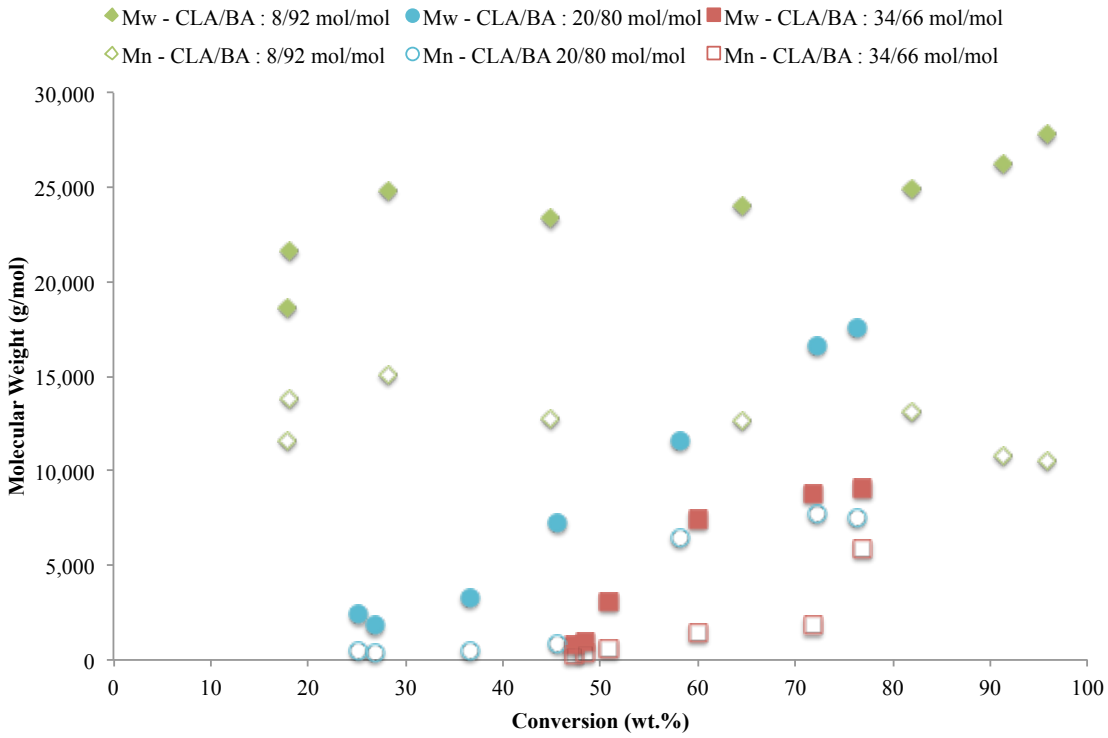

Figure 6.4: Weight-average molecular weight versus conversion for CLA-BA polymer systems

6.2 Bulk terpolymerizations with CLA/Sty/BA

This work was performed as a preliminary study before attempting emulsion terpolymerization and to clarify the terpolymerization kinetics. As a continuity to the copolymer experiments, low cost CLA was chosen. Mass balances via the ^{1}H-NMR spectroscopy results confirmed that oleic acid and saturated fatty acids were not incorporated into the polymer chains. A pseudo-kinetic model was developed to include

the oleic acid's ability at trapping electrons and was successful at predicting polymer composition when the conversion was known (see Figures 6.5 and 6.6). All parameter values previously optimized for the copolymer systems were used as is and no further parameter estimation was necessary.

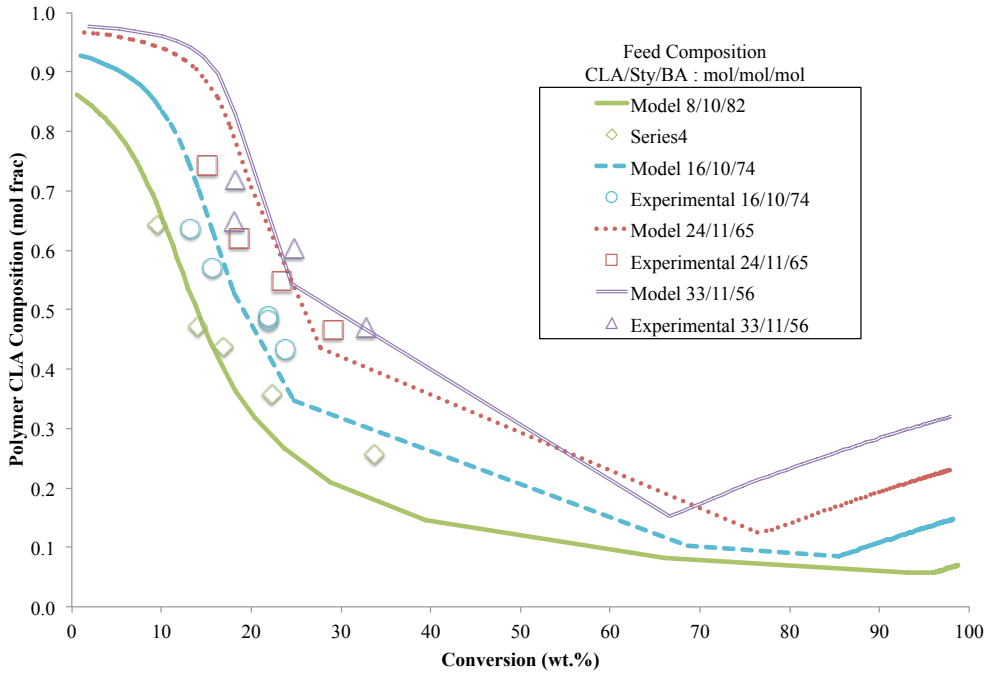

Figure 6.5: Terpolymer CLA composition versus conversion (higher BA feed concentration)

Parameter optimization for the copolymer systems led to the conclusion that the terms for Sty and BA initiation reactions were negligible compared to that of CLA. The significance of the CLA initiation term suggests that CLA readily reacts with initiator,

more so than would Sty and BA. During the initial reaction stages, CLA-rich oligomeric species are generated because oleic acid, which acts as an electron trap, quickly terminates any initiated polymer chains. As the reaction proceeds and the oleic acid is deactivated (i.e., space for electron trapping is filled), Sty and BA begin to dominate the polymerization due to their higher rates of propagation; this is due to their smaller size relative to CLA in the face of increasing reaction viscosity. In other words, the CLA propagation parameter reflects a viscosity impediment and is thus, an "effective" rate parameter (recall that we refer to this as a pseudo-kinetic model).

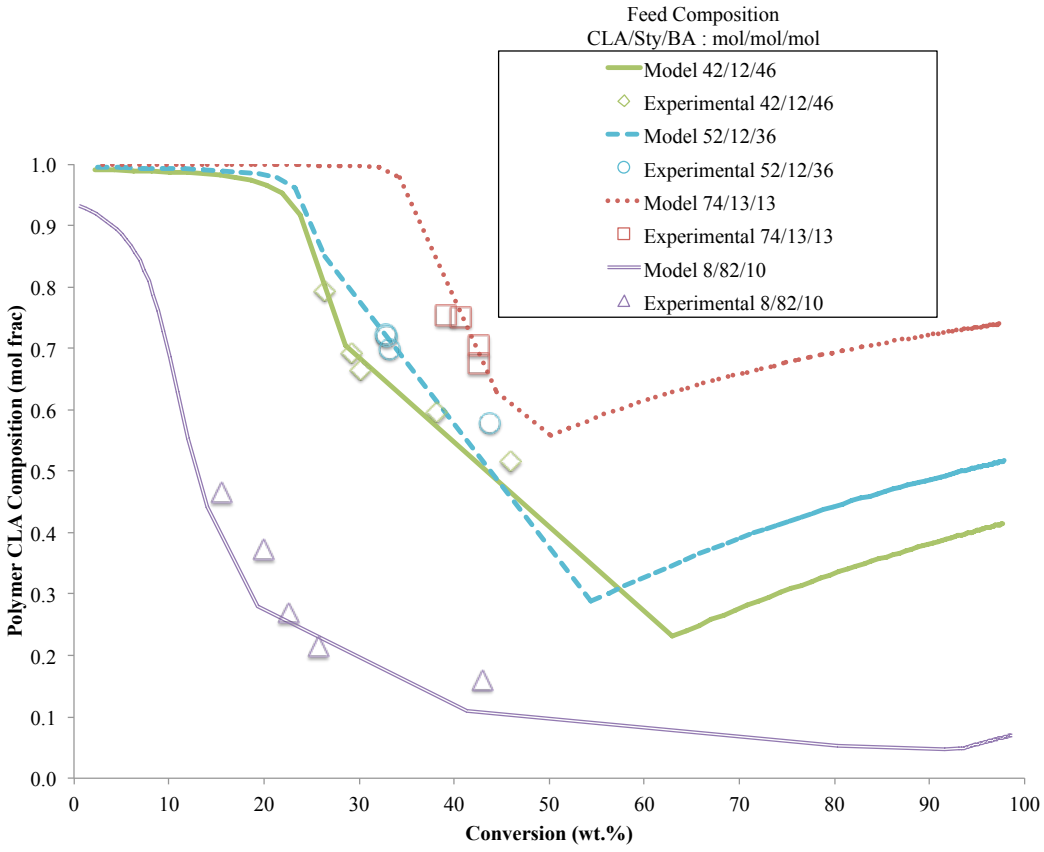

Figure 6.6: Terpolymer CLA composition versus conversion (lower BA feed concentration)

Molecular weight results for the terpolymer system produced similar observations when compared to the copolymer systems (see Figure 6.7). With an 8 mol% CLA feed concentration, an increasing molecular weight profile was observed when the feed was rich in BA and a decreasing molecular weight profile was observed when the feed was rich in Sty. With 16, 24, and 33 mol% CLA feed concentrations, a relatively flat molecular weight profile was observed with decreasing molecular weights when the CLA feed concentration was increased. At higher CLA feed concentrations, the molecular weights are relatively quite low and show a steeply sloping increase with conversion. This is entirely consistent with the presence of greater amounts of oleic acid in the system. Only low molecular weight oligomers are formed at the early stages of the reaction, while the molecular weights increased significantly after the effect of oleic acid has abated. Despite its interference with the polymerization kinetics, some oleic acid in the feed could be favourable towards the incorporation of CLA into the polymer and could be used to adjust polymer molecular weight.

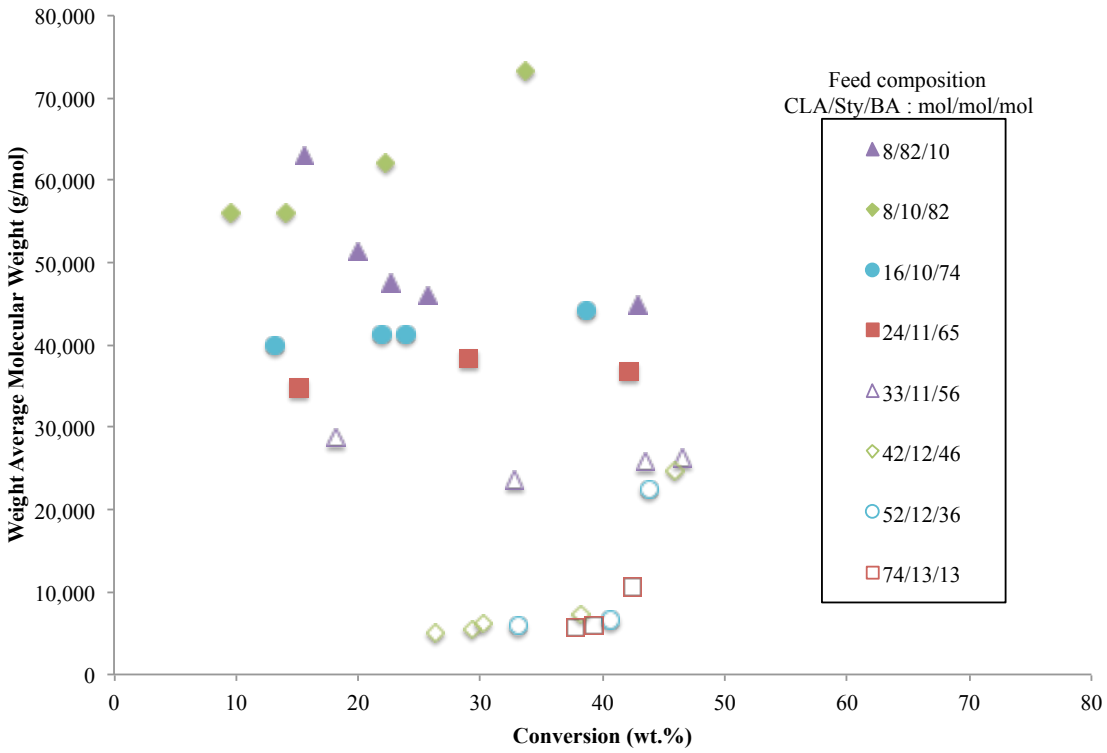

Figure 6.7: Weight-average molecular weight versus conversion for CLA/Sty/BA terpolymers.

6.3 Emulsion terpolymerizations with CLA/Sty/BA

This work was performed to evaluate the influence of terpolymer composition, chain transfer agent (CTA) concentration, DVB concentration, molecular weights, viscosity and particle size on tack, peel strength and shear strength of PSA's by using a constrained mixture design. This part of the project was used to evaluate the feasibility of incorporating CLA into a practical polymer application. As a continuity to the previous experiments, low cost CLA was chosen. The conversion results indicated that the presence of CLA causes a dramatic decrease in reaction rate after nucleation and limits

the maximum conversion one can achieve (see Figure 6.8). In Figure 6.8, an additional run containing no CLA was added for comparison as the dotted line.

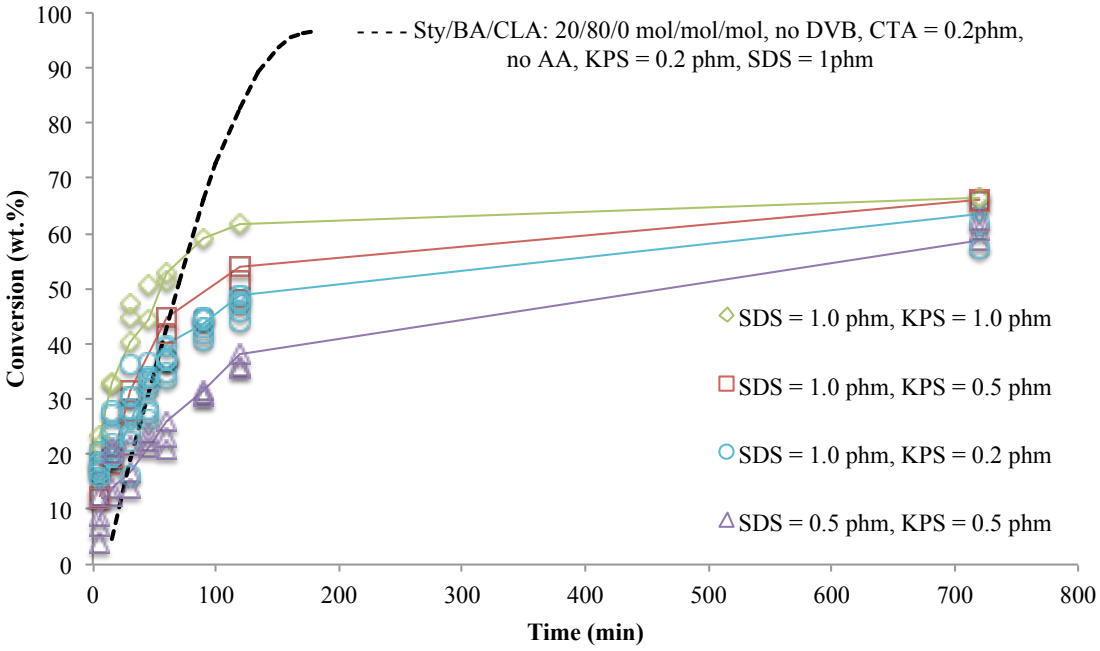

Figure 6.8: Conversion vs. time from preliminary emulsion screening experiments

The ^{1}H-NMR spectroscopic results indicated an initial CLA-rich terpolymer production, followed by the dominant consumption of the co-monomers Sty and BA (see Figure 6.9). The Sty composition reaches a maximum at ~30 wt.% overall conversion which coincides more or less with the complete depletion of Sty monomer in the system where the Sty feed concentration was 10 mol%. On the other hand, the BA composition increases throughout the polymerization.

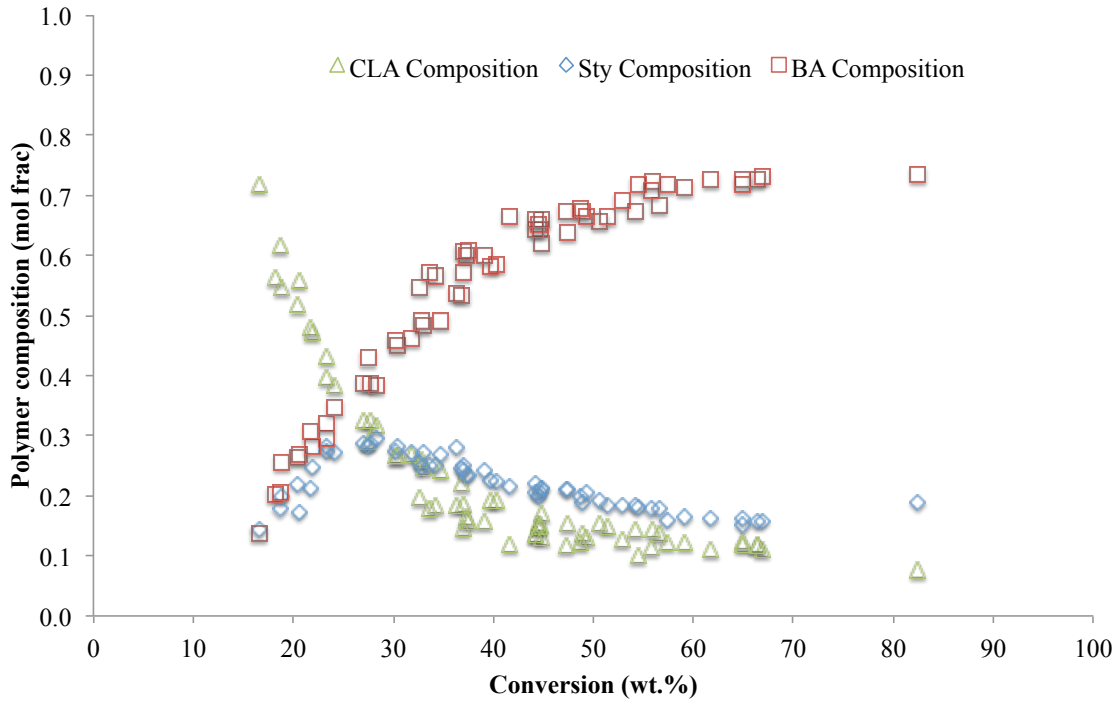

Figure 6.9: Terpolymer composition from preliminary emulsion screening experiments.

All the results from the constrained mixture design were combined to enable the development of empirical models to describe PSA performance. All the models described a statistically significant amount of variation in the data, showed no trend in the residuals and showed no lack of fit. From the models, 3D response surfaces were generated (see Figures 6.10 to 6.12) to illustrate regions where improvements to adhesive performance could be made. These 3D response surfaces are very useful when faced with the usual adhesive design conundrums where optimum conditions for tack and peel strength will differ from the optimum conditions for shear strength. In other words, optimal values for each of tack, peel strength and shear strength cannot be achieved simultaneously. Rather, we were able to achieve three separate formulations in a sub-optimal performance range (see Figures 6.10 to 6.12). These points all fall within an

acceptable range for commercial removable adhesives: tack – 1 to 4 N/cm^2; peel strength – 2 to 10 N/cm; shear strength – 30 to 600 minutes. Therefore, the control of the polymer molecular weight, demonstrated by changing the CLA feed compositions, and CTA and DVB concentrations, allowed us to achieve improved PSA performance suitable for the removable adhesive categories where low shear and low to medium tack and peel strength are required. Further exploration into the optimal adhesive performance region using the empirical models developed here is now possible. Most importantly, the goal of incorporating high amounts of a renewable monomer (i.e., CLA) into a practical application (i.e., PSA) has been achieved with 30 wt.% incorporation.

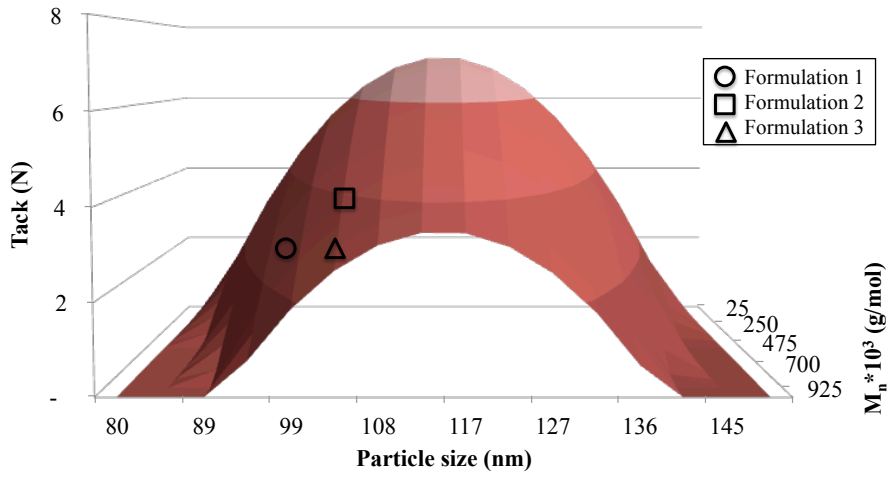

Figure 6.10: 3D response surface for tack model.

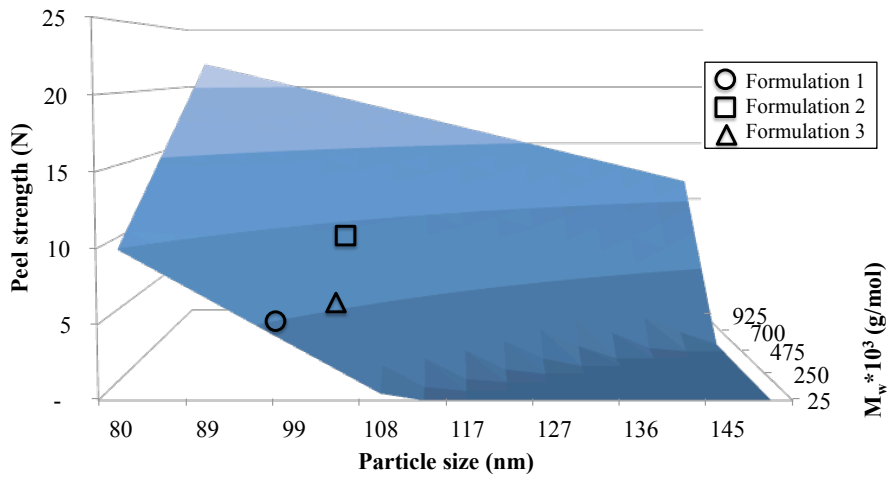

Figure 6.11: 3D response surface for peel strength model.

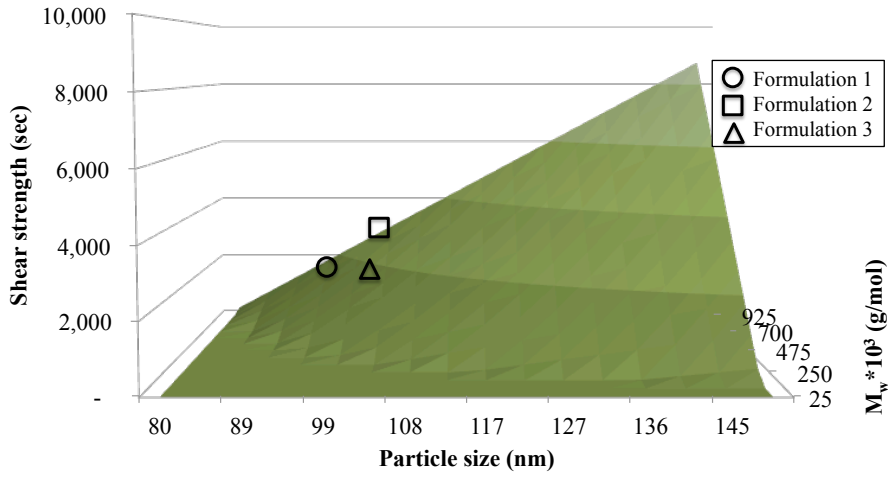

Figure 6.12: 3D response surface for shear strength model.

6.4 IR monitoring of polymerizations with CLA

Throughout this research project, IR monitoring was applied and this work was performed to evaluate the feasibility of ATR-FTIR monitoring on CLA polymerizations. After performing a peak assignment on the system, a multivariate calibration was

developed from the entire spectral region. An optimum number of factors was chosen for each calibration and a predictive relationship between the factors and off-line measurements could be built. The successful off-line and in-line monitoring of bulk and emulsion CLA/Sty/BA co- and terpolymerizations was achieved (see Figures 6.13 and 6.14). The calibration models were validated using off-line data and no significant differences between the ATR-FTIR results and the off-line data were found.

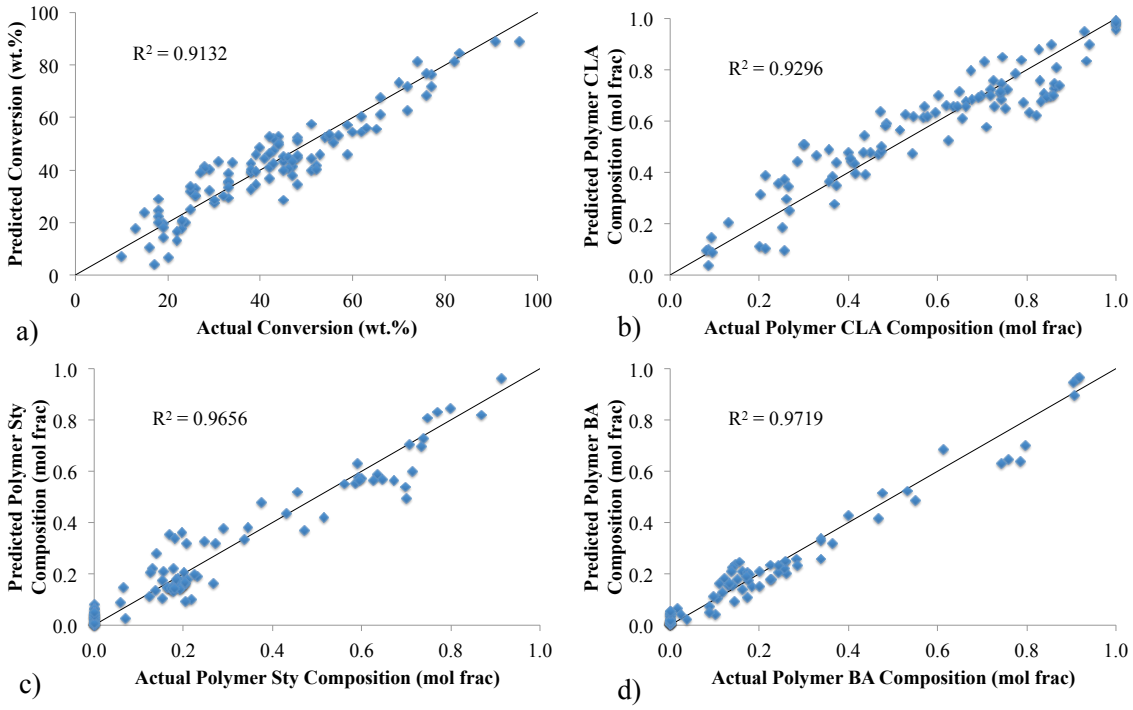

Figure 6.13: PLS predictions for bulk polymerizations: a) overall conversion, b) CLA polymer composition, c) Sty polymer composition, and d) BA polymer composition.

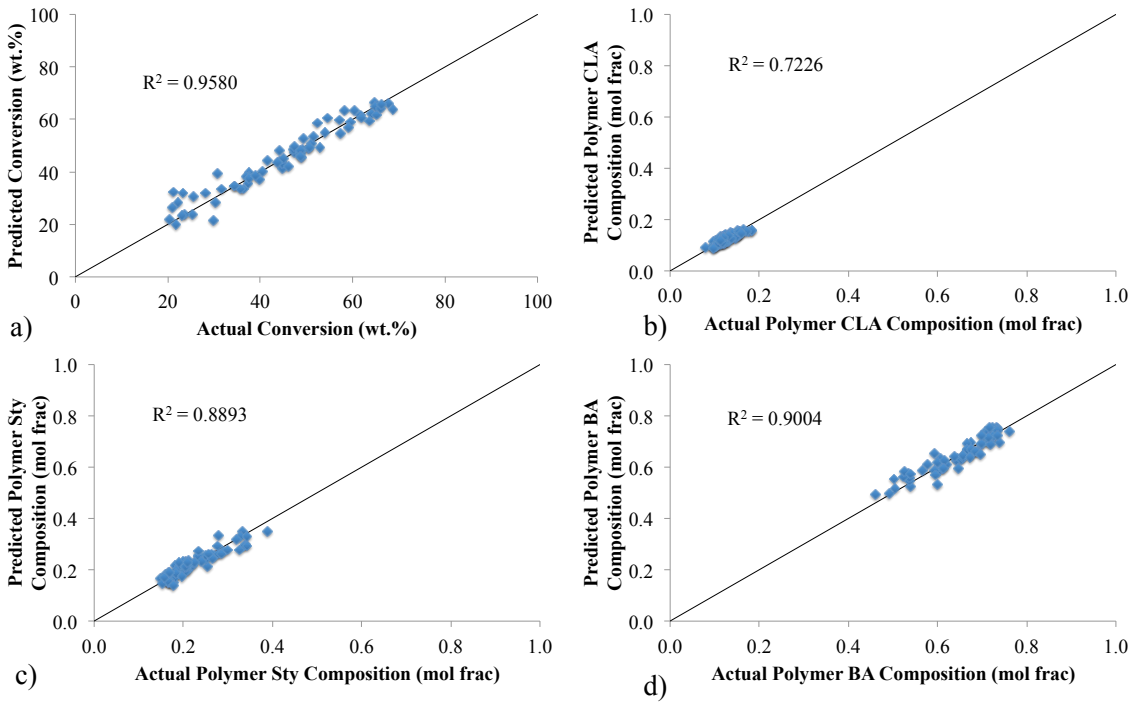

Figure 6.14: PLS predictions for emulsion polymerizations: a) overall conversion, b) CLA polymer composition, c) Sty polymer composition, and d) BA polymer composition.

A valuable consequence of in-line data collection involves the monitoring of fast kinetics (see Figure 6.15). In Figure 6.15, two large peaks at ~1190 cm^{-1} and at ~1730 cm^{-1} increased quickly during the first 5-10 min of the reaction, and then decreased. These changes were rapid enough to make the monitoring of the true trajectory via off-line sampling difficult. According to our peak assignments, both of these peaks relate to both CLA polymer and BA monomer, i.e., the CLA polymer and BA monomer peaks overlap at both 1190 and 1730 cm^{-1}. This trajectory confirms earlier speculation on the behaviour of the oleic acid impurity found in the CLA. An initial production of CLA-rich oligomers is reflected by the sharp increase in the two peaks for the first 5-10 min. When the effect of oleic acid, acting as an impurity, has abated, the consumption of BA

monomer then causes the decrease of those same peaks due to their overlapping functional groups with that of the CLA polymer. Of course, if the peaks were strictly assigned to a monomer, one would expect the peaks to reach an absorbance near zero. That is clearly not the case and the peaks level off due to the produced CLA polymer (oligomers). It should be added that the oleic acid and saturated fatty acid peak assignments overlap with that of the CLA. As the oleic acid and saturated fatty acid are not consumed, the peaks associated to these should not be affected. The kinetic observations demonstrated the value of a continuous in-line monitoring procedure when fast kinetics precludes the ability to monitor a reaction using intermittent, costly and time-consuming off-line measurements

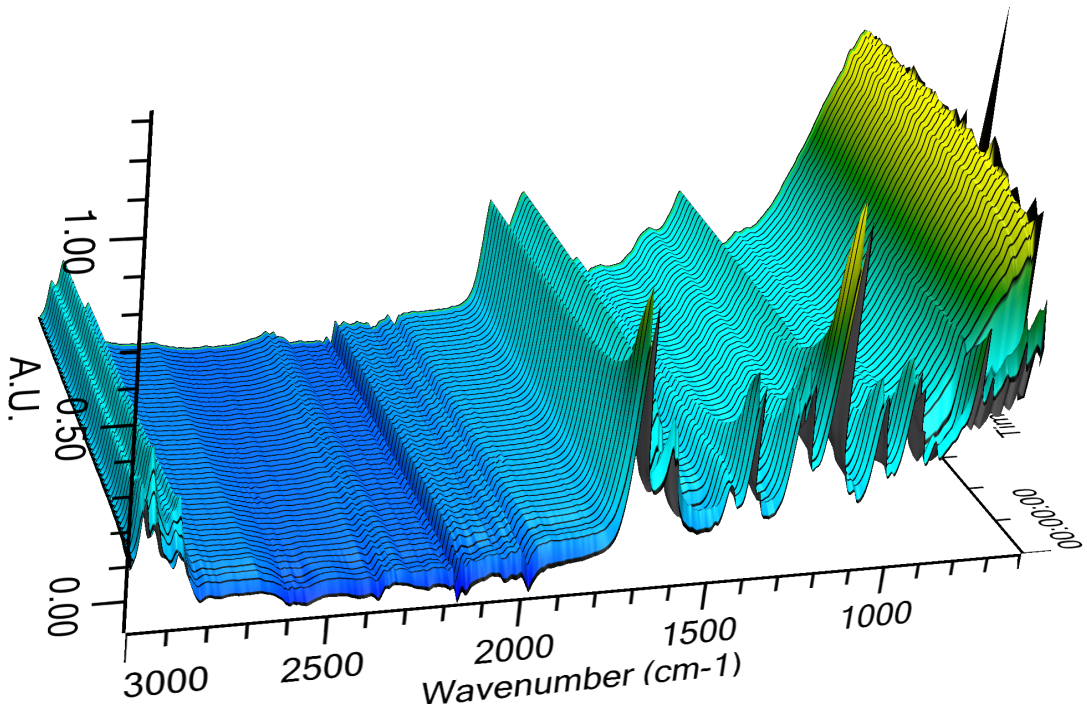

Figure 6.15: Example IR reaction spectra for CLA/Sty/BA: 8/10/82 mol/mol/mol feed composition.

6.5 Main contributions and findings

The main contributions and findings emanating from this thesis are enumerated below.

1. A novel approach was used, for the first time, to estimate reactivity ratios by solving two pseudo-kinetic models simultaneously during the parameter fitting process. This can be considered an extension to the Mayo-Lewis model for reactivity ratio estimation. It should allow the estimation of reactivity ratios for different polymerization systems containing oleic acid such as low-cost fatty acids.

2. Reactivity ratios for the CLA/Sty and the CLA/BA polymer systems were identified for the first time. A semi-batch feed policy can now be used to control polymer properties (i.e., composition) when CLA is being polymerized.

3. Pseudo-kinetic models were successfully developed for the prediction of bulk copolymer composition as a function of conversion. These pseudo-kinetic models provide an improved understanding of the reaction mechanisms involved in the bulk copolymerization of CLA/Sty and CLA/BA when oleic acid is present. To our knowledge, this is the first time that pseudo-kinetic models have been built for the bulk copolymerization of low-cost fatty acids.

4. We successfully incorporated CLA into bulk co- and terpolymers (i.e., CLA/Sty, CLA/BA and CLA/Sty/BA) thus providing a new generation of more sustainable bulk

polymers. To our knowledge, this is the first time that CLA has been successfully incorporated into a bulk polymer matrix without adding any functionalization steps to CLA.

5. We demonstrated that electron trapping from oleic acid improves CLA incorporation in bulk and emulsion co- and terpolymerizations. This finding enables improved economics for sustainable polymerizations with CLA. To our knowledge, this if the first time that oleic acid has been shown to improve CLA incorporation in polymerizations.

6. Electron trapping from oleic acid was also shown to increase oligomer production in bulk and emulsion co- and terpolymerizations. This improves control over polymer molecular weight when low-cost fatty acids are polymerized. To our knowledge, this is the first time that oleic acid has been shown to increase the oligomer production in the polymerization of CLA-containing systems.

7. Bulk terpolymer composition was predicted as a function of conversion using a newly developed pseudo-kinetic model, which was an extension of our previously developed copolymer models. This model provides an improved understanding of the reaction mechanisms involved in the bulk terpolymerization of CLA/Sty/BA in the presence of oleic acid. Hence, it should provide improved control over bulk terpolymer composition.

8. A means to achieve a sub-optimal performance for CLA-containing PSAs was demonstrated for the removable adhesives category. The use of a novel statistical

approach for optimizing PSA performance involving multiple factorial designs, multiple downward regressions of the database followed by 3D response surface analyses led to the identification of optimized regions for PSA performance.

9. We successfully incorporated CLA into an emulsion terpolymer, CLA/Sty/BA, for the first time, to our knowledge. This presents a new polymer product with improved sustainability. The CLA was successfully incorporated without adding any functionalization steps.

10. We successfully applied an off-line and continuous in-line ATR-FTIR monitoring technique to the bulk and emulsion, co- and terpolymer composition and conversion. This enables (along with the reactivity ratios noted earlier) a means to control polymer composition when CLA is being polymerized. Of note was the ability to monitor the reaction in the face of relatively fast polymerization kinetics. To our knowledge, this is the first time that such a monitoring tool has been successfully applied to the monitoring of CLA polymerizations.

In addition to the above contributions, it is worth recalling the principle objectives of this project were guided by the twelve principles of green chemistry. Reflecting on how these principles were addressed reveals that the following principles were directly addressed:

1. Design safer chemicals and products: CLA is considered a non-hazardous material.

2. Use renewable feedstock: CLA is a renewable monomer.

3. Avoid chemical derivatives: no additional functionalization of the CLA was required in this project.

4. Use safer solvents and reaction conditions: using a water-based (emulsion) polymerization technique replaces the conventional solvent-based adhesive production method.

5. Design chemicals and product to degrade after use: CLA is a degradable monomer and fatty acid polymers are biodegradable if not too heavily cross-linked. While not specifically tested for degradability, the addition of CLA to the polymer matrix should, in theory, increase degradability of the product.

6. Analyze in real time to prevent pollution: we employed real-time process monitoring with the ReactIR 45m™ ATR-FTIR probe.

The above contributions were published/submitted as four articles in peer-reviewed publications:

1. S. Roberge, M. A. Dubé, Bulk Copolymerization of Conjugated Linoleic Acid with Styrene and Butyl Acrylate: Reactivity Ratio Estimation. J. Macromol. Sci., Pure Appl. Chem., 2015, 52, 961-970.

2. S. Roberge, M. A. Dubé, Bulk Terpolymerization of Conjugated Linoleic Acid with Styrene and Butyl Acrylate. Sust. Chem. Eng., 2015, DOI: 10.102/acssuschemeng.5b01106.

3. S. Roberge, M. A. Dubé, Emulsion Terpolymerization of Conjugated Linoleic Acid with Styrene and Butyl Acrylate. Int. J. Adhes. Adhes., **submitted December 2015.**

4. S. Roberge, M. A. Dubé, Infrared Process Monitoring of Conjugated Linoleic Acid/Styrene/Butyl Acrylate Bulk and Emulsion Terpolymerization. J. Appl. Polym. Sci. **submitted December 2015.**

6.6 Recommendations for future work

As is the case in many research projects, we have answered many questions regarding CLA/Sty/BA bulk and emulsion-based polymers. At the same time, we have generated many new questions. As a result, we suggest the following steps for future work:

1. In this thesis, reference to the use of reactivity ratios in a semi-batch feed policy to control polymer composition was made frequently. In order to gain improved control over latex properties, which are a significant function of polymer composition, a feedback control policy using the ATR-FTIR spectroscopy probe could be coupled with a semi-batch policy. This would ultimately lead to improved tailoring of desirable latex and polymer performance properties.

2. The main focus in this thesis was the development of a PSA. However, by adjusting the Sty/BA ratio in the polymer numerous other polymer products (e.g., coatings, resins)

could be devised. For example, increasing the amount of Sty would lead to a harder polymer.

3. Obviously, many additional monomers could be copolymerized with CLA. This could include monomers suitable for PSA applications and others suitable to other applications.

4. Different sources of low-cost CLA should be investigated. These may contain differing oleic acid and saturated fatty acid concentrations. Examination of these alternatively sourced CLAs could be used to further validate our findings. By extension, should a more cost-effective pure CLA (and oleic acid) become available, further validation studies could be performed.

5. The ability of oleic acid to trap electrons could be characterized in more detail with crystallographic experimental methods or catalytic experimental methods. More insight into the reaction mechanisms of oleic acid could be revealed this way.

6. Given the high levels of CLA incorporation into our polymers, significant commercial interest is likely. Of course, a likely partner in any future investigations would be Omnova Solutions. In particular, using CLA as a replacement (or partial replacement) for butadiene in styrene-butadiene rubber (SBR) formulations would be high on the list of interesting products.

6.9 Final remarks

The ultimate goal of this thesis was to provide contributions toward a more sustainable future. The incorporation of 30 wt.% CLA into a practical PSA application has brought us one step closer to sustainability. The knowledge gained along the path to reaching this goal will contribute to the body of scientific knowledge already accumulated on sustainable polymers in general and on CLA in particular. These findings on sustainable polymer production provide an economic incentive to the polymer industry and facilitate the eventual transition to petroleum-free polymers. One such incentive comes from the ability to incorporate more CLA in the presence of oleic acid and thus, using a feed component at a competitive price. Another such incentive comes from the ability to incorporate significant amounts of low-cost CLA into a removable adhesive application with obvious extensions to a wide range of other polymer products. Since the different components of plant oils (i.e., fatty acids) were studied instead of one single plant oil (i.e., soybean oil), the findings in this thesis can now be applied to different plant oils around the world.

Appendix A – Sample Calculations

Conversion and Composition Calculations

Mass conversion based on the total polymer in the reaction mixture was measured using gravimetry. The reaction sample was left to dry in a fumehood for ~7 days, then under vacuum for ~7 days until a constant weight was reached. ^{1}H-NMR was used to determine the polymer composition (refer to Equations A1 to A8) from the areas under the appropriate absorption peaks of the spectrum.

$$F_{CLA} = \frac{\text{mole CLA poly}}{\text{mole CLA poly+mole Sty (or BA) poly}} \tag{A1}$$

where

$$Sty\ poly = \frac{\left(\text{peak @ 6.2–7.2 ppm} - \frac{\text{peak @ 7.3–7.5 ppm}}{4} * 2\right)}{5} \tag{A2}$$

$$Sty = \frac{\text{peak @ 7.3–7.5 ppm}}{4} \tag{A3}$$

$$BA\ poly = \frac{\text{peak @ 4.0 ppm}}{2} \tag{A4}$$

$$BA = \frac{\text{peak @ 4.2 ppm}}{2} \tag{A5}$$

$$CLA = \text{peak @ 5.9 ppm} \tag{A6}$$

$$oleic\ acid\ = \frac{\text{peak @ 5.2 ppm} - \text{peak @ 5.9}}{2} \quad \text{(A7)}$$

$$saturated + CLA\ poly = \frac{\text{peak @ 0.9 ppm}}{3} - BA\ poly - BA - CLA - oleic\ acid \quad \text{(A8)}$$

The polymer composition and conversion could then be calculated as follows (see Equations A8 to A13):

$$mole\ CLA\ poly = \frac{CLA\ in\ feed\ sample\ (g) - CLA\ in\ reaction\ sample(g)}{280.5\ (\frac{g}{mol})} \quad \text{(A8)}$$

$$CLA\ in\ feed\ sample\ (g) = sample\ mass(g) * wt\%\ CLA\ in\ feed \quad \text{(A9)}$$

$$CLA\ in\ reaction\ sample\ (g) = \ sample\ mass\ (g) * wt\%\ CLA\ from\ NMR \quad \text{(A10)}$$

$$Sty\ poly\ (mole) = \frac{sample\ mass\ (g) * wt\%\ Sty\ poly\ from\ NMR}{104.1\ (\frac{g}{mol})} \quad \text{(A11)}$$

$$BA\ poly\ (mole) = \frac{sample\ mass\ (g) * wt\%\ BA\ poly\ from\ NMR}{128.17\ (\frac{g}{mol})} \quad \text{(A12)}$$

$$Conversion = \frac{CLA\ poly\ (g) + Sty(or\ BA)poly(g)}{CLA\ feed\ (g) + Sty\ (or\ BA)feed(g)} \quad \text{(A13)}$$

To illustrate the calculation procedure, an emulsion terpolymerization performed during this PhD will be analyzed. The low-cost CLA sample containing impurities was

analyzed for composition through ^{1}H-NMR. For this experiment, the low-cost CLA composition was, in wt.%, 70.56% CLA, 14.91% Oleic acid, 14.53% Saturated fatty acid. The reaction recipe is shown in Table A1.

Table A1: Emulsion terpolymerization recipe

Ingredients	Mass (g)	Weight% (%)
CLA	78.752	10.15
Sty	27.690	3.57
BA	254.990	32.88
Oleic	16.641	2.15
Saturated	16.217	2.09
CTA	3.950	0.51
AA	15.780	2.03
DVB	1.220	0.05
DDI water	354.880	45.73
SDS	3.941	0.51
NaHCO3	0.588	0.08
KPS	1.972	0.25

A sample was taken from the emulsion experiment at 722 minutes and it weighted 9.802 g. After drying, the sample weight was 5.046 g. This dry sample was analyzed for

composition through ^{1}H-NMR (refer to Figure A1) and the identified peak areas are shown in Table A2.

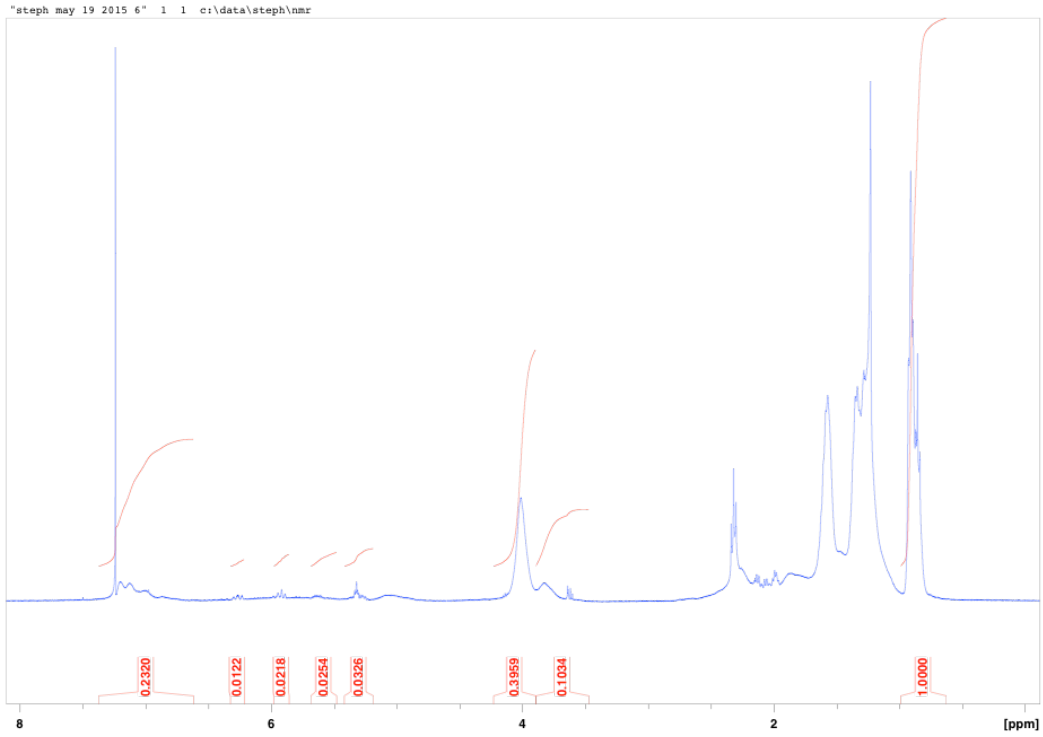

Figure A.1: ^{1}H-NMR spectrum with peak integration for sample calculations

Table A2: Dry emulsion sample ^{1}H-NMR peak areas

Identified Peaks	Peak Areas
Sty	0.0000
poly-Sty	0.2320
CLA	0.0122
Oleic+CLA	0.0326
BA	0.0000
poly-BA	0.3959
Saturated+Oleic+CLA+BA+poly BA+poly CLA	1.0000

The dry sample weight was corrected to exclude the weight of CTA, SDS, NaHCO3 and KPS. The dry sample composition and conversion were calculated with Equations A1 to A13 as follows:

$$Sty\ poly = \frac{\left(0.232 - \frac{0}{4} * 2\right)}{5} = 0.0464\ mol$$

$$Sty\ = \frac{0}{4} = 0\ mol$$

$$BA\ poly\ = \frac{0.3959}{2} = 0.19795\ mol$$

$$BA\ = \frac{0}{2} = 0\ mol$$

$$CLA = \ 0.0122\ \text{mol}$$

$$oleic\ acid\ = \frac{0.0326 - 0.0122}{2} = 0.0102\ mol$$

$$saturated + CLA\ poly = \frac{1}{3} - 0.19795 - 0 - 0.0122 - 0.0102 = 0.11298\ mol$$

The dry sample composition was calculated in mol% and wt% and those results are shown in Table A3.

Table A3: Dry emulsion sample composition

Ingredients	Mass (g)	Weight% (%)	Mole (mol)	Mol% (%)
Sty	0.000	0.00	0.0000	0.00
poly-Sty	0.348	7.08	0.0033	12.22
CLA	0.247	5.02	0.0009	3.21
Oleic	0.208	4.23	0.0007	2.69
BA	0.000	0.00	0.0000	0.00
poly-BA	1.828	37.20	0.0143	52.13
Sat+polyCLA	2.284	46.47	0.0081	29.75

The amount of poly-CLA in the dry sample was calculated as follows:

$$CLA\ in\ feed\ sample\ (g) = 9.802 * 10.15\% = 0.995\ g$$

$$CLA\ in\ reaction\ sample\ (g) = \ 4.914 * 5.02\% = 0.247\ g$$

$$CLA\ poly\ (mole) = \frac{0.995 - 0.247}{280.5} = 0.0027\ mol$$

The dry polymer composition and conversion could then be calculated as follows:

$$Sty\ poly\ (mole) = \frac{4.914 * 7.08\%}{104.1} = 0.0033\ mol$$

$$BA\ poly\ (mole) = \frac{4.914 * 37.20\%}{128.17} = 0.0143\ mol$$

$$\mathrm{F_{CLA}} = \frac{0.0027}{0.0027 + 0.0033 + 0.0143} = 13.15\ mol\%$$

$$\mathrm{F_{Sty}} = \frac{0.0033}{0.0027 + 0.0033 + 0.0143} = 16.49\ mol\%$$

$$\mathrm{F_{BA}} = \frac{0.0143}{0.0027 + 0.0033 + 0.0143} = 70.36\ mol\%$$

$$Conversion = \frac{0.748 + 0.348 + 1.828}{0.995 + 0.349 + 3.219} = 64.08\ wt\%$$

Appendix B – Extra Figures and Tables

Figures B.1, B.2, B.3, B.4, B.5: Monomers IR spectrum

Figure B.6, B.7, B.8, B.9, B.10: Monomers ^{1}H-NMR spectrum

Figure B.11: Polymer ^{1}H-NMR spectrum from “Sample Calculations”

Figure B.12: Low-cost CLA DSC curve

Figure B.13, B.14, B.15, B.16: Examples of Polymer DSC curve

Figure B.17: Example of terpolymer GPC results

Figure B.11: Example of temperature profile from emulsion experiment

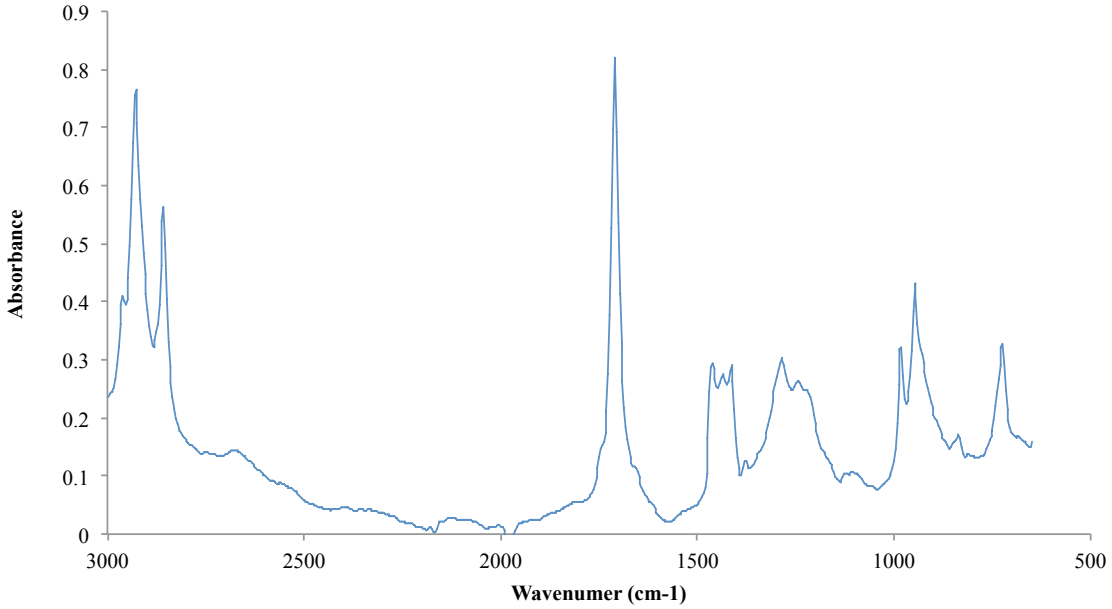

Figure B.1: IR spectrum for low-cost CLA.

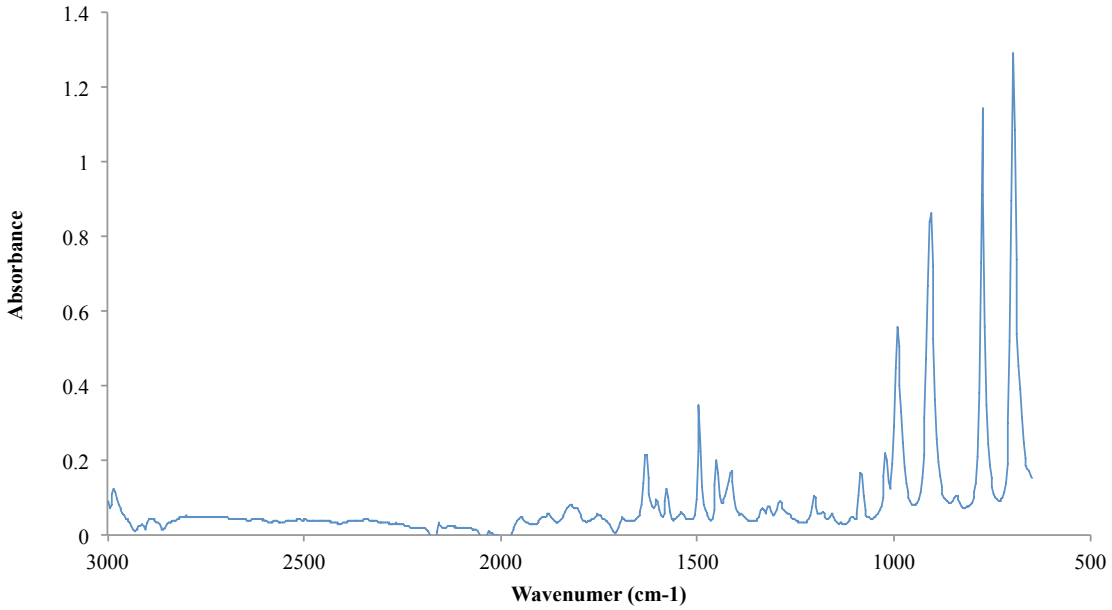

Figure B.2: IR spectrum for styrene

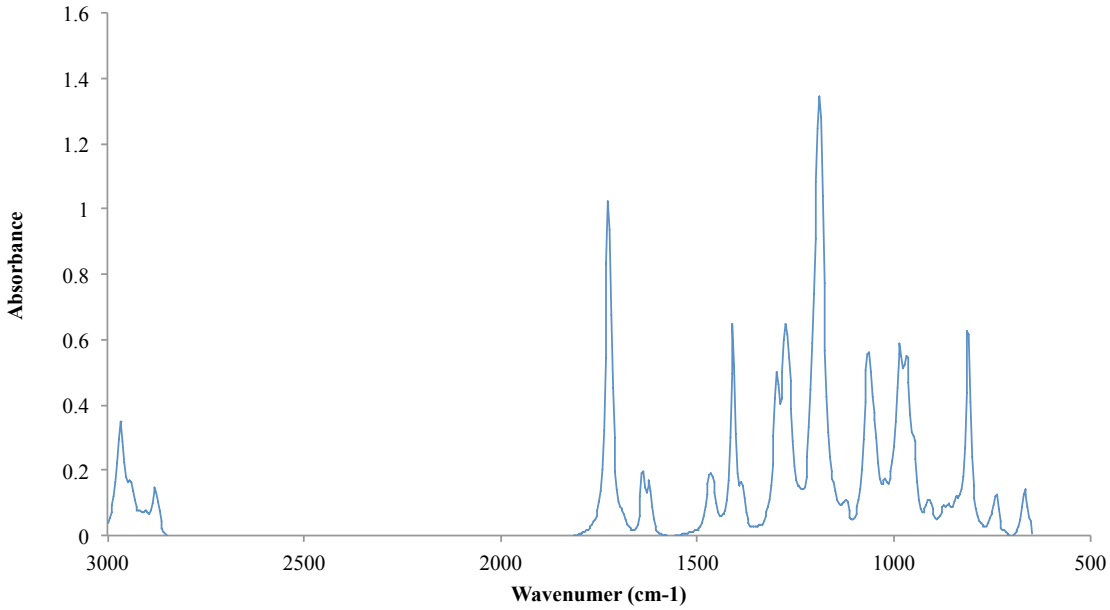

Figure B.3: IR spectrum for butyl acrylate

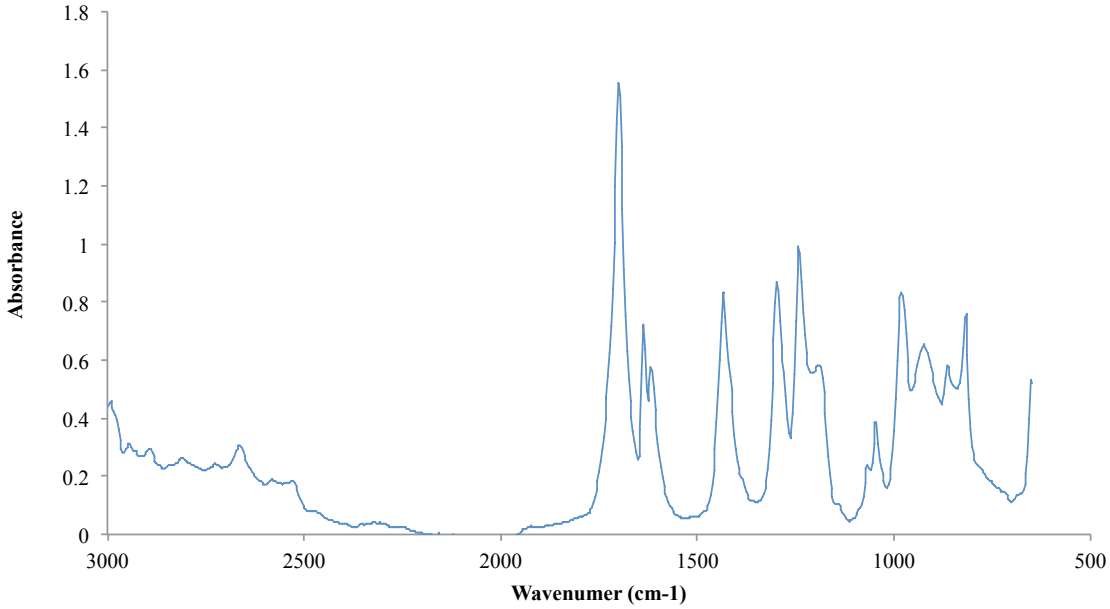

Figure B.4: IR spectrum for acrylic acid

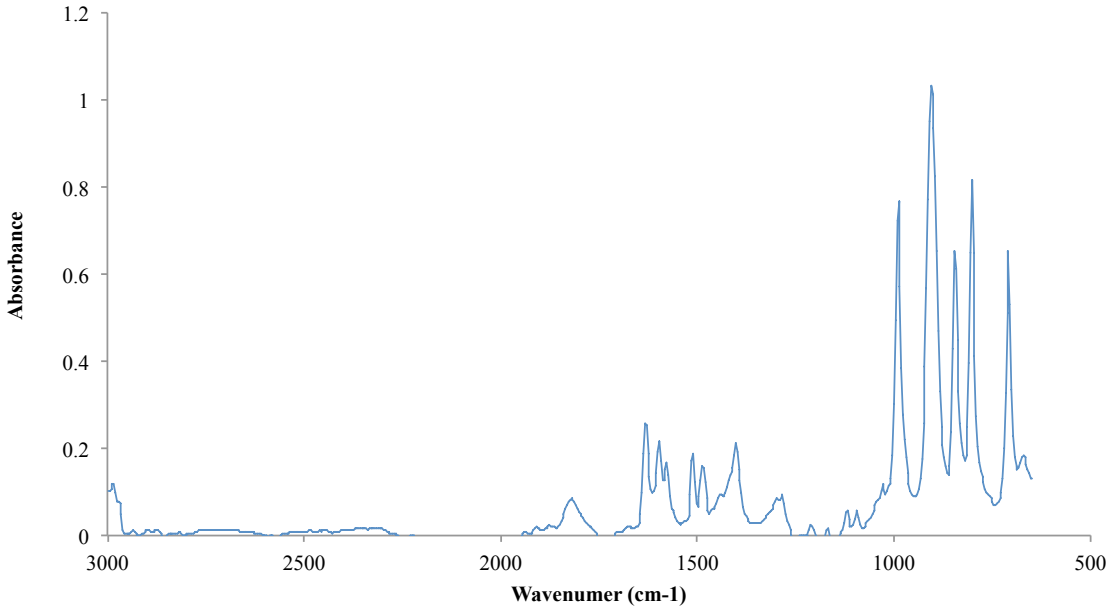

Figure B5: IR spectrum for divinylbenzene

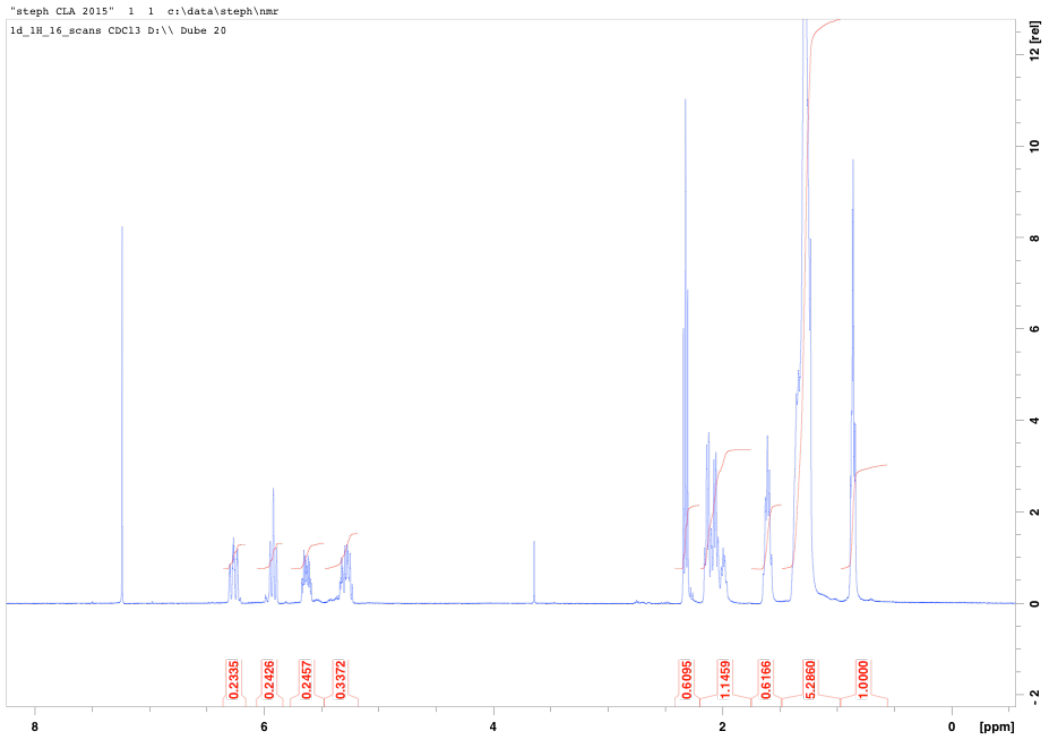

Figure B.6: ^{1}H-NMR spectrum for low-cost CLA.

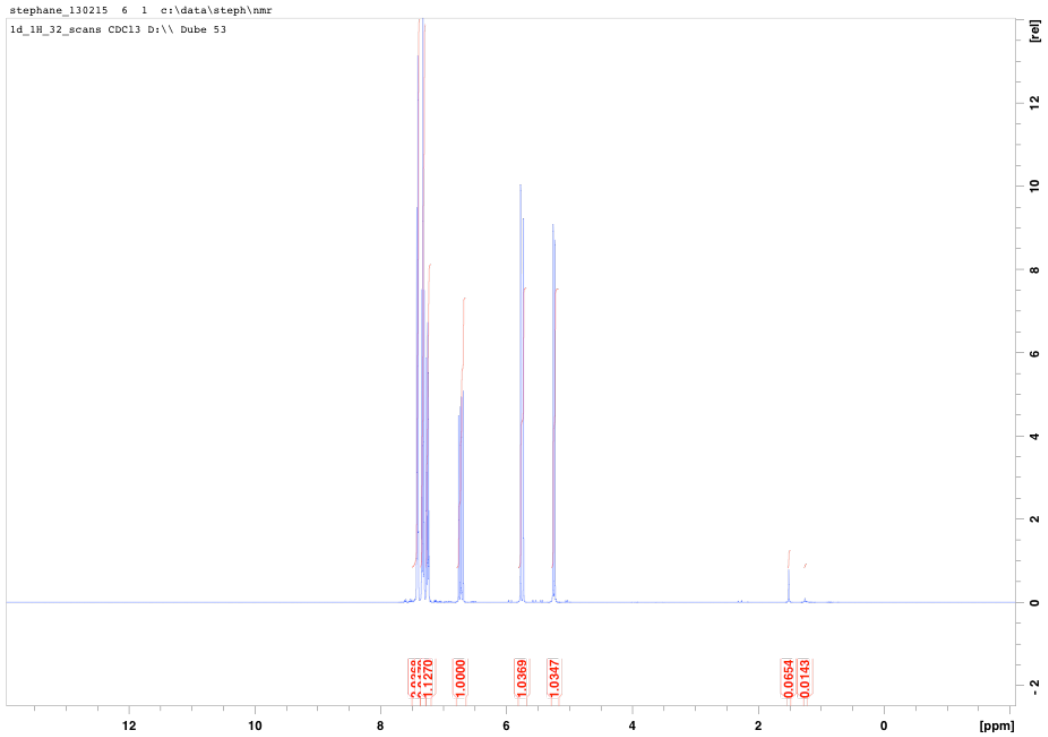

Figure B.7: ^{1}H-NMR spectrum for styrene

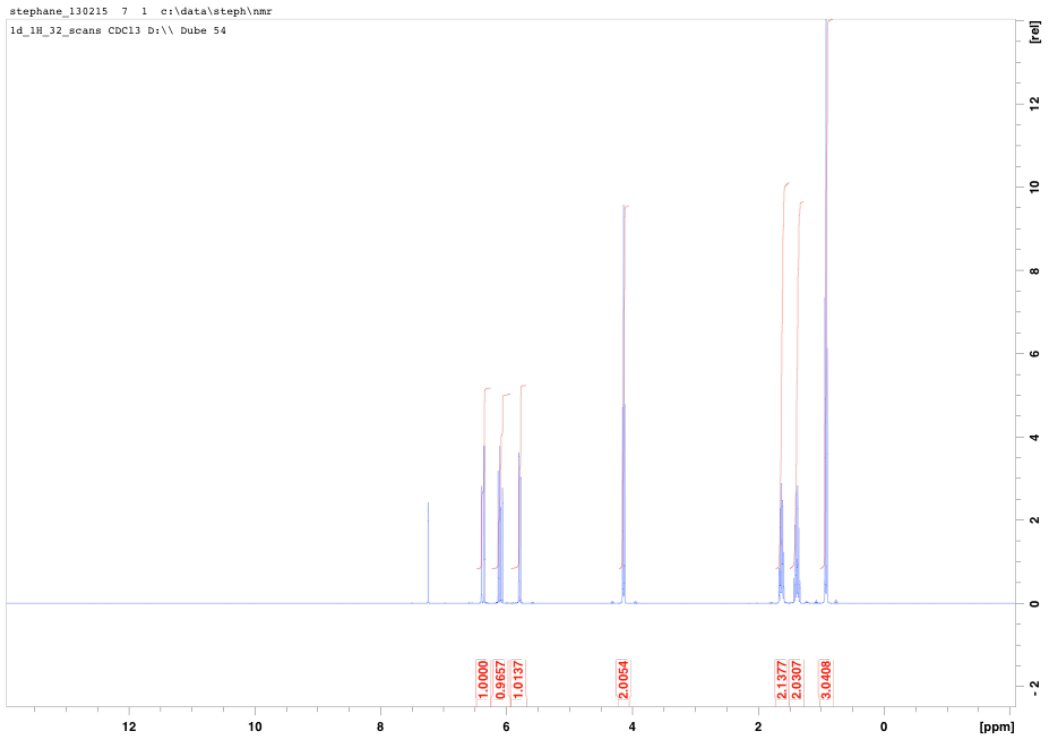

Figure B.8: ^{1}H-NMR spectrum for butyl acrylate

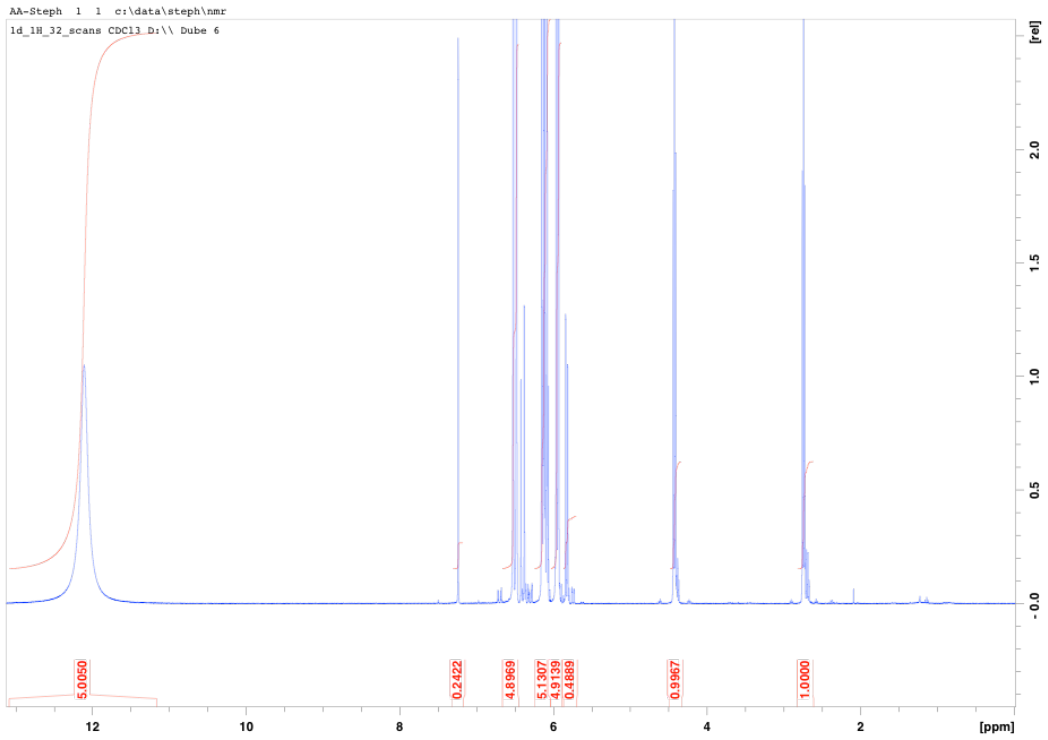

Figure B.9: ^{1}H-NMR spectrum for acrylic acid

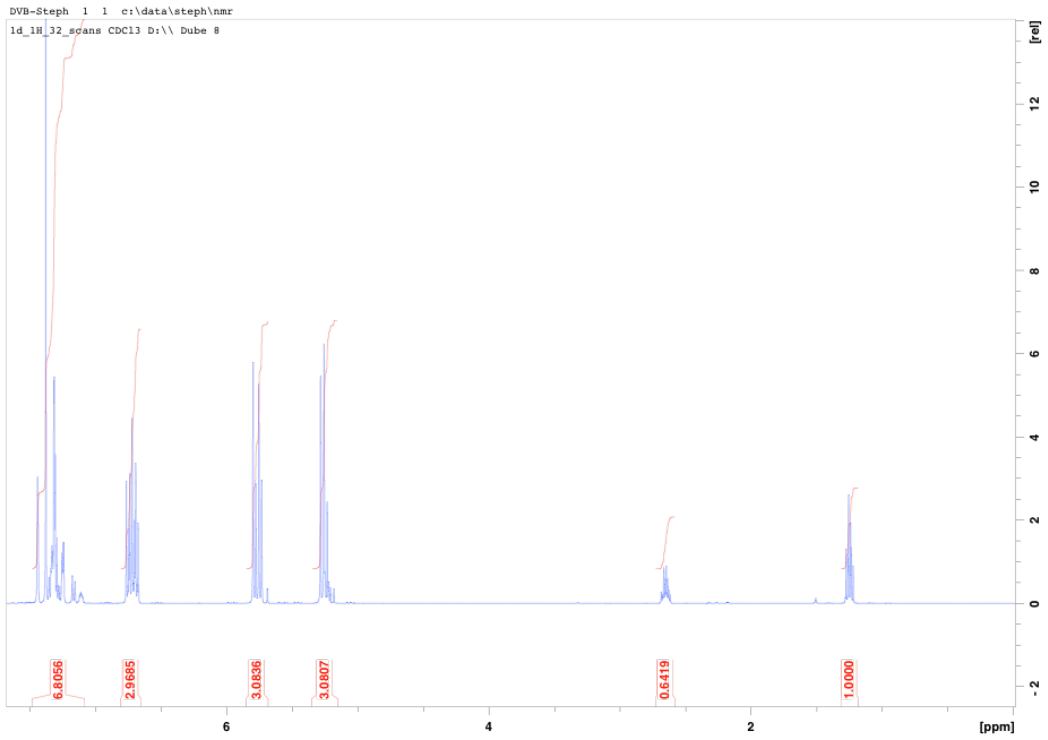

Figure B10: ^{1}H-NMR spectrum for divinylbenzene

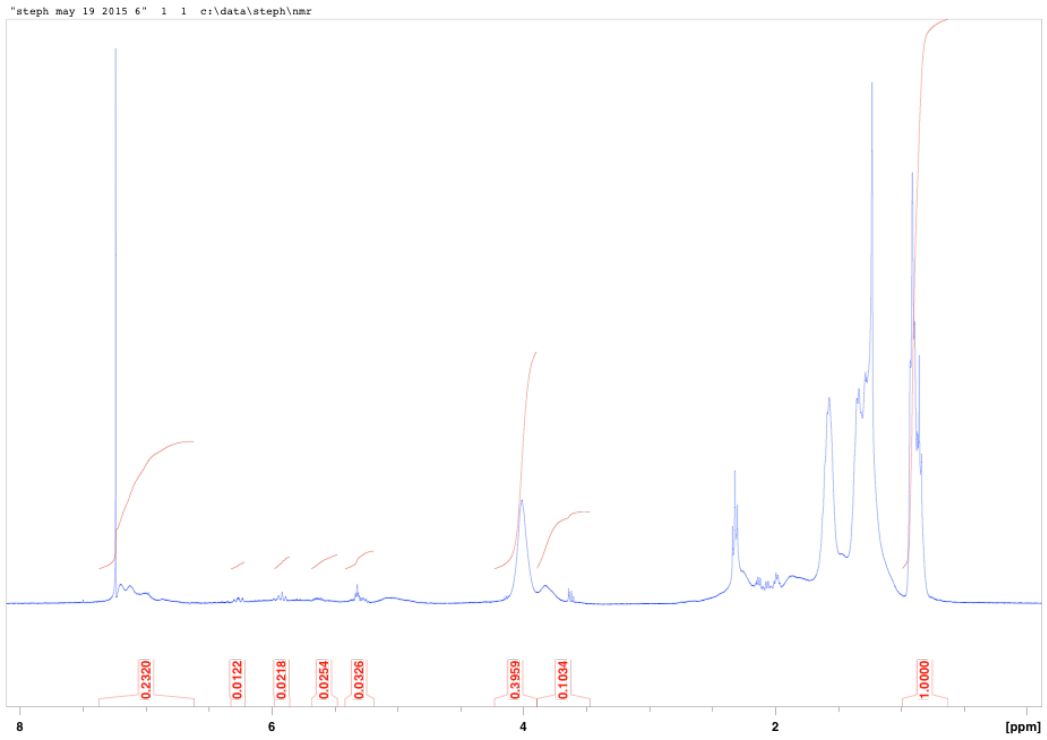

Figure B.11: ^{1}H-NMR spectrum of terpolymer from “Sample Calculations”

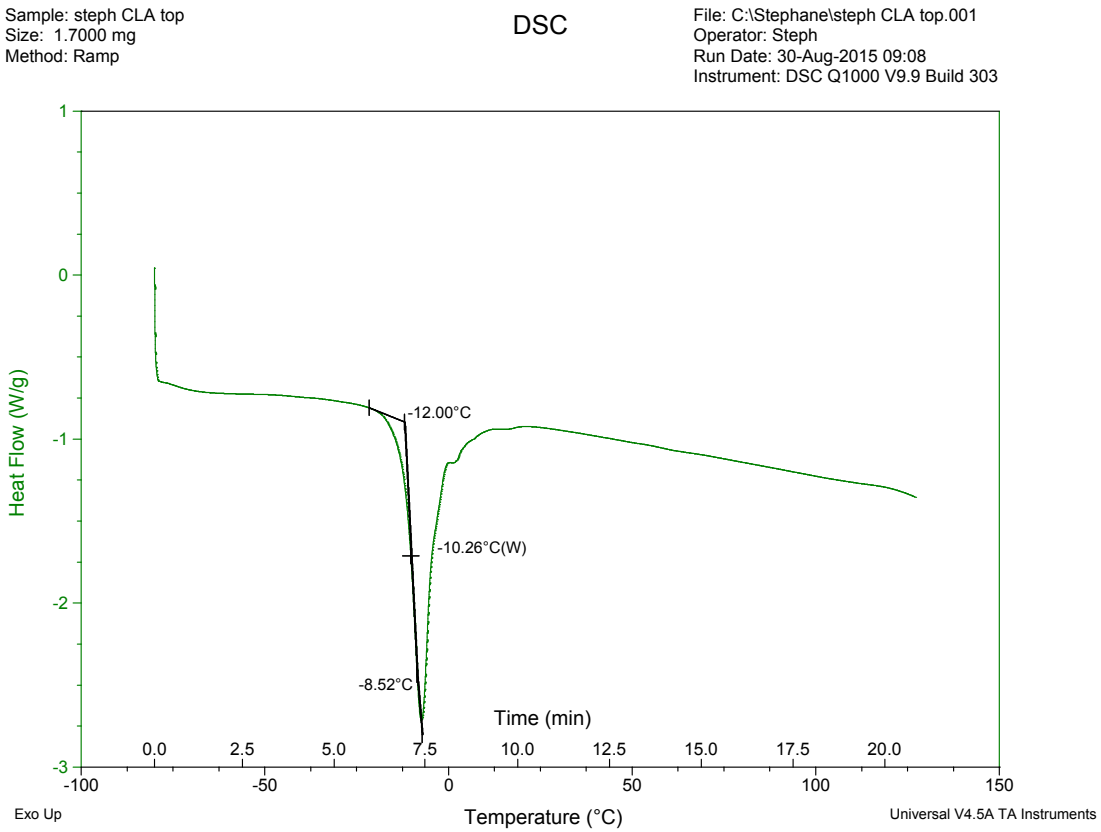

Figure B.12: DSC curve for low-cost CLA

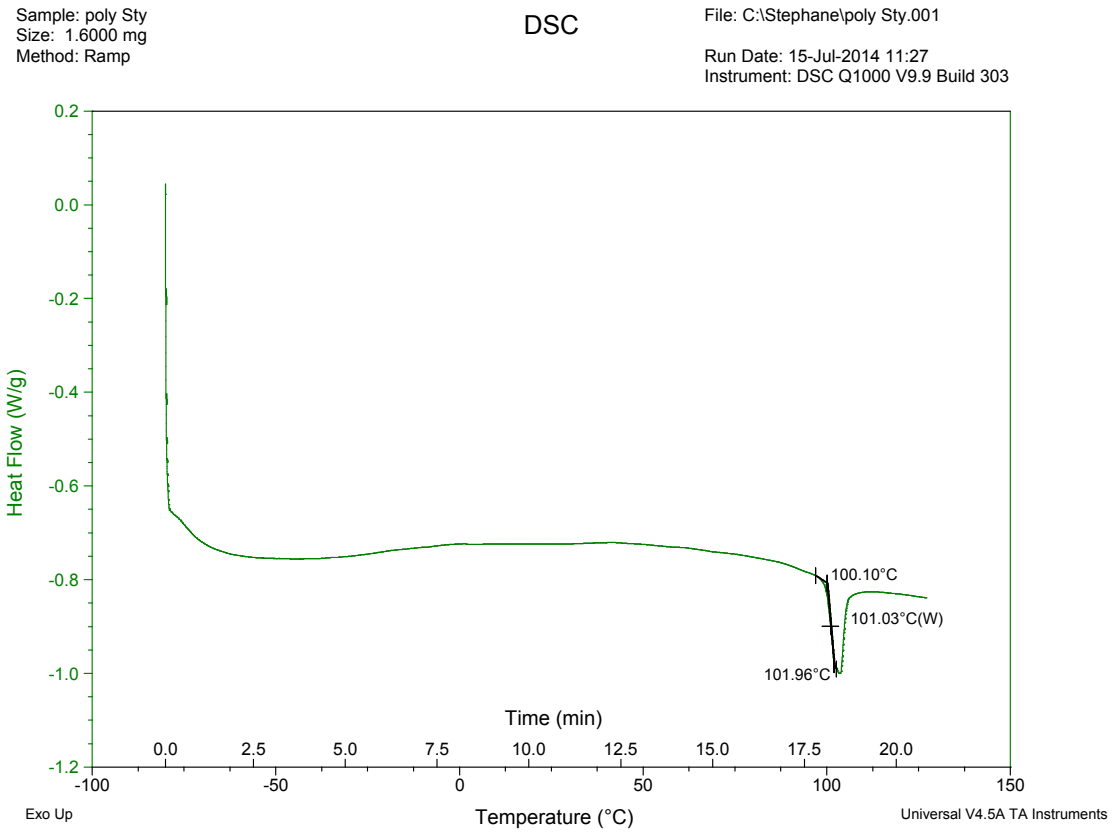

Figure B.13: DSC curve for styrene homopolymer

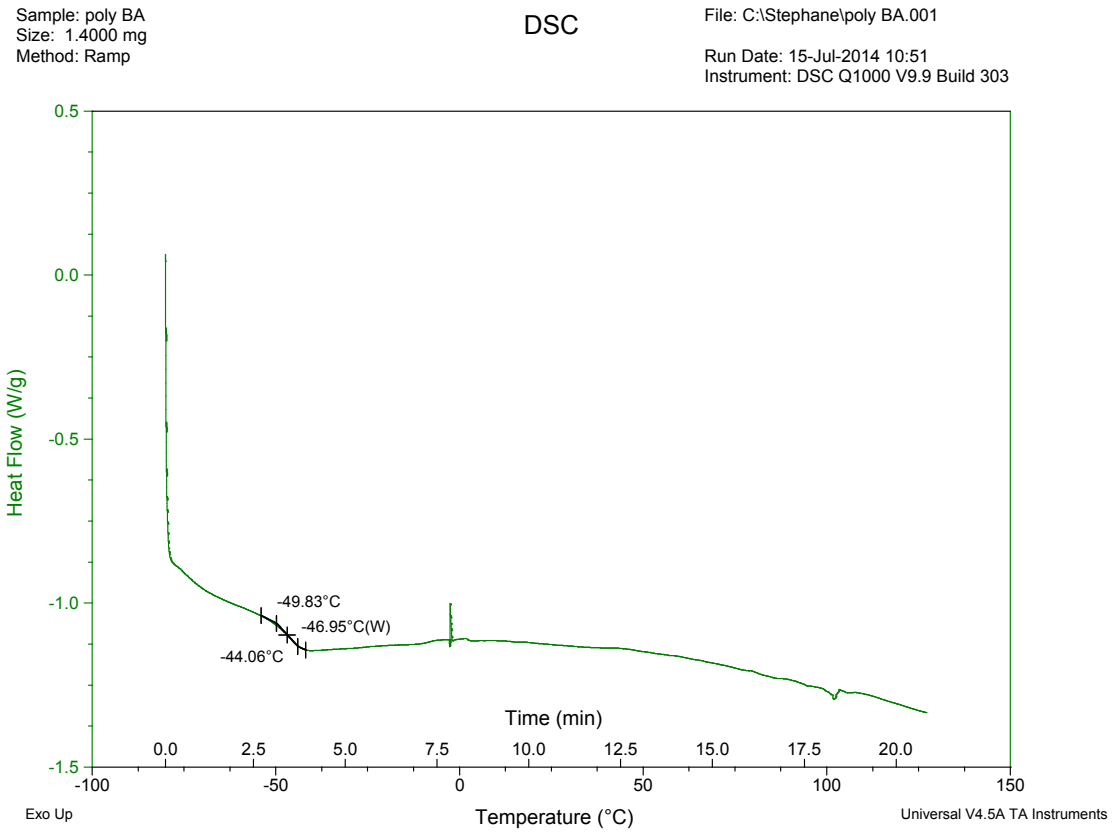

Figure B.14: DSC curve for butyl acrylate homopolymer

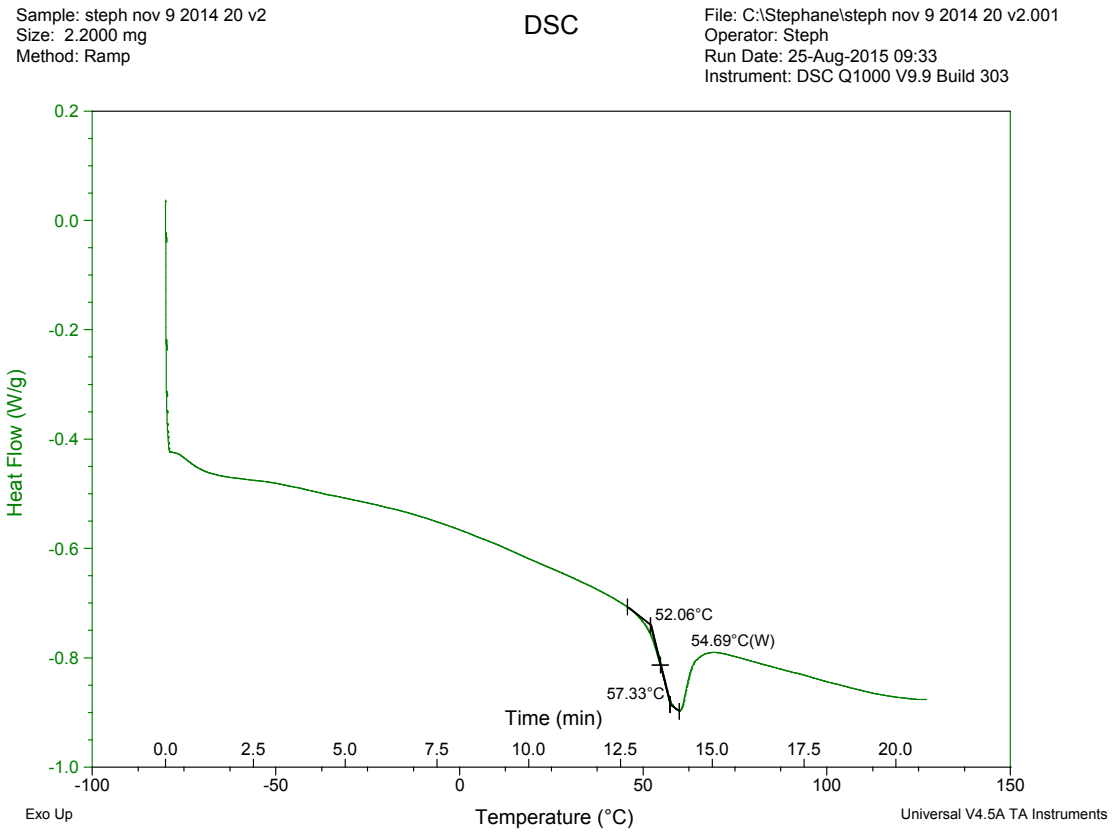

Figure B.15: DSC curve for high styrene terpolymer (CLA/Sty/BA)

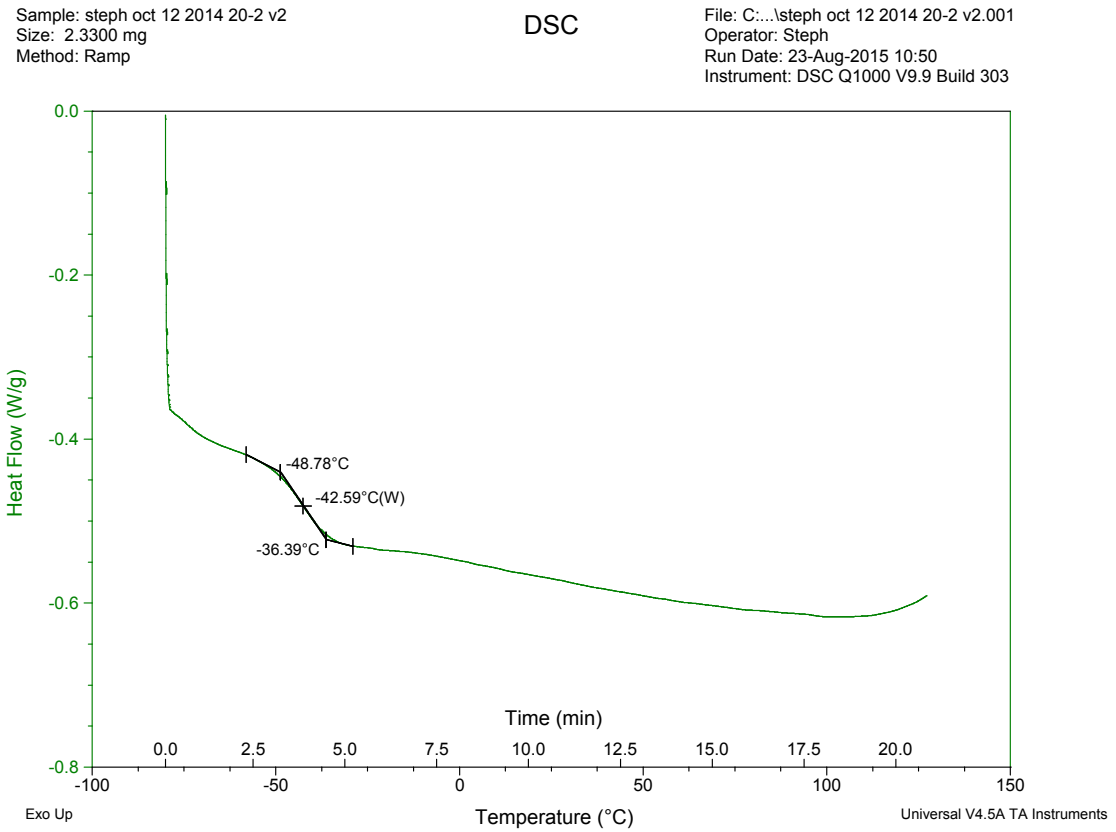

Figure B.16: DSC curve for high butyl acrylate terpolymer (CLA/Sty/BA)

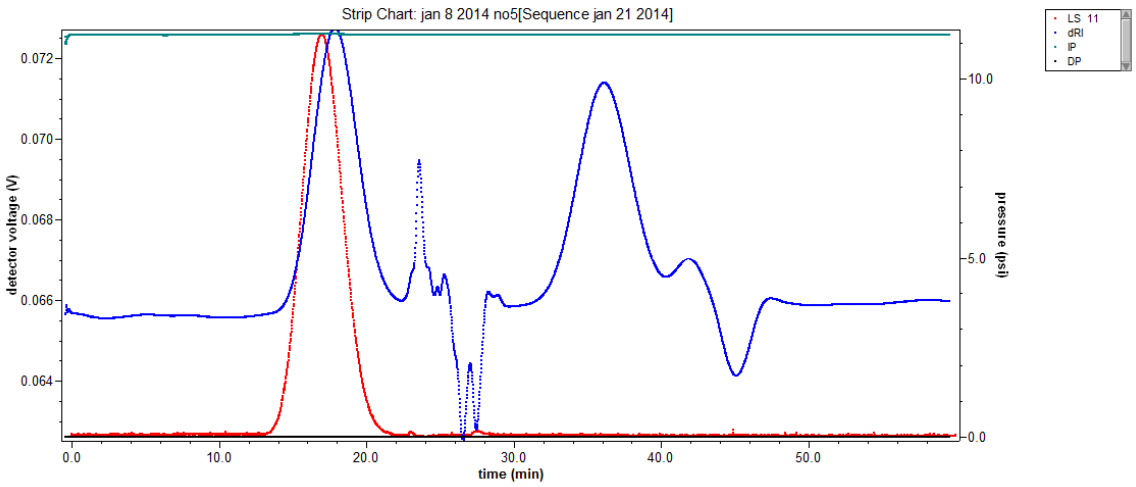

Figure B.17: Example of terpolymer GPC results

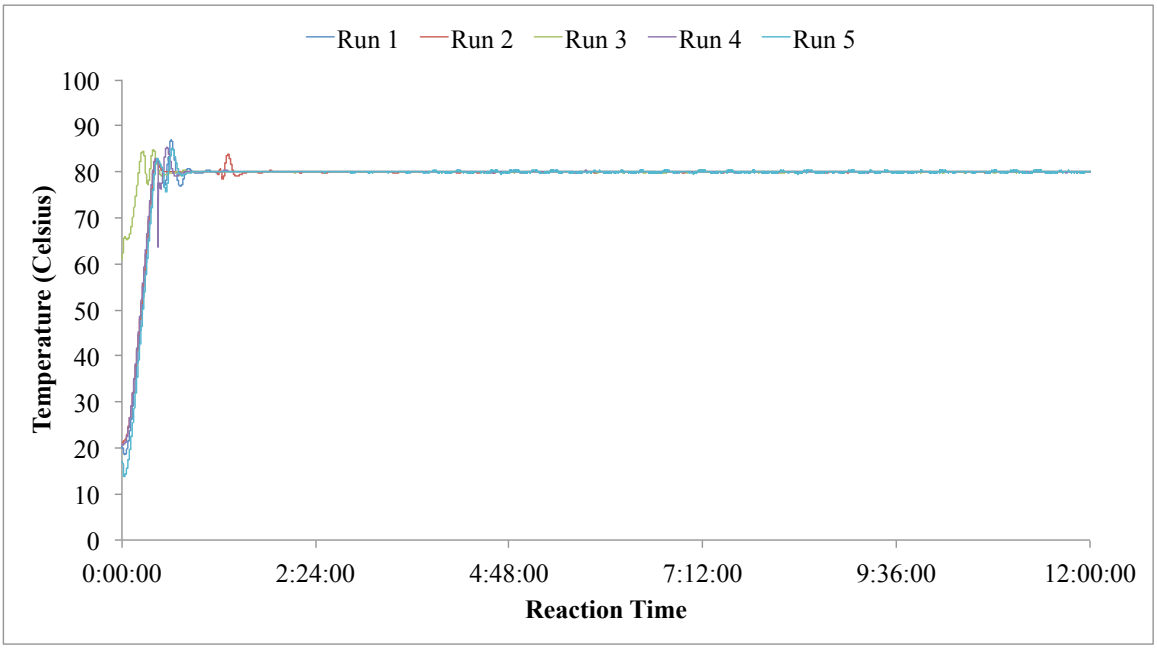

Figure B.18: Example of temperature profile from emulsion experiment

Appendix C – Matlab Code for Bulk Copolymerization

Matlab version: Mathworks, R2014b, 8.4.0.150421, 64-bit (maci64)

The following function “f2” was created:

```
function rk = f2(t,y)

kd=2.47E-5; %s-1 for BPO at 80 deg C
Izero=0.0694; %mol/L initiator (2 phm w/w)
Idot=Izero*exp(-kd*t); %mol/L initiator radicals

kIA=1; %L mol-1 sec-1
kIB=0;
kIO=0;
kpAA=0.03;
kpAB=0.6;
kpBA=0.3;
kpBB=3024;
ktAO=1000;
ktBO=2000;

a=-kIA*Idot*y(1)-kpAA*y(4)*y(1)-kpBA*y(5)*y(1); %change of CLA
b=-kIB*Idot*y(2)-kpAB*y(4)*y(2)-kpBB*y(5)*y(2); %change of BA or Sty
c=-kIO*Idot*y(3)-ktAO*y(4)*y(3)-ktBO*y(5)*y(3); %change of activated Oleic
d=kIA*Idot*y(1)-kpAB*y(4)*y(2)+kpBA*y(5)*y(1)-ktAO*y(4)*y(3); %ending in A
e=kIB*Idot*y(2)+kpAB*y(4)*y(2)-kpBA*y(5)*y(1)-ktBO*y(5)*y(3); %ending in B
```

```
rk = [a; b; c; d; e];
```

The following “m file” was created as the main program:

```
time = 0:10:70000;
initial = [0.4255, 5.2288, 0.3, 0, 0];
[t,y] = ode45(@f2, time, initial);
figure;
plot(t,y(:,1),'b');
title('Models'), xlabel('seconds'), ylabel('mol/L');
hold on;
plot(t,y(:,2),'r');
plot(t,y(:,3),'m');
plot(t,y(:,4),'k');
plot(t,y(:,5),'g');
legend('CLA','BA', 'Oleic', 'Ra', 'Rb');
hold off;
```

The mol/L of CLA, Sty, BA and oleic acid were plotted as a function of time for a quick assessment when possible. Time was varied from 0 to 70,000 sec, R_A, R_B were initialized for all feeds as 0 and A, B, O were initialized for each feed as follows (see Table A2).

Table C1: Feed Concentrations for Matlab Modeling

CLA (mol/L)	BA (mol/L)	Oleic (mol/L)	Oleic effective
0.4255	5.2288	0.1000	0.30
0.9281	3.7870	0.2133	0.64
1.2150	2.6707	0.4033	1.21

CLA (mol/L)	Sty (mol/L)	Oleic (mol/L)	Oleic effective
0.5225	6.2879	0.0867	0.26
0.9601	4.3618	0.3200	0.96
1.5136	2.9118	0.2500	0.75

I_0 was 2 phm on weight basis (calculated mole/L for each feed)

(BA: 0.0694, 0.0705, 0.0713; Sty: 0.0703, 0.0712, 0.0719)

Appendix D – Matlab Code for Bulk Terpolymerization

Matlab version: Mathworks, R2014b, 8.4.0.150421, 64-bit (maci64)

The following function “f3” was created:

```
function rk = f3(t,y)

kd=2.47E-5; %s-1 for BPO at 80 deg C

Izero=0.07; %mol/L initiator (2 phm w/w)

Idot=Izero*exp(-kd*t); %mol/L initiator radicals

kiA=0.0003; %L mol-1 sec-1

kiB=0;

kiC=0;

kiO=0;

kpAA=0.03;

kpAB=0.3;

kpAC=0.6;

kpBA=0.03;

kpBB=341;

kpBC=357;

kpCA=0.3;

kpCB=15205;

kpCC=3024;

ktrAO=1000;

ktrBO=1000;

ktrCO=2000;

a=-kiA*Idot*y(1)-kpAA*y(5)*y(1)-kpBA*y(6)*y(1)-kpCA*y(7)*y(1); %change of CLA
```

```
b=-kiB*Idot*y(2)-kpAB*y(5)*y(2)-kpBB*y(6)*y(2)-kpCB*y(7)*y(2); %change of Sty
c=-kiC*Idot*y(3)-kpAC*y(5)*y(3)-kpBC*y(6)*y(3)-kpCC*y(7)*y(3); %change of BA
d=-kiO*Idot*y(4)-ktrAO*y(5)*y(4)-ktrBO*y(6)*y(4)-ktrCO*y(7)*y(4); %change of
activated Oleic
e=kiA*Idot*y(1)-kpAB*y(5)*y(2)-kpAC*y(5)*y(3)+kpBA*y(6)*y(1)+kpCA*y(7)*y(1)-
ktrAO*y(5)*y(4); %ending in CLA
f=kiB*Idot*y(2)+kpAB*y(5)*y(2)-kpBA*y(6)*y(1)-kpBC*y(6)*y(3)+kpCB*y(7)*y(2)-
ktrBO*y(6)*y(4); %ending in Sty
g=kiC*Idot*y(3)+kpAC*y(5)*y(3)+kpBC*y(6)*y(3)-kpCA*y(7)*y(1)-kpCB*y(7)*y(2)-
ktrCO*y(7)*y(4); %ending in BA
rk = [a; b; c; d; e; f; g];
```

The following “m file” was created as the main program:

```
time = 0:1:70000;
initial = [1.6360, 0.4469, 1.7794, 0.6338, 0, 0, 0];
[t,y] = ode45(@f3, time, initial);
figure;
plot(t,y(:,1),'y');
title('Models'), xlabel('seconds'), ylabel('mol/L');
hold on;
plot(t,y(:,2),'m');
plot(t,y(:,3),'c');
plot(t,y(:,4),'r');
```

```
plot(t,y(:,5),'g');
plot(t,y(:,6),'b');
plot(t,y(:,7),'k');
legend('CLA','Sty','BA', 'Oleic', 'Ra', 'Rb', 'Rc');
hold off;
```

The mol/L of CLA, Sty, BA and oleic acid were plotted as a function of time for a quick assessment when possible. Time was varied from 0 to 70,000 sec, R_A, R_B, R_C were initialized for all feeds as 0 and A, B, C, O were initialized for each feed as follows (refer to Table A1).

Table D1: Feed concentrations for Matlab modeling

Run	CLA (mol/L)	Sty (mol/L)	BA (mol/L)	Oleic effective (mol/L)	Initiator (mol/L)
1	0.4352	0.5908	4.7206	0.3151	0.07
2	0.8071	0.5431	3.8348	0.3852	0.07
3	1.1223	0.5065	3.0494	0.4845	0.07
4	1.4100	0.4777	2.3999	0.4854	0.07
5	1.6360	0.4469	1.7794	0.6338	0.07
6	1.8614	0.4243	1.2655	0.6408	0.07
7	2.1906	0.3735	0.3733	0.8487	0.07
8	0.5025	5.4686	0.6864	0.2807	0.07